sid.inpe.br/mtc-m21d/2021/07.22.11.18-TDI

# ASSESSMENT OF THE IMPACT CAUSED BY FIRES IN THE BRAZILIAN LEGAL AMAZON FROM 2001 TO 2020

Wesley Augusto Campanharo

Doctorate Thesis of the Graduate Course in Remote Sensing, guided by Drs. Liana Oighenstein Anderson, and Thiago Fonseca Morello Ramalho da Silva, approved in July 29, 2021.

URL of the original document:
<http://urlib.net/8JMKD3MGP3W34T/455DTUL>

INPE
São José dos Campos
2021

**PUBLISHED BY:**

Instituto Nacional de Pesquisas Espaciais - INPE
Coordenação de Ensino, Pesquisa e Extensão (COEPE)
Divisão de Biblioteca (DIBIB)
CEP 12.227-010
São José dos Campos - SP - Brasil
Tel.:(012) 3208-6923/7348
E-mail: pubtc@inpe.br

sid.inpe.br/mtc-m21d/2021/07.22.11.18-TDI

# ASSESSMENT OF THE IMPACT CAUSED BY FIRES IN THE BRAZILIAN LEGAL AMAZON FROM 2001 TO 2020

Wesley Augusto Campanharo

Doctorate Thesis of the Graduate Course in Remote Sensing, guided by Drs. Liana Oighenstein Anderson, and Thiago Fonseca Morello Ramalho da Silva, approved in July 29, 2021.

URL of the original document:
<http://urlib.net/8JMKD3MGP3W34T/455DTUL>

INPE
São José dos Campos
2021

Cataloging in Publication Data

Campanharo, Wesley Augusto.

C151a Assessment of the impact caused by fires in the Brazilian Legal Amazon from 2001 to 2020 / Wesley Augusto Campanharo. – São José dos Campos : INPE, 2021.

xx + 156 p. ; (sid.inpe.br/mtc-m21d/2021/07.22.11.18-TDI)

Thesis (Doctorate in Remote Sensing) – Instituto Nacional de Pesquisas Espaciais, São José dos Campos, 2021.

Guiding : Drs. Liana Oighenstein Anderson, and Thiago Fonseca Morello Ramalho da Silva.

1. Wildfire. 2. Amazon. 3. Econometrics. 4. Environmental valuating. 5. Geoprocessing. I.Title.

CDU 630*43:528.8(811)

MINISTÉRIO DA CIÊNCIA, TECNOLOGIA E INOVAÇÕES

**INSTITUTO NACIONAL DE PESQUISAS ESPACIAIS**

Serviço de Pós-Graduação - SEPGR

## DEFESA FINAL DE TESE DE WESLEY AUGUSTO CAMPANHARO
## BANCA Nº 197/2021 REG 142409/2017

No dia 29 de julho de 2021, as 10h00min, por teleconferência, o(a) aluno(a) mencionado(a) acima defendeu seu trabalho final (apresentação oral seguida de arguição) perante uma Banca Examinadora, cujos membros estão listados abaixo. O(A) aluno(a) foi APROVADO(A) pela Banca Examinadora, por unanimidade, em cumprimento ao requisito exigido para obtenção do Título de Doutor em Sensoriamento Remoto. O trabalho precisa da incorporação das correções sugeridas pela Banca Examinadora e revisão final pelo(s) orientador(es).

**Título: "ASSESSMENT OF THE IMPACT CAUSED BY FIRES IN THE BRAZILIAN LEGAL AMAZON FROM 2001 TO 2020"**

**Membros da banca:**

Dr. Luiz Eduardo Oliveira e Cruz de Aragão - Presidente - INPE
Dra. Liana Oighenstein Anderson - Orientadora - CEMADEN
Dr. Thiago Fonseca Morello Ramalho da Silva - Orientador - UFABC
Dra. Ane Alencar - Membro Externo - IPAM
Dr. Irving Foster Brown - Membro Externo - UFAC

Documento assinado eletronicamente por **Thiago fonseca morello ramalho da silva (E)**, **Usuário Externo**, em 03/08/2021, às 21:23 (horário oficial de Brasília), com fundamento no § 3º do art. 4º do Decreto nº 10.543, de 13 de novembro de 2020.

Documento assinado eletronicamente por **Luiz Eduardo Oliveira E Cruz de Aragão**, **Chefe da Divisão de Observação da Terra e Geoinformática**, em 05/08/2021, às 08:37 (horário oficial de Brasília), com fundamento no § 3º do art. 4º do Decreto nº 10.543, de 13 de novembro de 2020.

Documento assinado eletronicamente por **Liana Oighenstein Anderson**, **Pesquisador**, em 16/08/2021, às 14:42 (horário oficial de Brasília), com fundamento no § 3º do art. 4º do Decreto nº 10.543, de 13 de novembro de 2020.

Documento assinado eletronicamente por **IRVING FOSTER BROWN (E)**, **Usuário Externo**, em 26/08/2021, às 10:20 (horário oficial de Brasília), com fundamento no § 3º do art. 4º do Decreto nº 10.543, de 13 de novembro de 2020.

Documento assinado eletronicamente por **Ane Auxiliadora Costa Alencar (E)**, **Usuário Externo**, em 27/08/2021, às 15:14 (horário oficial de Brasília), com fundamento no § 3º do art. 4º do Decreto nº 10.543, de 13 de novembro de 2020.

A autenticidade deste documento pode ser conferida no site http://sei.mctic.gov.br/verifica.html, informando o código verificador **7930029** e o código CRC **5E4F7F3E**.

DON’T PANIC !

[Douglas Adams]

## ACKNOWLEDGEMENTS

It has been a long time since this journey began, and it was not easy at all. However, like a rollercoaster, it has its ups and downs, but for a good adventurer this will always be exciting. The scientific side of my life started with the endless curiosity to understand and see how things work and what happens if we change them. However, the desire to get a doctorate degree appeared in the middle of the journey, when I began teaching and instructing how to use SIG programs and how to delimit watersheds.

I am very grateful for all things that already happened to me, and I need to be ready for things that will come. In this doctorate's period, it was not different. I am very thankful for Dr. Liana O. Anderson to have chosen me among other dreamers to guide in this new path, including a brand-new area, the wildfire study. Also, I am grateful to be introduced to Dr. Thiago Morello, who helped me to understand the Econometrics language of Economists and how they behave. Jokes apart, those moments of listening and learning provided by both of them were very important to my personal and professional growth.

In this Doctorate, it is impossible to forget the “sandwiched” period in Italy, where I lived one year under the JRC bubble. It was a world of technology and possibilities inside a small old town, called Ispra. I am very thankful to have met Dr. Jesus San-Miguel and his colleagues, Rosana, Duarte, Tomas, Daniele, David, Alfredo, Pieralberto, Roberto, Hans and Tracy, who helped me in the fire fields research and to survive in Italy.

Besides that, the COVID experience in JRC allowed me to meet Dr. Maria Christofoletti, who showed me the Instrumental Variable method, which solved a big issue that I faced during this thesis. Every burned cake and melted ice-cream were worthy thanks to the thoughts and discussions that followed them.

As said by Emicida, "who has friends, has everything", so I am very lucky to have found such incredible people in this process. I am grateful for Debora, Juliana, Carol, and Jessica, who started a simple and random class work and stayed together during all the journey.

To the Trees lab, for the friendship that was possible to have and the people to interact ("gringos" and native ones). Especially to Celso, Igor José, Thais and Igor Broggio (Former "Sala 02") for all edifying thoughts. Also to Aline, who is a very good friend and an incredible paper partner.

To my fellow roommates, Philip, Andeise, and Victor, for being respectful during a very stressful doctorate life.

And to Diego, that was patient and persistent during this long doctorate process that we both faced almost at the same time, which was many times aggravated by the distance imposed.

I am thankful for all grants received along these years in the doctorate, including the CAPES, CNPq and my mother. Especially the last one, who did not understand very well what I was always looking at on the computer (known as programming process), but never stopped believing in my potential or asking for a full report.

Lastly, but still important, thanks for all those people that directly or indirectly contributed to this Thesis either physically or by helping me to maintain my mental health.

My sincere thanks | Muito Obrigado | Grazie mille

## ABSTRACT

Humans were only able to evolve thanks to the use and the control of fire learned some million years ago. However, with great power comes great responsibility, and for now it seems that the fire is uncontrolled or not well managed. The damages documented so far can be sensed directly (human life loss, burning production, damaging infrastructure, reducing biodiversity, affecting cultural resources) or indirectly (changing the climate, increasing hospitalizations, reducing tourism, promoting species migration, and affecting transport of people and goods), both occurring at any kind of scale (locally, regionally, globally). The Amazon region is the primary source of biodiversity in the Neotropics, being the genetic pool to other places and also providing important ecosystem services. The Brazilian Legal Amazon (BLA), is a geopolitical region, that is responsible for 8.5% of the Gross Domestic Product (GDP), besides being home for more than 24 million inhabitants, including indigenous and traditional communities. Only in the past 20 years, severe droughts with major associated wildfires were reported in the region. This phenomenon brings several consequences, and most of them are still uncountable or not well characterized. This thesis, hence, aims to quantify the impact of fire in the BLA in recent years (from 2001 to 2020), accessing the damage either by a monetary aspect or by a tangible form, categorizing it in a disaster context (environmental, material, and human damages). The thesis was based on three main chapters, the first one is a case study, the second is a methodological update, and the third one shows the total damage accounted for the last 20 years. The case study focused on Acre state aimed to establish a methodological basis to allow the up scaling the results to the entire BLA region. In the local scale, the use of fire was closely linked to the agricultural sector, especially connected to large proprieties as a tool for deforestation and pasture management. The total damages between 2008 and 2012 in Acre caused by fire represents 0.51%±0.10 of the state's GDP in normal climatic years, reaching up to 7.03% ±2.45 in drought years (2010). In this case study, the estimate of the relation between hospitalization and fires was not entirely elucidated. The second chapter, which covers the whole Amazon, therefore, was delineated to use an Instrumental Variable (IV) approach to determine how respiratory hospitalizations are associated with air pollution induced by fires, using a large data set. The results revealed a positive effect of fire-pollution on the hospitalization due to respiratory diseases in general and, specifically, due to Asthma, which the model predicts that approximately 4,000 people are yearly affected. The results indicate that the estimates could have been further improved by using other pollutant indicators, neighborhood effects, time lag or even downscaling the series. Finally, the last chapter analyzes the main pattern of the fire and its impacts over the BLA through the last 20 years. The results exposed that approximately 17% of the BLA region already suffered with fire at least once, mostly in small patches ($\leq$ 40 ha). Nevertheless, this pattern changes over the years, with an increase of: (1) the minimum area per month, (2) the occurrence of anomalous months, and (3) the total burned area of the first months of the year. Over these 20 years, the equivalent damage caused by the use of fire is around 6.28%±1.1p.p per year considering the BLA's GDP. Therefore, this thesis provided a methodological structure and information to understand the extent, the magnitude and the damage caused by fire in the BLA, contributing to assist managers in the construction of public policies and clarifying the side effects of fire over the time.



Keywords: Wildfire. Amazon. Econometrics. Environmental valuating. Geoprocessing.

# AVALIAÇÃO DOS IMPACTOS CAUSADOS POR INCÊNDIOS NA AMAZÔNIA LEGAL BRASILEIRA ENTRE 2001 E 2020

## RESUMO

A espécie humana só foi capaz de evoluir graças ao uso e ao controle do fogo aprendidos há milhões de anos atrás. Porém, com grande poder vem grande responsabilidade, e por enquanto parece que o fogo está descontrolado ou mal administrado. Os danos documentados até agora podem ser relacionados diretamente (perda de vidas, queimando produções agrícolas, danificando infraestrutura, reduzindo a biodiversidade, impactando recursos culturais) ou indiretamente (mudando o clima, aumentando as hospitalizações, reduzindo o turismo, promovendo a migração de espécies e afetando o transporte de pessoas e bens), ambos ocorrendo em qualquer escala (local, regional, global). A região amazônica é a principal fonte de diversidade na região Neotropical, fornecendo várias linhagens para outras localidades, gerando importantes serviços ecossistêmicos. A Amazônia Legal Brasileira (AMZL), por sua vez, é uma região político administrativa responsável por 8,5% do Produto Interno Bruto (PIB), além de abrigar mais de 24 milhões de habitantes, entre comunidades indígenas e tradicionais. Somente nos últimos 20 anos, secas severas desencadearam grandes incêndios florestais na região. Esse fenômeno traz várias consequências, e a maioria delas ainda são desconhecidas ou mal caracterizadas. Desta maneira esta Tese visa quantificar o impacto do uso do fogo na AMZL nos últimos anos (2001 a 2020), tanto pelo aspecto monetário como também pela forma tangível, categorizando-o sob o contexto de desastre (separando em classes de danos ambientais, materiais e humanos). Para tanto, a tese está fundamentada em três capítulos principais, o primeiro é um estudo de caso, o segundo é uma atualização metodológica e o terceiro mostra os danos totais contabilizados nos últimos 20 anos. O estudo de caso focado no estado do Acre teve como objetivo estabelecer uma base metodológica capaz de ser extrapolada para toda a região da AMZL. Sob esta escala local, o uso do fogo está intimamente ligado ao setor agrícola, principalmente como ferramenta de desmatamento e manejo de pastagens em grandes propriedades. O total de danos causados pelo fogo entre 2008 e 2012 no Acre representa 0,51% ± 0,10 do PIB do estado em anos climáticos normais, chegando a 7,03% ± 2,45 em anos de seca (2010). Porém, neste estudo de caso, a estimativa da relação entre as taxas de hospitalizações e área queimada apresentou-se complexa e não totalmente válida. Assim, o capítulo dois foi delineado para se utilizar uma abordagem econométrica por meio de Variável Instrumental (IV) para determinar as hospitalizações respiratórias associadas à poluição derivadas do uso do fogo na região da AMZL, usando um grande conjunto de dados. Os resultados revelaram um efeito positivo do fogo no total de hospitalizações por doenças respiratórias e também por Asma, prevendo que cerca de 4.000 pessoas sejam afetadas anualmente. Os resultados indicam que as estimativas podem ser melhoradas utilizando outros indicadores de poluentes, efeitos de vizinhança, defasagem de tempo ou mesmo reduzindo a escala da série. Por fim, o último capítulo analisa, o padrão característico do fogo e seus impactos sobre a AMZL ao longo dos últimos 20 anos. Os resultados evidenciaram que cerca de 17% da região já sofreu com incêndios pelo menos uma vez, sendo pequenas manchas (≤ 40 ha) as mais recorrentes. No entanto, esse padrão muda ao longo dos anos, com o aumento:

(1) da área mínima mensal, (2) da ocorrência de meses anômalos e (3) da área total queimada dos primeiros meses do ano. Nestes últimos 20 anos, o dano equivalente causado pelo uso do fogo é de 6.28%±1.1p.p ao ano, considerando o PIB da AMZL. Desta maneira, esta Tese forneceu uma estrutura metodológica e informações para se entender a extensão, a magnitude e os danos causados pelo fogo na AMZL, contribuindo para auxiliar os gestores na construção de políticas públicas e esclarecendo os efeitos colaterais do fogo ao longo do tempo.

Palavras-chave: Incêndios. Amazônia. Econometria. Valoração ambiental. Geoprocessamento.

## LIST OF FIGURES

**Page**

## LIST OF TABLE

**Page**

**CONTENTS**

**Page**

# 1 INTRODUCTION

This millennium is known as the *Pyrocene*, because humanity is altering the global fire regime (PYNE, 2020; VAUGHAN, 2019). Just during the last years, strong fire events occurred globally, such as those in Portugal in 2017, (TURCO et al., 2019), Greece in 2018 (LAGOUVARDOS et al., 2019), California in 2018 (CAL FIRE, 2021), in the Amazon during 2015/2016 and 2018/2019 (ARAGÃO et al., 2018; BRANDO et al., 2020), in Australia in 2019/20 (HUGHES et al., 2020), and among others places.

This scenario is alarming since weather is becoming more favourable to uncontrolled fires across time, a change that will be exacerbated in the near future according to the available forecasts (IPCC, 2021a). This is true especially in the Brazilian Amazon, where the frequency and intensity of drier conditions are expected (LI; FU; DICKINSON, 2006; AVILA-DIAZ et al., 2020), including the expansion of ecological drought, aridity and fire weather conditions that will affect negatively a wide range of sectors (IPCC, 2021b). In this sense, fire in the Amazon region, which is mainly human driven (ALENCAR; RODRIGUES; CASTRO, 2020; BARLOW et al., 2020), will have a significant transformation potential over the years, either by the economic or by the social impact.

Whereas agricultural fires generate benefits accruing to those that use them, the cost extend to whole society, including loss of human lives (AHRENS; EVARTS, 2020); destruction of productive inputs and outputs (DE MENDONÇA et al., 2004), damage to infrastructure (DIAZ, 2012), reduction of biodiversity (BARLOW et al., 2003; NOLASCO, 2006; BRANDO et al., 2014; PAOLUCCI et al., 2017; SILVA et al., 2018a), impact on cultural heritage (RYAN et al., 2012) and tourism (BOUSTRAS; BOUKAS, 2013), and a massive release of polution into the atmosphere with health and climate change consequences (ANDREAE et al., 2004; ANDERSON et al., 2011; GONÇALVES; MACHADO; KIRSTETTER, 2015; DERYUGINA et al., 2019; ROCHA; SANT'ANNA, 2020).

Policy and strategic planning are needed to reduce the fire risk and its impacts. However, it is critical to determine and unfold the components associated with specific socio environmental damages caused by fires. Quantification of fires' impacts, by informing policymaking, would contribute to establish a legal basis for managing natural resources,

to the assessment of damage by a wide range of stakeholders, to the development of mechanisms for environmental compensation (MENDELSOHN; OLMSTEAD, 2009) and to the design of prevention and suppression initiatives (CARMENTA et al., 2013; MORELLO et al., 2017a, 2017b; TASKER; ARIMA, 2016, MOTTA et al., 2002). These achievements would also pave the way to the compliance with international agreements such as the Sendai Framework[1] and the Paris Agreement for climate change mitigation and adaptation[2].

## 1.1 Motivation and objectives

Due to the lack of historical information about the social, economic and environmental impact caused by fire across the Brazilian Legal Amazon (BLA), the main objective of this thesis was to establish a methodology capable of quantifying a set of economic, social and environmental impacts caused by fire, and then implement it using the remote sensing product of burned area. With that the thesis answers two main questions (1) what was the magnitude of fire-related losses for the BLA in the last 20 years? and, (2) is this loss significant compared to the total value of goods and services produced, as captured by the gross domestic product in the BLA ?".

In this way, the quantification of fire impacts conducted in this thesis was supported by three questions detailed below, divided by Chapter. Each Chapter was grounded on specificities of the fire phenomenon as it occurs in the Amazon.

In Chapter 3 it is explored and developed a method for estimating the fires' economic losses for Acre state, as a pilot Study. The motivation regarding this chapter relies on the fact that Acre, even being among the Amazon states with lower deforestation rate, has registered a growing frequency of fires, especially in extreme drought years. It remains unclear whether the impacts during regular years are substantial enough, compared to extreme drought years, to justify policy action or if policy should prioritize strictly

[1] Sendai Framework is a successor instrument to the Hyogo Framework for Action, whose objective is to substantially reduce the risk of disasters, loss of life, livelihoods, and health, as well as economic, physical, social, cultural and environmental assets of people, companies, communities and countries (UNDRR, 2015).

[2] 21st Conference of the Parties (COP21) established during the Paris Agreement in 2015 which aims to enhance the global response to the threats of climate change, whose objective is to increase adaptive capacity, strengthen resilience and reduce vulnerability to climate change, with a view to contribute to sustainable development (UNFCCC, 2015).

preparedness for extremely drought years. Therefore, the following question was proposed:

Q1: Is, in the context of Acre state, the impact of fires in terms of greenhouse gases (GHG) emissions, agricultural production losses and health larger in extreme drought years?

- H1.0: no, even with fires being more frequent in extreme drought years, the difference in terms of impact is negligible. This is probably due to the fact that the land use processes that drive fires and are not directly affected by extreme meteorological conditions remain the dominant source of impact.
- H1.1: yes, impacts are larger by orders of magnitude in extreme drought years, so that the contribution of extreme meteorological conditions stands out even after considering land use processes not directly affected by such conditions.

The second research object, covered in the Chapter 4, is the effect on the health of regional inhabitants due to the pollution released by biomass burning. The motivation is based on the knowledge that fire is widely used in the Amazon constituting a persistent land cover change and agricultural practice used for all types of landowners and population. Regardless of its purpose, fires release a large amount of pollutants in the atmosphere, with severe consequences for human health. With that in mind, a question (Q2) was proposed.

Q.2: Is the hospitalization induced by fire-pollution detectable, with the available data, over different ages and correlated diseases across the entire Brazilian Legal Amazon?

- H2.0: no, other causes of hospitalization , such as the decrease in temperature and increase in humidity in the wet season, as well as other non-seasonal factors (such as healthcare supply), have a contribution which masks the fire-affected population data. This way, fire's contribution does not stand out from data analysis.
- H2.1: yes, fire emission plays an important role in the region's hospitalization counts, even after accounting for season and non-seasonal factors. The emission load released by biomass burning leads to an increase in hospitalization, especially during the fire season.

Finally, the third perspective of this research related to the phenomenon is that controlled fires may turn into accidental fire spreads, which affects agricultural production, infrastructure, and it also contributes to global climate change due to the emission of greenhouse gases (GHG). This is explored in Chapter 5. The premise adopted is that the BLA suffers from uncontrolled fires every year, with emphasis on drought-and non-drought-related events that are becoming more frequent. The lack of an estimation of the magnitude of losses, in ecological and monetary terms is a knowledge gap. Filling this gap is crucial to support and design policy to mitigate and prevent such events. This is the background of the third question (Q3).

Q.3: Are the negative impacts caused by fire in BLA over the last 20 years sufficiently large to demand attention in national and international policy?

- H3.0: no, the damage is negligible even accounting for the impacts on climate, agriculture and health.
- H3.1: yes, the damage is considerable both whether totalized or whether its environmental, economic and health dimensions are assessed isolated.

## 1.2 Thesis outline

This document is organized in a paper-format, which aggregates one paper that has already been published and two in the process of being finalized. In the following sections it will be described: Chapter 2 is a literature review of fire impacts in a context of disaster management, separating the affected components between Environmental, Material and Human damage, and also establishing how each component connects and influences one another; Chapter 3 presents a case study about Acre state, using a few components to determine the damages of fire in normal climatic years and anomalous ones; Chapter 4 introduces an econometric approach to quantify the hospitalizations due to fire-smoke pollution in the BLA region; Chapter 5 presents a monetary quantification caused by fire between 2001 and 2020 in the BLA; Finally, Chapter 6 aggregate the general discussion from the analysis used between the local approach and the regional estimates.

Chapter 2 presents the main concepts used in Brazil about fire, regarding its classification and types. In addition to summarize the main damages caused by fire under an disaster perspective, where those damages were categorized into three class (environmental,

material and human nature damage). With all this discretized, a fire impact chain was produced, showing how each component connects and influences on another, classifying them by category, extension (local, regional or global) and degree of impact (direct and indirect).

The case study of Acre state between 2008 and 2012, aimed for stablishing a methodological baseline, which adequate to be extrapolated to the entire BLA region. This chapter brings the quantification of impacts in normal climatic years and in years of extreme drought in the state, accounting for the environmental losses represented by the loss of biomass and the consequent emissions of carbon dioxide ($CO_2$) into the atmosphere; the social impacts, evaluating hospitalizations due to respiratory diseases during this period; and material impacts, related to the burning of property fence and loss of agricultural production.

Such chapter included a first simplified attempt to quantity health impacts based on the correlation coefficient which is not suitable to measure the causal effect of fires on health and to reveal the precision (or volatility) with which such effect may be estimated (what would be informative regarding the inherent degree of uncertainty). With that in mind, an improved assessment of the health impact was carried out in Chapter 4. The econometric method of Instrumental Variables was used to measure the causal effect of fire-induced pollution on respiratory hospitalizations, thus obtaining more reliable measures given the many tests of methodological consistency and robustness required by the technique.

Finally, in Chapter 5, building on Chapters 3 and 4 in terms of the performance of the quantification techniques applied, an integrated analysis was performed for the entire BLA from 2001 to 2020, quantifying and valuing the total damage generated by fires from three sources, namely, production losses, $CO_2$ emissions and hospitalizations.

## 2 LITERATURE REVIEW

The impact of the fire in a region is complex because each damaged feature is part of a entangled chain of interconnected cycles, and the consequences can be propagated in different scales and components (RYAN et al., 2012; NELSON et al., 2013). However it can be clarified if the fire were considered as a disasters, because it can be categorized in three major groups (Human, Material and Environmental), as proposed by the Disaster Risk Management Classification (DE CASTRO, 2007).

Based on the most common impacts driven by wildfire, a theoretical fire chain impact (Figure 2-1) was propose, which each point will be discussed in the following sections.

Figure 2-1. Schematics of Fire impacts in an ecosystem with details of different scales and effect.

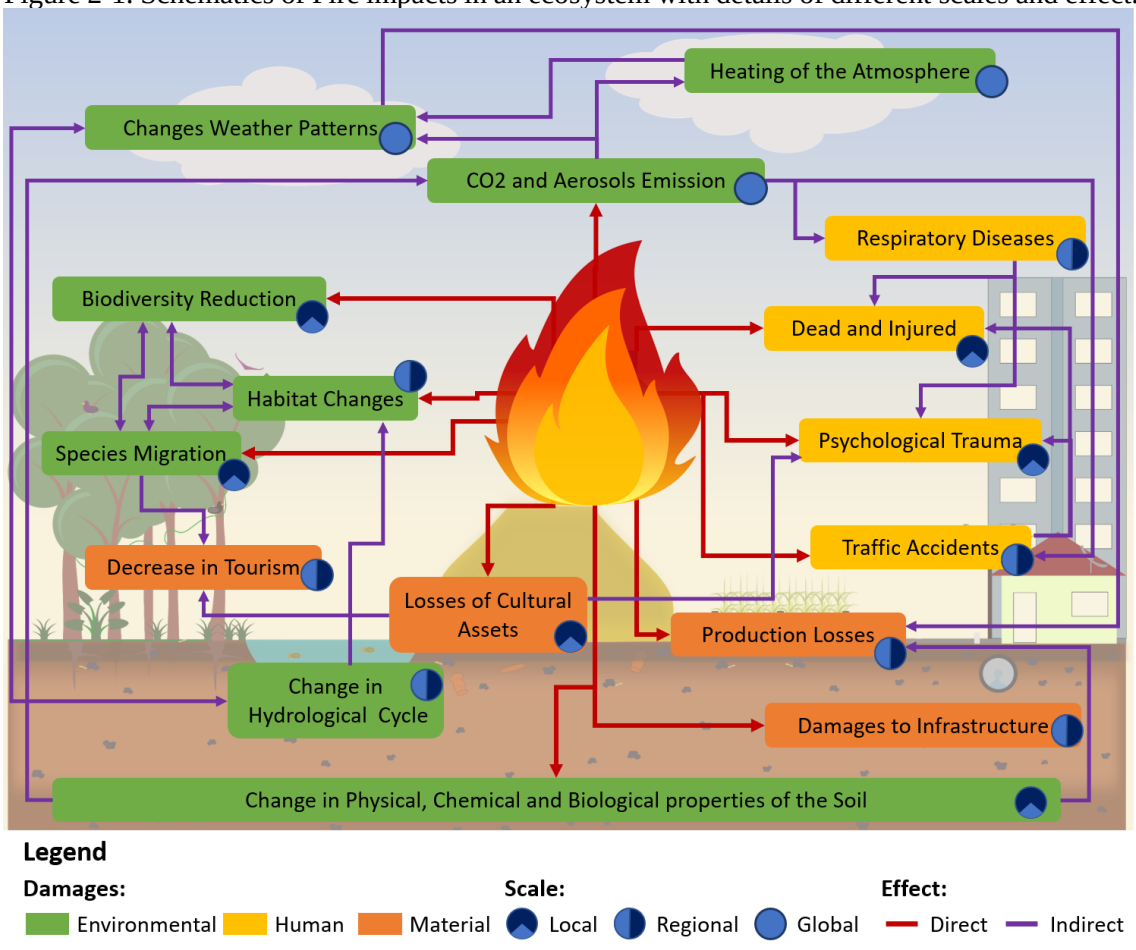


Note: Human damages – are those related to the people affected by the disasters Material damages – are those associated to goods, proprieties, and facilities. Environmental damages – are those related to the contamination or degradation of the water, soil, air, and biodiversity. Direct effect – is the one caused by the fire itseld or by the contact with ashes and smoke.Indirect effect – is second-order effect, caused by the direct effect.
Source: From author.

## 2.1 Human damages

Forest fires cause serious environmental disasters, they kill and injure people, destroy private and public goods, towns and villages. According to FAO's report (NOLASCO, 2006), during the 1990s, fires in South America caused 742 deaths and 429 people were injured, including volunteers, firefighters and civilians. The National Fire Protection Association (NFPA) (AHRENS; EVARTS, 2020) reports that, for all incidents involving fire in 2019 in The United States of America, the number of people affected was approximately 20.000 across the country, in which 18% died. However, the Federal Emergency Management Agency (FEMA) (FEMA, 2016), indicates that the trend of injured and death rates is in opposite directions, generally because the age groups is a very relevant factor. The agency believes that due to the debilitated cognition and mobility of elderly people, they were less likely to escape from the effects of the fire and therefore suffered fatal injuries.

It is important to point out that during the process of burning, there is a large amount of ashes, smokes and gases being released. These can cause traffic and air accidents, due to the lack of visibility (ANDERSON et al., 2011; NEPSTAD; MOREIRA; ALENCAR, 1999), and hospitalizations owing to the bad air quality (DE MENDONÇA et al., 2004; DERYUGINA et al., 2019; ROCHA; SANT'ANNA, 2020; SHELDON; SANKARAN, 2017; WANG et al., 2020). Health impacts of smoke are determined by: chemical composition and concentrations of pollutants in the smoke; the intensity and duration of exposure to smoke during an event; the protection of individuals from exposure; and the number of individuals exposed (WILLIAMSON et al., 2016). A study carried out by Da Motta et al (2002) found out that in the period from 1996 to 1999, the relation between the total number of respiratory morbidity associated with the smoke by the burning biomass in the Brazilian Amazon varied from 3% to 8%. This percentage depends on the age group, because children and elderly people are more vulnerable and more impacted (ARAGÃO et al., 2016; SMITH et al., 2014). The smoke also has a cross boundary impact in respiratory hospitalization, affecting from regional (WANG et al., 2020) to international scale (SHELDON; SANKARAN, 2017; REDDINGTON et al., 2015). Psychological problems such as posttraumatic stress disorder, depression and adverse physical side effects can also appear in both affected communities (victims, families),

firefighters and associated staff (e.g. police, rescue team) (CAAMANO-ISORNA et al., 2011; LAUGHARNE; VAN DE WATT; JANCA, 2011).

## 2.2 Material damages

In relation to quantifying wildfire impacts, Diaz (2012) indicates that the most common damages in a community infrastructure are the ones in highways, communication facilities, power lines, and in water delivery systems. Following a report made by the National Agency of Electric Energy (ANEEL), between 2013 and March 2017, more than 14.000 forced energy shutdowns in Brazil were recorded. Of those cases, around 9% was related to uncontrolled fires, representing the fifth main factor of interruption in the system (ANEEL, 2018).

The material impacts of fire, however, go beyond direct and local damages. Economic goods should be also taken into account, for example: services; consumer goods (cars, houses, food); and capital goods (equipment, buildings, installations). De Mendonça et al. (2004) considered the impact of fire for farmers in the Amazon region, registering damages in the production, losses in the pasture and plantations, house destructions, damages in fences and equipment. Boustras and Boulas (2013), additionally, determined the impact of fires on tourism activities in Greece and Cyprus. The authors explain that the impact is multidimensional, going from damages in tourist facilities, signposts, trails, viewpoints and even changes in the tourists' behaviors and in the attractiveness of the landscape. Nonetheless, cultural resources can also be affected by the fire. Those resources are defined by Ryan (2012) as material and non-material items that represent the physical, spiritual presence and practices of society, connecting people with their traditions, histories and their ancestors. The author explains that those resources are often tangible and fragile objects, but they can also be resources that incorporate all elements of the environment that support culture, such as the living organisms (plants, animals) and the physical characteristics of the region (mountains, hills, plains, rivers) which are susceptible to fires.

### 2.2.1 Environmental damages

Within the environmental damages, the impacts related to the atmosphere, biodiversity, soil, and water are detailed in what follows.

#### 2.2.1.1 Atmosphere

Fires have a great effect on the emission of greenhouse gases and aerosols. Nolasco (2006) shows that in the last decades, the smoke released by forest fires had affected whole urban areas and have caused serious problems to the health and the air traffic. Reductions of scenic beauty and in the market value of real estate can also be consequences of the smoke. For example, in August 2019, the city of São Paulo had a moment that the day became night due to the smoke and ashes from Amazon fires (SETZER, 2019).

The composition of a wildfire smoke depends on the fuel type, the temperature of the fire, and the weather conditions (URBANSKI; HAO; BAKER, 2008). However, the smoke is usually composed by primary pollutants, such particulate matter (PM), carbon monoxide (CO), nitrogen oxides ($NO_x$), and non-methane organic compounds (NMOC), which some of it react to form secondary pollutants (REISEN et al., 2015).

Da Rocha and Yamasoe (2013), who worked with the aerosol optical depth (AOD) and its correlation with fires in the Amazon, presented that during the fire season, the AOD levels can rise up to 280% in sites with fire, but the effects were also perceived in more distant places. The increase of aerosol levels in the atmosphere, which impacts the human health (showed in the Section 2.1), the smoke and its components affect the weather, for reducing the size of cloud drops; delaying the onset of precipitation; strengthening upward currents, causing intense storms until hail; releasing latent heat in the upper layers of the atmosphere, affecting regional and global circulation systems; and changing the water cycle (ANDREAE et al., 2004; GONÇALVES; MACHADO; KIRSTETTER, 2015).

Fires are also directly associated to greenhouse gas emissions (GATTI et al., 2021). Between 2015 to 2012, the average of $CO_2$ emissions estimated by (SEEG, 2018) for Brazil, considering all sectors, was 1.352 Tg. Fires associated with deforestation contributed with an annual average of $454 \pm 496$ Tg of $CO_2$ per year in the Amazon (ARAGÃO et al., 2018), and these values can be bigger than the emission of deforestation in drought years.

#### 2.2.1.2 Biodiversity

When the fire reaches vegetation formations, in addition to consuming the organic material deposited in the soil, it eliminates plants and animals and decreases the local biodiversity. Large or resistant trees that had been damaged are generally able to resist for years, or they die later not necessarily because of the fire, but probably because of the attack of pathogens. The determinant of the mortality will be the consequence of the heat of the organs (leaf, stem and root), which will affect the physiology and other characteristics that change the resilience of the organism, and also by the injuries caused by the fire, opening a space to a pathogens attack (LIESENFELD; VIEIRA; MIRANDA, 2016).

Brando et al. (2014) shows that the tree mortality in the Amazon forest can increase to 226% due to the fire damages, and that number reaches 462% during drier years. It was also registered a cascade effect in deaths of trees, causing a decrease in the canopy cover (23% to 31%), in the above-ground biomass (12% to 30%), and increasing the invasion of grass (80%) over the edge of the forest fragment, where fires are more intense and common. In a long-term, it has been suggested that 36% of the trees will die in the following year and around 48% in the next three years (BARLOW et al., 2003), and this process can continue for up to 8 years after the fire (SILVA et al., 2018a).

Negative effects in large groups of animals, such as birds, mammals and reptiles, have been reported as well. Even though such groups and many mobile animals are able to escape from the flames, the surviving animals may not be able to withstand these frequent fires due to the reduced availability of resources and habitats (NOLASCO, 2006). Paolucci et al. (2017) claims that some groups of animals change because of the degradation of the forest and the consequent changes in the phytophysiognomy.

#### 2.2.1.3 Soil

Related to the soil damages, Santín and Doerr (2016) summarized the impacts in each soil component, indicating the possible forms of burning and its range (Figure 2-2).

Figure 2-2. Different effects of burnings over the chemical, physical and biological soil proprieties.

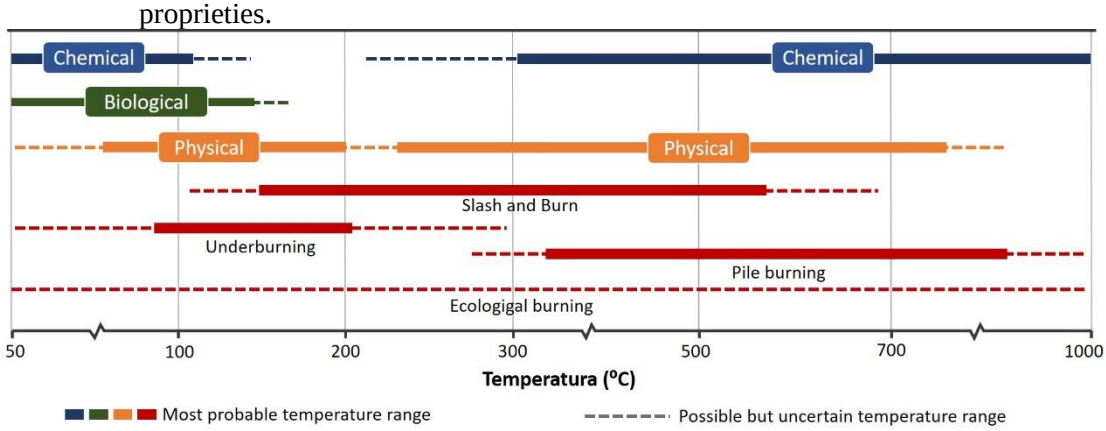


Source: Adapted from Santín and Doerr (2016).

The authors found that biological properties, in general, are affected at temperatures below 200°C, in which there is a reduction of microbiotic biomass and a destruction of the seed bank and fine roots. The first group of chemical properties of the soil to be affected is the stored water, which is evaporated. The second group occurs at temperatures above 300°C, related to the combustion of organic matter in the soil, the production of pyrogenic organic matter, the increase in the soil pH, and in the transformation of minerals (Calcium and Iron).

Regarding the physical properties of the soil, in the first moment (temperatures below 200°C) there is an increase in aggregation and water repellency. However, with the increase in temperature, there is a breakdown of clods and repellency, in addition to the collapse and melting of clays. The authors also address that some of the most significant impacts on the soil are indirect and happen gradually during and after the fire, such as an increased runoff, erosion, distribution, and incorporation of ashes into the soil. However, not all impacts are negative, some consequences may have benefits in boosting the soil fertility, organic carbon content, weathering and assisting the formation of organic soils.

#### 2.2.1.4 Water

According to Neary et al. (2005) the main impacts in the water quality are: the introduction of sediments, the potential increase in nitrates, the possible introduction of heavy metals from soils and nearby geological sources.

The introduction of fire-retardant chemicals in streams can reach toxic levels for aquatic organisms, causing an increase in the pH because of the ashes and also an increase in the water temperature, which may also enhance the biological activity. Nonetheless, the fire impacts can indirectly influence water bodies by changing hydrological cycles (see Section 2.2.1.1) that will also change the flow regimes; affecting riparian environments; changing the biodiversity (see Section 2.2.1.2) with consequent changes in the physical properties of the basin (e.g. evapotranspiration, infiltration, surface runoff) that affect the flow regime, and altering the quality of the water, either by the changes in the flow regime and the riparian vegetation or by the deposition of ashes and particulate.

The magnitude of these effects depends on the fire characteristic (size, intensity, and severity), the watershed (topography, land conditions, hydrography), and the weather conditions (precipitation, temperature).

# 3 ECONOMIC LOSSES CAUSED BY FIRES FROM 2008 TO 2012 IN ACRE STATE, BRAZILIAN AMAZON[3]

## 3.1 Introduction

Fire-dependent ecosystems, such as the Brazilian Cerrado and the African Savannah, evolved in the presence of periodic or episodic fires and depend on them for maintaining their ecological processes (PIVELLO, 2011). However, in the Amazon, natural fires are rare in the absence of humans and fire's presence can be an indicator of human activity (BUSH et al., 2004, 2007). The use of fires in this region is a usual agricultural practice for farmers, for both clearing new areas and preparing productive lands (DA MOTTA et al., 2002; DE MENDONÇA et al., 2004), to increase the soil fertility and the amount of organic carbon in a short period (DE SOUZA BRAZ; FERNANDES; ALLEONI, 2013; SANTÍN; DOERR, 2016), and to prevent massive fires by reducing fire fuels (FALLEIRO; SANTANA; BERNI, 2016). Additionally, fire is part of the culture of many indigenous and traditional communities, and is used for hunting and religious rituals as well (POSEY, 1985; MISTRY; BILBAO; BERARDI, 2016).

Over the past 20 years, severe droughts were reported in the Amazon (BRANDO et al., 2014; MARENGO; ESPINOZA, 2016) and major wildfires were associated with them (ARAGÃO et al., 2007; LIMA et al., 2012; ANDERSON et al., 2015; ARAGÃO et al., 2018). Usually, the severe droughts are caused by one or a combination of climatic phenomenon, such as the El Niño-Southern Oscillation (ENSO), the Atlantic Multidecadal Oscillation (AMO), and warming of the Tropical North Atlantic (TNA), where the environmental conditions, characterized by high temperatures and low air humidity, are more suitable for the rapid spread of fires (BRANDO et al., 2014; MARENGO; ESPINOZA, 2016).

Moreover, many studies suggest an increase in drought frequencies in the Amazon (LI; FU; DICKINSON, 2006; AVILA-DIAZ et al., 2020) with a collateral increase of fires in forests adjacent to anthropic areas (SILVA JUNIOR et al., 2018). As a consequence, burnings can escape and escalate into wildfires, causing several environmental and

[3] This chapter is a adapted version of the paper: CAMPANHARO, W.A.; LOPES, A.P.; ANDERSON, L.O.; SILVA, T.F.M.R.; ARAGAO, L.E.C.O. Translating Fire Impacts in Southwestern Amazonia into Economic Costs. **Remote Sensing**, v11, (2019).

socioeconomic losses (SILVA; LIMA, 2006; DA ROCHA; YAMASOE, 2013; BRANDO et al., 2014; NEPSTAD et al., 2014; SMITH et al., 2014; ARAGÃO et al., 2016). With that, this phenomena may have a greater environmental change potential than the drought event itself (ARAGÃO et al., 2007; LIMA et al., 2012; BRANDO et al., 2014).

The State of Acre, located in the southwestern flank of the Brazilian Amazon, has suffered from the high frequency of extreme climatic events since 2005 (LEWIS et al., 2011; MARENGO et al., 2011; MARENGO; ESPINOZA, 2016) and more recently in 2016 and 2017 (DOLMAN et al., 2018). In the first two decades of the 21st century, socioeconomic impacts, caused by such events, have been particularly critical in Acre, especially in relation to the direct and indirect impacts of wildfires (ARAGÃO et al., 2016; BROWN et al., 2006, 2011). Brown et al. (2006), for instance, estimated that during the 2005 drought, more than 400 thousand people were affected by fire-related air pollution and over 300 thousand hectares of forests burned, with direct losses surpassing US$ 50 million and approximately US$100 million in economic, social, and environmental losses.

As a consequence of the 2005 drought, Acre's authorities created a temporary Situation Room to effectively monitor forest fires and gather meteorological data for fire risk analysis, aiming to assist the placement of fire-fighting crews in the field (BROWN et al., 2011). In 2013, after many extreme events such as floods, droughts, and wildfires, the Situation Unit of Hydrometeorological Monitoring was permanently established under the Secretariat of the Environment of Acre, for following purposes: Monitoring critical hydrologic events, supporting prevention actions to cope with extreme events, gathering information about critical events, and managing platforms for collecting and integrating pluvial and fluviometric data (REIS et al., 2015).

Additionally, in the last decade, Acre State established environmental policies for reducing deforestation, designing mechanisms of payments for environmental services, and creating new governmental and non-governmental sectors to directly deal with solutions for mitigating disasters in the region. All these policies are aligned with the Sendai Framework, of which Brazil has been a signatory country since 2015. This framework includes measures to reduce direct economic losses due to disasters, as well

as the establishment of techniques for assessing losses associated with economic, social, environmental, and cultural heritage (UNDRR, 2015). Nevertheless, information on economic losses from disasters remains critically lacking for entities and governmental institutions, especially in countries under development. The United Nations Office for Disaster Risk Reduction - UNDRR (WALLEMACQ; HOUSE, 2018) showed that only 37% of all disasters cataloged between 1998 to 2017 had estimated economic losses, suggesting that the direct costs of the majority of disasters (63%) worldwide are unknown or not well documented.

Techniques for valuing disaster-related environmental and socioeconomic costs have a great and critical role in public policies. These techniques are essential for characterizing the magnitude of the problem and for supporting regional development models (DA MOTTA et al., 2002). Moreover, information on costs can facilitate the communication of the value of nature or any affected good to different people using a unique language that unites political and economic visions (KUMAR et al., 2013). Finally, this type of analysis can provide a legal basis for managing natural resources, assessing damage, and developing mechanisms for environmental compensation (MENDELSOHN; OLMSTEAD, 2009).

It is clear that quantitative information about the impact of wildfires on ecosystems and humans is mandatory for supporting the development of strategies and public policies for the prevention of disasters and related impact assessment. Therefore, in this study, our objective is to investigate the spatiotemporal pattern of fires, their attribution regarding fire occurrence and land tenure, and the environmental, social, and economic impacts of fire in Acre state. More specifically, this study aims to answer the following: (1) What are the spatiotemporal variabilities of fires during anomalously dry years and years with regular climatic conditions? (2) Who are the actors, in terms of land tenure, to which fire occurrence can be attributed to? and (3) What is the potential magnitude of the environmental, social, and economic impact caused by fires and their consequences for Acre's economy?

In this study, we go beyond the analysis of ecological impacts on natural resources to show that, during droughts, the increase in fire events, in comparison to normal climatological years, raises the annual estimated cost related to infrastructure damages,

production losses, $CO_2$ emissions, and respiratory morbidities around 15-fold. This estimate represents 7.03±2.45% of Acre's gross domestic product (GDP). The observed increment in costs was driven by the spatially extensive impact of fires on forests, which enhanced gross carbon emission from biomass burning and its associated costs to society.

## 3.2 Materials and methods

### 3.2.1 Study area

Acre state has an area of approximately 164,124 km$^2$ and is located in the southwest flank of the Brazilian Amazon, with borders with Peru and Bolivia (Figure 3-1). Approximately 68,000 km$^2$ (41%) of its territory is covered by conservation units, including indigenous areas. Approximately 12% of its total area was deforested until 2010 (INPE, 2021b), concentrated in Acre's southeastern region, around urban centers, and along the state's road network, especially BR-364, BR-317, and AC-40. Although deforestation rates decreased between 2004 and 2010, forest clearing and burning for agricultural activities are still the major agents of regional landscape transformation (RODRIGUES, 2014).

Figure 3-1. Location of the study area.

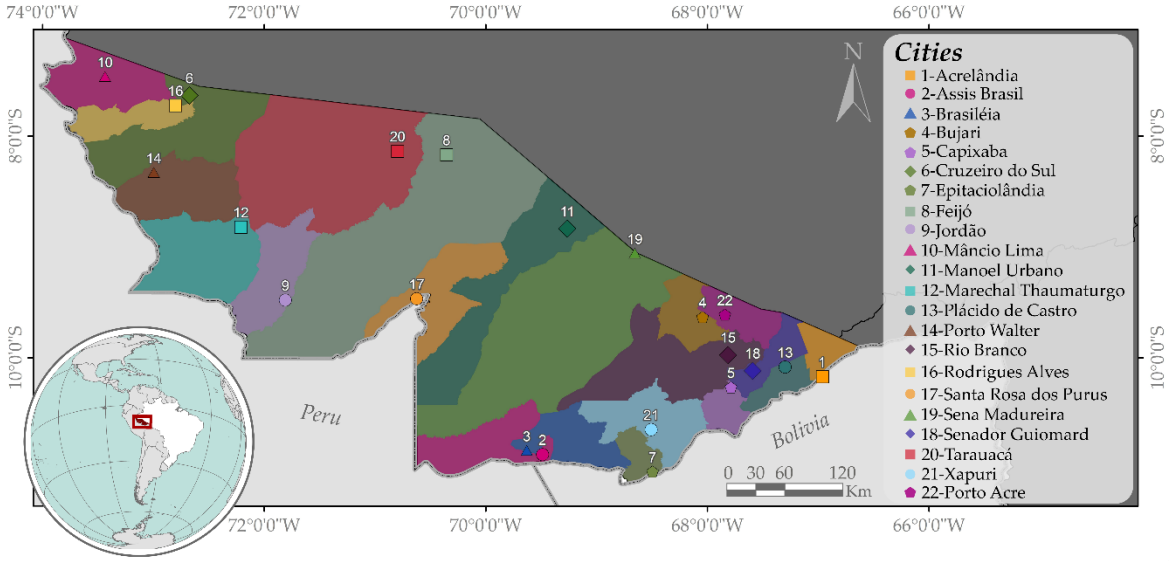


Source: From Author.

The climate in this region is characterized, under the Köppen system, as tropical (A) with 30% of the state area in a tropical monsoon climate (Am), characterized by the compensation of the short dry season by large amounts of precipitation throughout the

year. The other 70% of the state is classified as a tropical rainforest climate (Af), which is characterized by average precipitation of at least 60 mm in every month (ALVARES et al., 2013). The rainy season occurs from October to April and the dry season between June and August, while May and September are characterized as transition months among these seasons (DUARTE, 2006).

### 3.2.2 Data

This study integrates different spatial data products (Table 3-1) and non-spatial datasets (Table 3-2). The spatially explicit information refers to georeferenced vector and raster data, while the non-spatial datasets are composed of tables and numerical values. All the data and products were gathered from open-source repositories and official government databases, journal articles, market research, and web-pages from governmental and non-governmental organizations. Details of each dataset are presented below.

Table 3-1. Summary of the spatial dataset used.

| Data | Structure | Spatial Resolution | Period | Source |
|---|---|---|---|---|
| Burned area map | Raster | 250 m | 2008 to 2012 | Anderson et al. (2015) |
| Aboveground carbon density map | Raster | 30 m | 2000s | Baccini (2017) |
| Land use and land cover map (LULC) | Raster | 30 m | 2010, 2008, and 2012 | Almeida et al. (2016) |
| Rivers and Roads | Polygons | Multi-scale | 2016 | (IBGE, 2018a) |
| Property boundaries and protected private areas (APPs and LRs) | Polygons | Multi-scale | 2017 | (SFB, 2018) |
| Rural module specifications | Table** | - | 2013 | (INCRA, 2018) |
| Municipal boundaries | Polygons | Multi-scale | 2015 | (IBGE, 2018a) |
| Conservation units (UCs) and Indigenous Lands (ILs) | Polygons | Multi-scale | 2016 | (MMA, 2018) e (FUNAI, 2018) |

Source: From Author.

Table 3-2. Costs, prices, and index used.

| Variable | Un. | Ag | 2008 | 2009 | 2010 | 2011 | 2012 | References |
|---|---|---|---|---|---|---|---|---|
| Morbidity cases (Jun–Dec) | # | | 2776 | 2708 | 2545 | 2706 | 2657 | *(DATASUS, 2020) |
| Cost of morbidity | MUS$ | | 34.25 | 24.87 | 28.76 | 36.58 | 41.27 | |
| Fence recovery | US$/m | mn | 49.46 | 42.24 | 33.12 | 38.01 | 22.20 | *(DNIT, 2018) |
| | | sd | 18.32 | 15.35 | 11.67 | 12.86 | 7.10 | |
| Pasture reestablishment | US$/ha | mn | 883.27[1] | 883.27[1] | 883.27 | 883.27[1] | 883.27[1] | **(TOWNSEND; COSTA, 2010) |
| | | sd | 300.01[1] | 300.01[1] | 300.01 | 300.01[1] | 300.01[1] | |
| Agriculture reestablishment | US$/ha | | 813.62[1] | 813.62[1] | 813.62 | 813.62[1] | 813.62[1] | |
| Maize productivity | t/ha | | 1.75 | 1.83 | 2.00 | 2.21 | 2.27 | *(CONAB, 2021a) |
| Maize price | US$/t | mn | 182.27 | 201.29 | 215.29 | 269.54 | 243.20 | **(CEPEA, 2018) |
| | | sd | 22.70 | 12.97 | 37.93 | 11.51 | 29.33 | |
| Cassava productivity | t/ha | | 21.71 | 18.73 | 20.67 | 19.00 | 15.33 | *(IBGE, 2017) |
| Cassava price | US$/t | mn | 62.39 | 86.62 | 134.14 | 103.60 | 107.09 | **(CEPEA, 2018) |
| | | sd | 2.44 | 17.27 | 9.79 | 12.69 | 27.72 | |
| Cattle Densidy[2] | #/ha | | 1.80 | 1.86 | 1.88 | 1.85 | 1.79 | *(IBGE, 2018b) / **(ALMEIDA et al., 2016) |
| Cattle productivity | @/ha/y | | 4.06[3] | 4.06 | 4.06[3] | 4.06[3] | 4.06[3] | *(SÁ; ANDRADE; VALENTIM, 2010) |
| Cattle price | US$/@ | mn | 36.10 | 45.32 | 53.15 | 54.26 | 46.40 | **(CEPEA, 2018) |
| | | sd | 3.06 | 1.71 | 6.97 | 1.59 | 1.30 | |
| $CO_2$ price | €/t | mn | 13.69[3] | 13.69 | 11.98 | 13.06 | 7.50 | **(MARKETS INSIDERS, 2018) |
| | | sd | 0.68[3] | 0.68 | 5.42 | 3.35 | 0.72 | |
| Euro change | US$/€ | mn | 1.15 | 1.59 | 1.40 | 1.24 | 1.23 | *(BCB, 2018) |
| | | sd | 0.10 | 0.10 | 0.07 | 0.04 | 0.07 | |
| Cumulative Inflation | %b.y | | 32.51 | 32.46 | 32.41 | 32.35 | 32.29 | *(IPEA, 2018) |
| US$ changes[4] | US$/R$ | | 0.43 | 0.57 | 0.60 | 0.53 | 0.49 | *(IPEA, 2018) |

Un. – Unit of measurement; Ag – type of aggregation, as mean value (mn) or standard deviation (sd); *-data form governmental institutes; **-data from literature; 1 –Used values from 2010; 2 – Calculated by the total of cattle from PPM-IBGE divided by the pasture area from TerraClass ;3 – Used values of 2009; 4 – Used to convert the market prices as *reais* to US dollars.
Source: From Author.

#### 3.2.2.1 Spatial datasets

Maps containing burned area information from 2008 to 2012 were provided by the Tropical Ecosystems and Environmental Science Laboratory (TREES) at the Brazilian National Institute for Space Research (INPE). This dataset was generated following a well-established methodology (ANDERSON et al., 2005; SHIMABUKURO et al., 2009; ANDERSON et al., 2015, 2017). These maps are derived from MODIS surface reflectance products collection 5, which were resampled to 250 m of spatial resolution and subsequently processed by applying a Spectral Mixture Analysis (SMA) with vegetation, soil, and shade endmembers (SHIMABUKURO; SMITH, 1991). Based on

the shade fraction image, a region growth segmentation procedure was applied, followed by a manual post-classification edition (ANDERSON et al., 2015). The final maps display information on the yearly burned area, corresponding to the cumulative burned area occurring during the dry season of each year. The validation of this product at a significance level of 5%, exhibited an overall accuracy of 99.20% with a lower and upper confidence interval of 97.67% to 99.48%, respectively, for forest areas and an overall accuracy of 96.30%, with a lower and upper confidence interval of 92.88% to 98.55%, respectively, for non-forest areas (ANDERSON et al., 2017).

For characterizing land use and land cover (LULC) in the region, we used maps provided by the TerraClass project (INPE, 2018) for the years 2008, 2010, and 2012. TerraClass is a project for monitoring LULC in the Brazilian Legal Amazon, providing 15 LULC types. To retrieve classes of LULC within the TerraClass project, an analysis of Landsat-5/TM images using SMA is performed, followed by a slicing procedure and visual interpretation. This analysis is supported by temporal information based on the normalized difference vegetation index (NDVI) product from MODIS (Moderate Resolution Imaging Spectroradiometer) and the mask of deforestation, forest, and hydrography from the PRODES project (ALMEIDA et al., 2016; COUTINHO et al., 2013).

For this study, we aggregated the LULC thematic classes into the following three generalist categories: Forests, agriculture, and pastures (Table 3-3). The land cover class "Forests" refers to old-growth and secondary forests. The "Agriculture" class refers to annual crops, generally mechanized agriculture, and the mosaic of uses, which is a mix of agriculture and pastures. Finally, the land use class "Pastures" refers to areas where pastures dominate the landscape. Seven LULC thematic classes were not used in this research because their contribution in terms of area coverage in the Acre state territory was not representative (<1%).

Table 3-3. Summary of TerraClass land use and land cover (LULC) types.

| TerraClass LULC types | Grouped LULC categories |
|---|---|
| Primary forests and secondary vegetation | Forests |
| Annual crops and Mosaic of uses | Agriculture |
| Herbaceous pasture, Scrubby pasture, Pasture with exposed soil and Regeneration with pasture | Pastures |

Source: From Author.

Data on aboveground carbon density (ACD) was acquired from three datasets. First, for the Forest category, we assigned the respective value of the pantropical biomass map developed by Baccini et al. (2017). This product consists of a single raster map at 30-meter resolution, representing the ACD of live woody vegetation for the 2000–2009 decade, created based on field measurements, vegetation height maps from GLAS-Lidar (Geoscience Laser Altimeter System), a digital elevation model from SRTM (Shuttle Radar Topography Mission), and Landsat-7 ETM+ surface reflectance products.

Secondly, for the Agriculture category we identified maize and cassava as the main agricultural crops of Acre state, according to the Brazilian Institute of Geography and Statistics -IBGE (IBGE, 2017). Due to the lack of regional reports, the maize values were based on dry biomass for the whole aerial part of plantations located in southern Brazil (VIAN et al., 2016), added by the maize grain mean annual yield in the own state of Acre (FNP, 2012), estimated at 3.07±0.72 $Mg.ha^{-1}$. The cassava's biomass was based on the aboveground dry biomass of plantations in central Brazil (FERNANDES et al., 2009), estimated at 5.48±0.43 $Mg.ha^{-1}$. To convert these biomass values to ACD, we used a conversion factor of 0.4, as described by Redin (2010). This can be considered as a conservative value of *C* content in the vegetation biomass. These reference studies reported intensive and homogeneous plantations, with a certain degree of technology, like those indicated by the TerraClass annual crop category. Therefore, for the agriculture land cover class, we attributed the mean ACD value of 1.71 $MgC.ha^{-1}$, calculated from the maize and cassava ACD, with a standard deviation of 0.17, estimated through the uncertainty propagation method (Equation 3.1 and Equation 3.2) (VUOLO, 1996).

$$\sigma_w^2=\sigma_x^2+\sigma_y^2 \tag{3.1}$$

$$\sigma_w=|e| \, . \, \sigma_x \tag{3.2}$$

where $\sigma w$ is the uncertainty resultant; $\sigma x$ and $\sigma y$ are the uncertainty of X and Y; *W* is the final result; and *e* is a constant error-free.

Finally, for the "Pasture" category, we used an average value of 38.61 $MgC.ha^{-1}$, with a standard deviation of 16.54, based on the sum of the total alive pools of aboveground wood biomass, grasses and herbaceous dicots, and the dead pools of fine litter and wood

debris, found in three different pasture areas in the Brazilian states of Rondônia and Pará (BOONE KAUFFMAN; CUMMINGS; WARD, 1998).

The final ACD map corresponds to the year 2008, with *C* values associated to each class, as follows: Forest, agriculture, and pasture, at each spatial location, as mapped by the TerraClass product for this same year.

The territorial information about land tenure was based on official data provided by the Brazilian government. We have integrated information from different databases, encompassing the following data: Rural private property boundaries, rural module specifications, protected private areas (Areas of Permanent Preservation, APPs, and Legal Reserves, LRs), and governmental protected areas (Conservation Units, CUs, and Indigenous Lands, ILs).

The boundaries of private rural properties and their respective APPs and LRs were obtained at the Rural Environmental Registry System (SICAR). These two kinds of protected areas are mandatory for all private property, according to the actual Brazilian Forest Code (FC, Federal Law nº 12.651 of 2012) (BRASIL, 2012). The LR is an area of native vegetation that must occupy at least 80% of the property area in the Amazonian biome, excluding the environmentally sensitive areas (e.g. riparian and hilltop zones), which are titled APPs (SOARES-FILHO et al., 2014).

We classified each private property according to the rural module (r.m.) specifications of each municipality. This classification was defined according to the Federal Law nº 8.629 of 25 February 1993 (BRASIL, 1993), which classifies the properties in smallholdings (area $\leq$ 1 r.m.), small (1 < area $\leq$ 4 r.m.), medium (4 < area $\leq$ 15 r.m.), and large properties (area > 15 r.m.). The rural module size for the Acre State ranges from 70 to 100 ha per municipality and it was defined in 2013 by the National Institute for Settlement and Agrarian Reform – INCRA (INCRA, 2018).

#### 3.2.2.2 Non-spatial datasets

Records of hospitalization cases caused by respiratory illness and the total cost of treatments are provided by the Brazilian Unified Health System (SUS). In its information system (Tabnet-DATASUS) (DATASUS, 2020), we searched for the number of hospitalization cases and the total economic cost according to the place of residence,

filtered for respiratory system diseases and distinguished by municipality and year/month of occurrence.

Among all the costs related to infrastructure, we computed only the impacts on the property fences due to the unavailability of data on all other costs and, thus, the infrastructure damage costs due to fires can be considered underestimated. This information was obtained from the National Department of Transport Infrastructure (DNIT), which provides the reference costs to repair and reconstruct different kinds of fences. Thus, we calculated the mean price of all the kinds of build and repair, which were described by DNIT annual reports (DNIT, 2018).

We assume that the cost related to land recovery was US$ 813.62 $ha^{-1}$ for agriculture and US$ 883.27 $ha^{-1}$ for pasture, both obtained by Townsend and Costa (2010) for areas in the Brazilian Amazon region. The costs of forest restoration were not considered because such practice is not usual in the region.

The value of crop production was generated by multiplying the productivity values by their market price in each year. For maize and cassava production (Table 3-2), we used the values provided by the National Supply Company – CONAB (CONAB, 2021a) and IBGE (IBGE, 2017) systems. The mean productivity for 2008 to 2012 was 2.01 $t.ha^{-1}$ for maize and 19.08 $t.ha^{-1}$ for cassava. The mean cattle weight gain for 2009 was 60.09 $kg.ha^{-1}.y^{-1}$, a value based on a technical report of the Brazilian Agricultural Research Corporation – EMBRAPA (SÁ; ANDRADE; VALENTIM, 2010). Market prices for those products were provided at an annual time-scale by the Center for Advanced Studies in Applied Economics (CEPEA) system (CEPEA, 2018).

For forest-related losses, we only considered commercial wood stocks, due to the data availability. For this, we used the value of US$ 5 $ha^{-1}$, quantified by De Mendonça et al. (2004), which denotes the mean price of marketable adult trees after a fire event that the lumber mill would be willing to pay to the landowners in an exploited forest in Eastern Amazonia.

Carbon emission values were accounted by using the market prices of carbon available at the Carbon Emission Future system (MARKETS INSIDERS, 2018) between 2009 and 2012 (Table 3-2). As these prices were in Euros, we converted these values into US

dollars using the exchange rates available from the Brazil Central Bank (BCB) system (BCB, 2018).

### 3.2.3 Data analysis

In the next sections, we describe all the procedures that were carried out to reach our three research goals. We also present a section of assumptions and uncertainties of our data and analysis.

#### 3.2.3.1 Quantifying the spatiotemporal variability of fire dynamics

To analyze the spatial dynamics of the burned areas, first we quantified the total burned areas by year, the wildfire frequency and recurrence, and the burned area anomalies. To understand how remotely fire sources could be inside Acre's territory, excluding common anthropic ignitions such as roads and urban centers, we built a grid of Euclidian distance from rivers and roads and then we determined the mean distance and standard deviation of burned areas by intersecting the fire scars and the Euclidian distance grid from these features.

#### 3.2.3.2 Fire occurrence and land tenure relationship

An intersection between burned area and the spatial data of land tenure and LULC was carried out for determining the areas affected by fires. Then, the annual burned areas were stratified by each LULC class, land tenure and protected areas inside and outside private properties. The year of 2010 was excluded from the time-series mean average due to the anomalous drought that occurred during that year, leading to extensive fires (ANDERSON et al., 2015).

#### 3.2.3.3 Estimating the environmental, social, and economic impacts of fires

The environmental impact is represented here by biomass loss and gross carbon emission by fire. It is quantified for each year, as shown in Figure 3-2. To determine the annual post-fire biomass loss, we first used the 2008 biomass map and then applied the relationship of biomass loss developed by Anderson et al., (2015), which states that the remaining above-ground biomass after fire is a function of the above-ground biomass prior the fire event. Then, for the areas mapped as Agriculture and Pastures, the reference biomass values (1.71 and 38.61 $MgC.ha^{-1}$, respectively) were attributed to the remaining

biomass map in order to simulate their seasonal renewal, resulting in the following year biomass map. For 2010 and 2012, we not only updated the biomass values but also dynamically revised the spatial location of Agriculture and Pasture areas, according to the available LULC maps.

Figure 3-2. Workflow for generating the annual maps of remaining and loss of biomass.

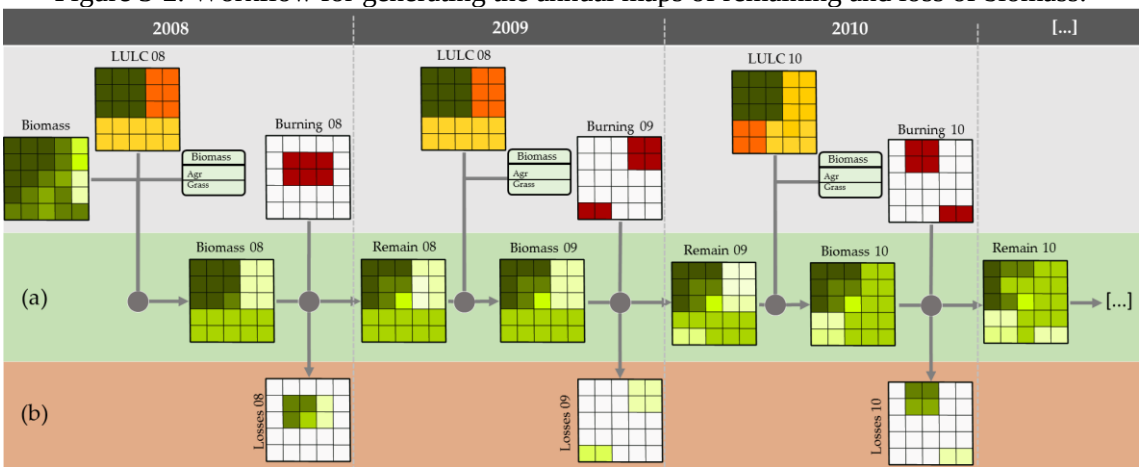


(a)The green panel represents the 2008–2010 annual potential biomass maps, which were processed from the annual burned area maps; 2008, 2010, and 2012 land use and land cover (LULC) maps; and a table of reference biomass values for each grouped LULC classes. (b) The red panel represents the 2008–2010 annual biomass loss maps, derived from an empirical relationship between pre and post-fire biomass applied to the potential biomass maps where a fire event was depicted by the burned area maps.
Source: From Author.

Finally, to quantify the total annual gross carbon emissions, we applied the $CO_2$ gross emission model (Equation 3.3) to the biomass loss maps (Figure 3-2b).

$$F_{CO_2} = \theta * (1 - \alpha) * \sum_{j=1}^{2} \lambda_j * \sum_x \sum_y Bi_{(x,y,j)} * A_{(x,y)} \quad (3.3)$$

where $F_{CO2}$ is the carbon dioxide gross emission (Mg $CO_2$) in the year of interest (immediate flux to the atmosphere); $\theta$ converts carbon to carbon dioxide (3.67); $\alpha$ is the slope of Anderson et al. (2015) equation's ($\alpha$ = 0.7084±0.034); $\lambda_j$ is the release constant specific for forest ($j$=1, $\lambda$=50%) and non-forest covers ($j$=2, $\lambda$=100%); $Bi_{(x,y,j)}$ is the pre-burn biomass (Mg C.ha$^{-1}$) for the pixel at the location ($x$,$y$), distinguished for forest and non-forest covers ($j$); and $A_{(x,y)}$ is the burned area (ha) at the pixel ($x$,$y$), for which the value in our studies is 0.09 ha at burned pixels.

The health data, considered here as social impact, was determined by building a relationship between fire and respiratory morbidity in Acre state. We computed a linear

correlation between the total burned area and the total cases of hospitalization by municipality and year. First, we summarized the total burned area by municipalities and aggregated the number of cases grouped in last semester, which includes the peak of the fire occurrence, in September. The dry season period was extended for three months in this analysis because not all health case manifests were registered at the same time as the fires.

We calculated five types of economic losses divided into two categories, directly and indirectly fire-related. The first direct cost is associated with infrastructure damages, for which we assume only fence losses. The second and third direct costs are the production losses, for which we considered costs related to crop reestablishment and affected future production. Finally, the quantified indirect costs were related to $CO_2$ emissions and respiratory morbidities.

Fence losses were calculated using the land property boundaries over burned Pasture and Agricultural fields, then extracting these vector lengths. This analysis can be considered conservative since fences are also usually used to separate pasture from agriculture inside the same property. The wildfire factor was applied and then the total cost of the fence reconstruction and repair was calculated using the respective prices for each year (Table 3-2).

Production losses were estimated by multiplying the production and reestablishment coefficients for each class and their market prices for each year. Just for the Agriculture class, we assume that there was the same proportion of cassava and maize crops.

Not all burned areas in rural properties are intentional, but the main losses are caused when fires escape and accidentally spread to adjacent areas. For that reason, we considered the wildfire factor of 45%, estimated by De Mendonça et al. (2004), to calculate the economic losses of infrastructure damages, crop reestablishment, and affected future production. This factor was estimated using an econometric model in the database from field research done by the Amazon Environmental Research Institute (IPAM). The database is related to an information set, acquired between 1994 and 1995, of 202 properties spread over five municipalities in the “Arco do Desmatamento” region,

specifically at Paragominas, PA, Santana do Araguaia, PA, Alta Floresta, PA, Ariquemes, RO, and Rio Branco, AC.

To quantify the costs of $CO_2$, we multiplied the total $CO_2$ emissions by the market prices and exchange rates. So, we didn't use the wildfire factor because the $CO_2$ emission is independent of the fire aim.

To evaluate the illness costs, we assumed that a factor of only 8% of respiratory morbidities can be attributed to smoke from fires and wildfires, as shown by De Mendonça et al. (2004), and then applied the respiratory morbidity costs for June to December.

Finally, we updated all values to the same year (2017), using the cumulative inflation rates (Table 3-2), available at the Brazilian Central Bank (BCB) (BCB, 2018) website using Equation 4. All the economic costs in Brazilian currency (*Reais)* were converted to US dollars, using an average exchange value of 0.31±0.01, which referred to the 2017 quotation given by the BCB (BCB, 2018).

$$Vf = Vp * (1+\sum IPCAy) \quad (3.4)$$

where *Vf* is the future value; *Vp* is the present value; and *IPCAy* is the annual inflation tax

#### 3.2.3.4 Assumptions and uncertainties

Assumptions were made in order to accommodate the limited data available with the method we developed. First, we assumed that (1) the TerraClass Agriculture and Mosaic of Uses classes cover all crops over the Acre state, ranging from mechanized to traditional agriculture; (2) the class Mosaic of Uses from TerraClass are a mix of agriculture and pasture of traditional agriculture, but it is reclassified in our analysis as Agriculture class as it is more representative of the landscape in these areas; (3) the delimitation of properties, APP and LR from Rural Environmental Registry (acronym CAR) have no remarkable spatial overlaps; and (4) the entire biomass loss is immediately combusted and released to the atmosphere, being accounted only in the period of one year, thus no decay rate or emissions from the decomposing pool were considered.

The CAR dataset is not used as official territorial delimitation due to overlaps between different properties, boundaries, and special areas, however, this dataset is the best spatially explicit public information on land tenure from the Brazilian Amazon.

The economic costs errors were estimated using the values and errors of the burned area, $CO_2$ equivalent emission, asset prices, and dollar exchange, by applying the methods of uncertainty propagation to compute each category uncertainty, and the total economic uncertainty, through the multiplication method, according to Vuolo (1996). Details about the method are provided below.

For the burned area error, we used the lower and upper values of the confidence interval of each land cover class related to the TREES product to estimate the uncertainty of the burned area. Thus, we propagated each burned class error to the total burned area error using the sum method (Equation 3.1).

The biomass error was first calculated using a multiplication method of uncertainty propagation (Equation 3.5) to estimate the uncertainty of each class, and second, the sum method (Equation 3.1) quantified the total biomass loss uncertainty. We used the burned area, the burned area uncertainty, the biomass value, and a standard deviation of each class. To the Agriculture and Pasture classes, we used a standard deviation available in the consulted literature. For the Forest class, we calculated the total standard deviation, based on the uncertainty map provided by Baccini et al. (2017). Therefore, the total forest biomass uncertainty was the product of the uncertainty map and the biomass map, with a subsequent numeric scale correction (dividing each pixel value by 1000) and a spatial scale correction from unit per pixel to hectares (multiplying each pixel value by 0.09 ha). Finally, we used a sum method of uncertainty propagation (Equation 3.1) to estimate the total standard deviation of the Forest class biomass.

The $CO_2$ emissions error followed the same principle of biomass error estimation, where the biomass total value, a biomass error, a CO2 equivalence conversion, and its error were used in a multiplication method of uncertainty (Equation 3.5), achieving the class error. This value was then applied to the sum method (Equation 3,1) to estimate the total $CO_2$ equivalent emission error.

$$\left(\frac{\sigma_w}{w}\right)^2 = \left(\frac{\sigma_x}{x}\right)^2 + \left(\frac{\sigma_y}{y}\right)^2 \quad (3.5)$$

where $\sigma w$ is the uncertainty resultant; $\sigma x$ and σy are the uncertainty of X and Y; $X$ and $Y$ are the measures values, and; $W$ is the final result

## 3.3 Results

### 3.3.1 Spatiotemporal variability of fire dynamics

During all the analyzed years, more than 2577 km² were burned. Of these, approximately 12% burned more than once and 3% occurred in following years, with a maximum three-year sequence (Table 3-4). Burning events in Acre (Figure 2) were concentrated near the major urban centers (Rio Branco, Cruzeiro do Sul, Sena Madureira, Tauaracá, Feijó, and Brasiléia), highways (BR-364, BR-317, AC-040, and AC-075) and waterways (Iaco, Muru, Acre, and Envira rivers).

Table 3-4. Total burned area in hectares (km²) that burned one time, more than once, and the number of burned scars in sequence of year.

| Year | Total | Frequency | | Recurrence | | |
|---|---|---|---|---|---|---|
| | | One | > One | 1 Years | 2 Years | 3 Years |
| 2008 | 218.85 | 218.85 | 161.82 | 57.04 | 2.47 | 0.53 |
| 2009 | 33.33 | 33.33 | 8.43 | 24.9 | 13.32 | 2.37 |
| 2010 | 2056.80 | 2056.8 | 1928.22 | 128.58 | 29.83 | 4.22 |
| 2011 | 178.52 | 178.52 | 135.74 | 42.78 | 8.5 | 0 |
| 2012 | 90.05 | 90.05 | 34.2 | 55.86 | 0 | 0 |
| **Total** | **2577.55** | **2577.55** | **2268.41** | **309.16** | **54.12** | **7.12** |

Source: From Author.

Every year new burn scars were mapped (Table 3-5). However, the number of polygons varied substantially (24–3521). Their size also had a large annual standard deviation (SD). The maximum SD reached 2.54 km² in 2010, while the minimum SD of 1.28 km² was recorded in 2011. In 2010 the highest number of polygons were observed (3521) and the largest total burned area (2056.8 km²) among all years analyzed was expressed, respectively, 19 times larger and 16 times higher than the mean of the other four years. The largest polygon observed in our time-series had more than 100 km², which occurred in 2010, while, in any other year the largest burned polygon had an area of 16.90 km².

Figure 3-3. Burn scars in Acre state (Brazil), mapped with 250 m spatial resolution, for the regular climate years of 2008, 2009, 2011, and 2012 (a) and for the 2010 drought year (b).

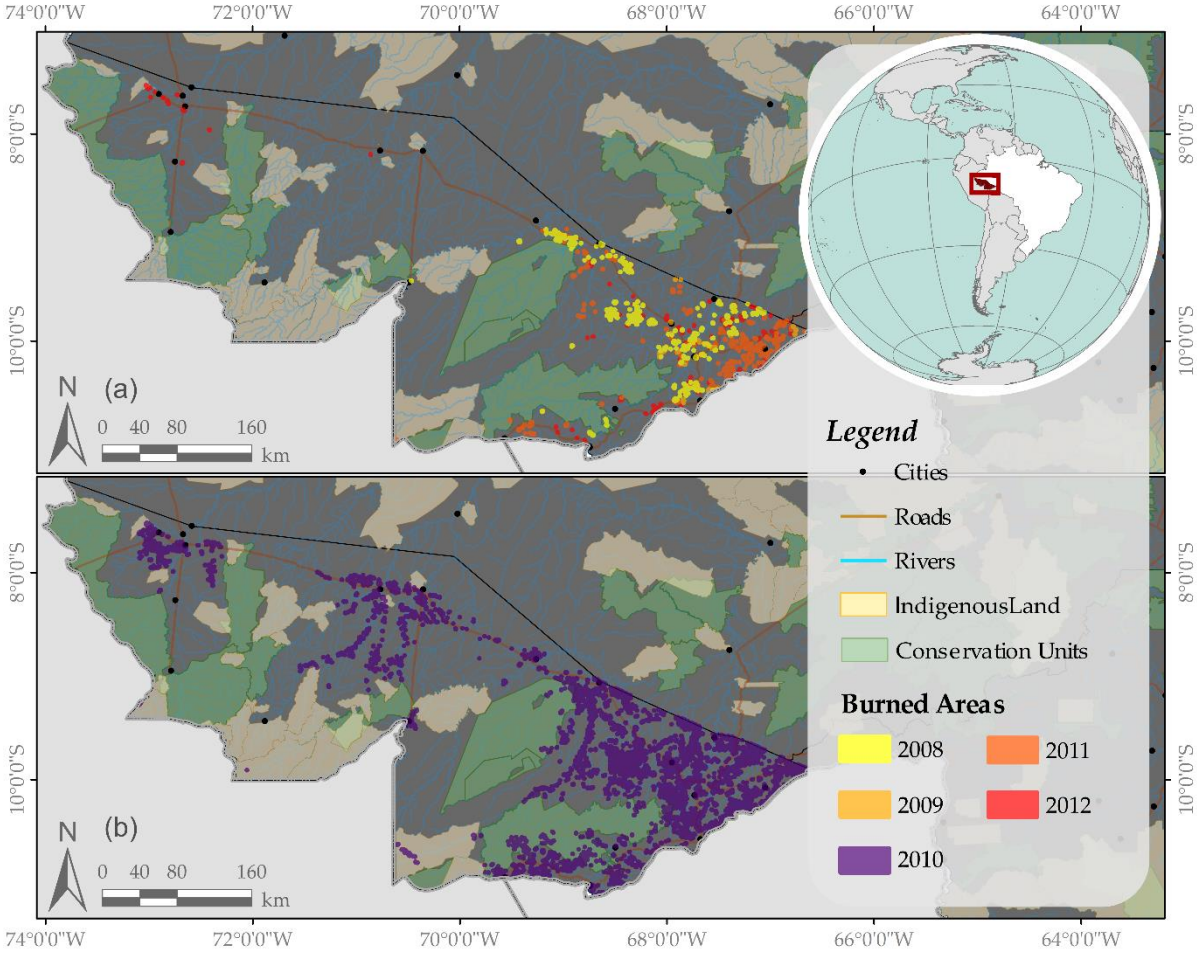


Source: From Author.

Considering that Acre's dry season (months with monthly rainfall < 100 mm) in 2010 extended by one month, totaling four months in this year, the 3521 observed burn scars (2056.8 km²) corresponded to around 29 burning events per day in the dry season, with an average of 16.85±0.52 km² each. During the three dry months of the regular climate year of 2012, conversely, only 146 burn scars (90 km²) were detected, corresponding to about 2 burning events per day in the dry season, with an average of 0.98±0.04 km² burned daily.

Analyzing the distance to roads (Table 3-6), we found that, in 2010, burn scars reached longer distances from the main highways (11.15±9.67 km) than the average distance of other years (7.27±6.52 km). These burned scars also occurred closer to the waterways in 2010 (1.49±1.15 km) than during the other years (1.66±1.13 km).

Table 3-5. Summary of burned scars between 2008 and 2012 for Acres state.

| Variable | Years | | | | |
|---|---|---|---|---|---|
| | **2008** | **2009** | **2010** | **2011** | **2012** |
| Number of scars | 267 | 24 | 3521 | 324 | 146 |
| Total area (km²) | 218.85 | 33.33 | 2056.80 | 178.52 | 90.05 |
| Maximum area (km²) | 16.41 | 5.03 | 104.34 | 16.90 | 10.74 |
| Mean area (km²) | 0.82 | 1.39 | 0.58 | 0.55 | 0.62 |
| Minimum area (km²) | 0.07 | 0.07 | 0.02 | 0.0009 | 0.01 |
| Standard deviation | 1.50 | 1.38 | 2.54 | 1.28 | 1.39 |
| Variance | 225.09 | 190.09 | 644.56 | 162.88 | 192.70 |
| Anomaly of quantity | −0.44 | −0.62 | 1.99 | −0.40 | −0.53 |
| Anomaly of area | −1.32 | −2.54 | 2.39 | −2.07 | −2.21 |

Source: From Author.

Table 3-6. Distance, in kilometers, of rivers (Ri) and roads (Rd) to burned scars.

| Distance (km) | 2008 | | 2009 | | 2010 | | 2011 | | 2012 | |
|---|---|---|---|---|---|---|---|---|---|---|
| | **Ri** | **Rd** | **Ri** | **Rd** | **Ri** | **Rd** | **Ri** | **Rd** | **Ri** | **Rd** |
| Minimum | 1.28 | 6.89 | 0.98 | 10.29 | 1.21 | 10.80 | 1.26 | 5.71 | 1.53 | 4.27 |
| Mean | 1.68 | 7.36 | 1.52 | 10.99 | 1.49 | 11.15 | 1.58 | 6.10 | 1.86 | 4.65 |
| Maximum | 5.39 | 28.88 | 3.72 | 41.86 | 6.20 | 56.54 | 5.69 | 34.28 | 5.73 | 24.81 |
| Standard deviation | 1.12 | 5.51 | 0.93 | 9.94 | 1.15 | 9.67 | 1.12 | 5.86 | 1.34 | 4.77 |
| Variance | 1.27 | 30.35 | 0.86 | 98.88 | 1.32 | 93.51 | 1.25 | 34.32 | 1.79 | 22.74 |

Source: From Author.

In all the analyzed years, there was a dominance of burned scars with areas up to 0.60 km² (Figure 3-4a). However, in 2009 there was a significant change in the proportions of burned scar classes, where the larger polygons (>0.25 km²) stood out over small polygons (< 0.25 km²).

In 2010, we observed the largest burned area (2056.80 km²) among all years analyzed, making this year anomalous in relation to the average burned area value (+2.39 SD, Table 3-5) and also to a number of burned scars (+1.99 SD, Figure 3-4b, and Table 3-5). Additionally, this year presented the larger number of outliers compared to the other years (Figure 3-4c and Table 3-5).

Figure 3-4. Evaluation of the annual burned area time series from 2008 to 2012.

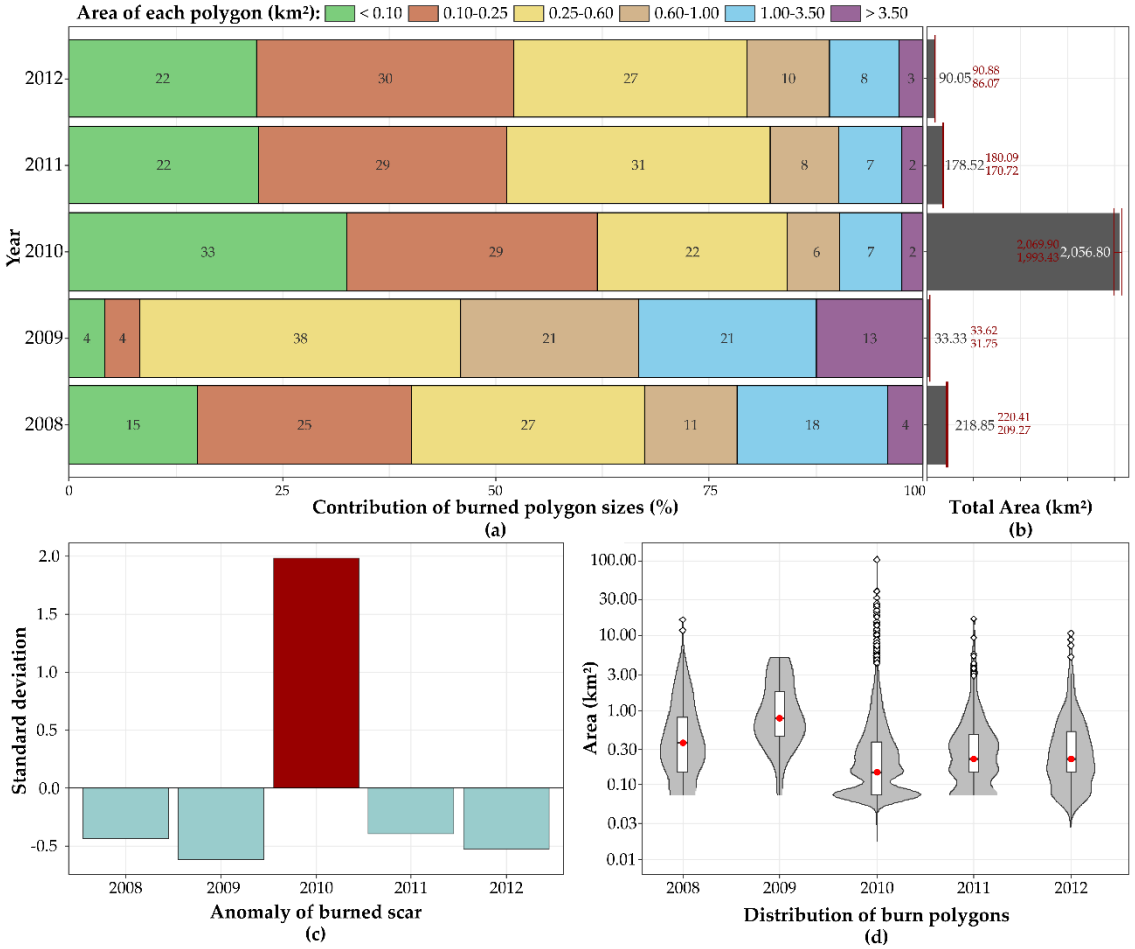


(a) Contribution of each burned polygon size to the total burned area; (b) total burned area (ha) with upper and lower limits; (c) anomaly of number of burned scars, normalized by its standard deviation (σ) for the 2008–2012 period; (d) Distribution of burn polygon sizes, where the sides of each violin is a kernel density function; the red dot represents the median; the white bar indicates the interquartile range; the straight vertical line represents the 95% confidence interval; and the white dots represent outlier polygons.
Source: From Author.

### 3.3.2 Fire occurrence and land tenure relationship

Usually, the extent of the fires' impact was greatest for private areas (98.8%) than for public governmental lands (1.2%). Burned areas were not observed in governmental lands in 2009 and were lower than 1% in 2008. However, in 2010, fire occurrences increased by 2.86 percentage points (p.p) within the areas managed by governmental institutes (Figure 3-5a).

Figure 3-5. The proportion of burned area by (a) management types; (b) land use and land cover; (c) propriety class.

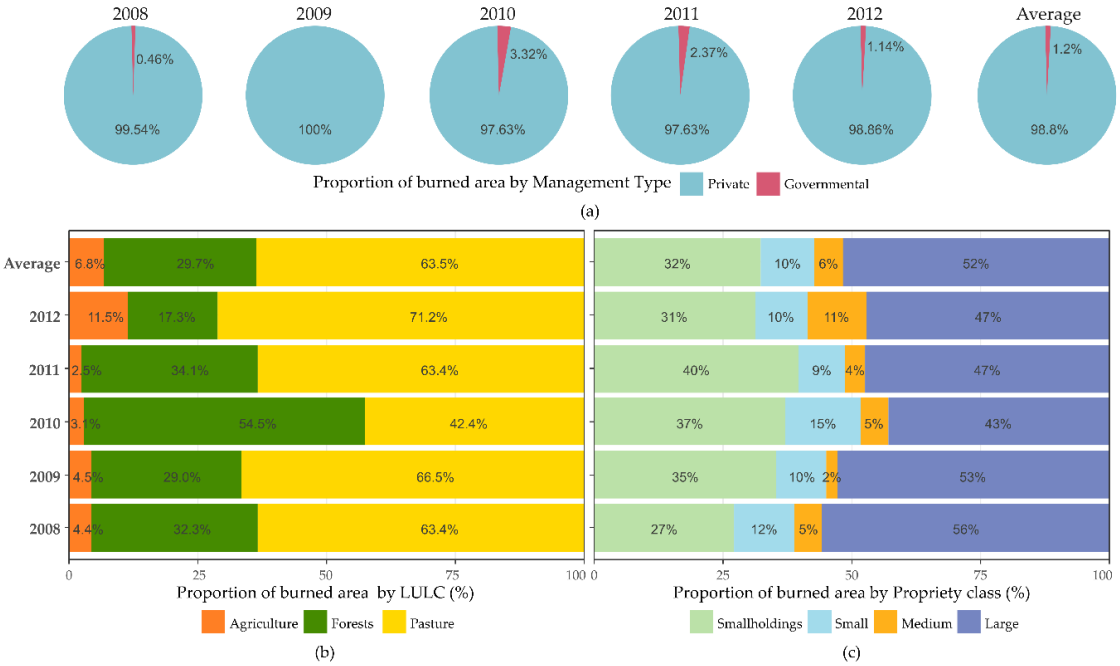


Source: From Author.

The dominant LULC in Acre is the Forest class (Table 3-7), representing 91% of all territory in the period studied. The area of Pasture and Agriculture corresponded to 8.3% and 0.7% of the territory, respectively. The Pastures class was the LULC predominantly affected by fire during regular years (63.5%). For the same period, the areas of Forests and Agriculture affected by fires corresponded, respectively, to 29.7% and 6.8% of Acre's territorial extent (Figure 3-5b). On the other hand, during the 2010 drought, the burned area increased by almost 25 p.p. in forests (contributing to 54.5% of the total area burned) and decreased in the other two classes (totaling 42.4% of Pasture and 3.1% of Agriculture).

Table 3-7. The proportion of each land use and land cover class in Acre state through the years.

| LULC | 2008 | 2010 | 2012 | Average |
|---|---|---|---|---|
| Forest | 91.0% | 91.2% | 90.5% | 91.0% |
| Agriculture | 0.9% | 0.6% | 0.7% | 0.7% |
| Pasture | 8.1% | 8.2% | 8.8% | 8.3% |

Source: From Author.

Acre registered, by 10 January 2018, 31901 proprieties with the Rural Environmental Registry (acronym CAR). From this total, 78% were classified as smallholdings, 18.5% as small, 1.9% as medium, and 1.5% as large properties. In regular years, around 38 large proprieties, 19 medium, 438 smallholdings, and 68 small proprieties were affected by fires. These numbers represent, for each class area respectively, 8%, 3.2%, 1.8%, and 1.2%. This same pattern persisted during 2010, with a change in the total amount of proprieties affected (Table 3-8). This pattern was not observed when we analyzed the total of the burned area (Figure 3-5c). Interestingly, a new configuration emerged in all regular climate and anomalous years, with large properties contributing to the largest affected areas, followed by smallholdings, then small, and finally medium properties.

Table 3-8. Number of proprieties affected by fires through the years.

| Class of Proprieties | Total | 2008 | 2009 | 2010 | 2011 | 2012 | Average |
|---|---|---|---|---|---|---|---|
| Smallholdings | 24964 | 658 (2.6%) | 80 (0.3%) | 6394 (25.6%) | 672 (2.7%) | 341 (1.4%) | 438 (1.8%) |
| Small | 5867 | 126 (2.1%) | 14 (0.2%) | 1368 (23.3%) | 91 (1.6%) | 42 (0.7%) | 68 (1.2%) |
| Medium | 593 | 35 (5.9%) | 3 (0.5%) | 215 (36.3%) | 22 (3.7%) | 16 (2.7%) | 19 (3.2%) |
| Large | 477 | 60 (12.6%) | 15 (3.1%) | 258 (54.1%) | 46 (9.6%) | 30 (6.3%) | 38 (8.0%) |
| **Total** | **31901** | **879 (2.8%)** | **112 (0.4%)** | **8235 (25.8%)** | **831 (2.6%)** | **429 (1.3%)** | **563 (1.8%)** |

Source: From Author.

When analyzing the occurrence of burned areas in governmentally protected areas (CU and IL), we found that the total burned area was predominant in 2008 and 2012, respectively by CU and IL (Figure 3-6a). In 2009, burned areas did not occur in governmentally protected areas. Inside the boundaries of private areas, common-use areas (AUC, 59.7%) were more affected by fires than protected areas (LR, 26.1% and APP, 14.2%) (Figure 3-6b).

Figure 3-6. The proportion of burned area by land use and land cover types (a) and by special areas (b), through the years analyzed.

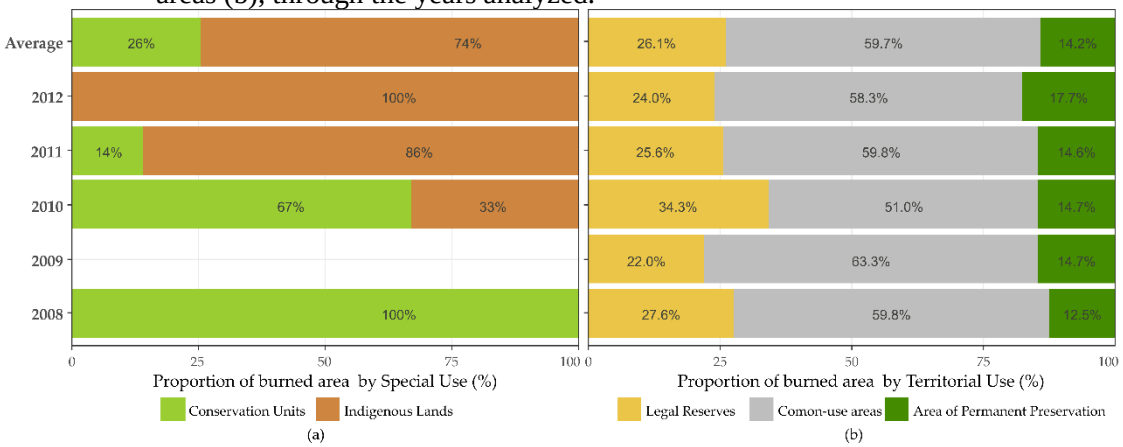


Source: From Author.

Five of the eleven CUs in Acre were affected by fires between 2008 and 2012 (Table 3-9). The RESEX Chico Mendes was the only one to burn every time that CU was affected. During 2010, we observed the highest number of CUs affected, reaching a total of 45.63 km² of area burned. In addition, less than 1% of the burnings occurred in Integral Protection reserves (PARNA Serra do Divisor), while about 99% occurred in sustainable-use reserves, such as the RESEX Chico Mendes (34.73 km²), RESEX Cazumbá-Iracema (7.76 km²), FLONA Santa Rosa dos Purus (1.87 km²), and ARIE Seringal Nova Esperança (1.26 km²).

Table 3-9. Area (km²) of Conservation Units affected by fire through the years analyzed.

| Type | Class (Acronym) | Nome | 2008 | 2009 | 2010 | 2011 | 2012 |
|---|---|---|---|---|---|---|---|
| UIP | National Park (PARNA) | Serra do Divisor | 0.00 | 0.00 | 0.02 | 0.00 | 0.00 |
| USU | Area of Relevant Ecological Interest (ARIE) | Seringal Nova Esperaça | 0.00 | 0.00 | 1.26 | 0.00 | 0.00 |
| USU | National Forest (FLONA) | Santa Rosa do Purus | 0.00 | 0.00 | 1.87 | 0.00 | 0.00 |
| USU | Extractive Reserve (RESEX) | Cazumbá-Iracema | 0.64 | 0.00 | 7.76 | 0.00 | 0.00 |
| USU | Extractive Reserve (RESEX) | Chico Mendes | 0.37 | 0.00 | 34.73 | 0.59 | 0.00 |
| **Total** | | | **1.00** | **0.00** | **45.63** | **0.59** | **0.00** |

UIP – Integral Protection; USU – Sustainable use.
Source: From Author.

In relation to the 31 ILs existing in Acre, only eleven of them were affected by fires between 2008 and 2012 (Table 3-10), which were the following: Alto Rio Purus;

Cabeceira do Rio Acre; Igarapé do Caucho; Kampa do Rio Amonea; Kampa e Isolados do Rio Envira; Katukina/Kaxinawá; Kaxinawá Colônia Vinte e Sete; Kaxinawá do Rio Humaitá; Mamoadate; and Poyanawa. The Mamoadate land had the greatest burned extent in 2010 (11.20 km²) and was the only one to burn in 2011.

Table 3-10. Area (km²) of Indigenous land affected by fire through the years analyzed.

| **Terra Indigena** | **2008** | **2009** | **2010** | **2011** | **2012** |
|---|---|---|---|---|---|
| Alto Rio Purus | 0.00 | 0.00 | 0.33 | 0.00 | 0.00 |
| Cabeceira do Rio Acre | 0.00 | 0.00 | 0.00 | 0.00 | 0.00 |
| Igarapé do Caucho | 0.00 | 0.00 | 0.96 | 0.00 | 0.00 |
| Kampa do Rio Amonea | 0.00 | 0.00 | 2.93 | 0.00 | 0.00 |
| Kampa e Isolados do Rio Envira | 0.00 | 0.00 | 0.15 | 0.00 | 0.00 |
| Katukina/Kaxinawá | 0.00 | 0.00 | 0.15 | 0.00 | 0.00 |
| Kaxinawá Colônia Vinte e Sete | 0.00 | 0.00 | 0.29 | 0.00 | 0.00 |
| Kaxinawá do Rio Humaitá | 0.00 | 0.00 | 0.13 | 0.00 | 0.00 |
| Mamoadate | 0.00 | 0.00 | 11.20 | 3.64 | 0.00 |
| Poyanawa | 0.00 | 0.00 | 6.46 | 0.00 | 1.03 |
| **Total** | **0.00** | **0.00** | **22.59** | **3.64** | **1.03** |

Source: From Author.

### 3.3.3 Environmental, social, and economic impacts of fire

The average biomass loss during normal climate years was about 0.3±0.5 $Tg.y^{-1}$, however, this value increased to 7.02±0.55 $Tg.y^{-1}$ in 2010 (Figure 3-7a). Fires in forested areas were responsible for almost 59% of biomass loss in Acre during all years, except for 2012 (Figure 3-7b)

Pastures contributed with approximately 58% of the total $CO_2$ emissions in normal years (0.78±0.20 $Tg.y^{-1}$) (Figure 3-7c). The Agriculture class, on the other hand, contributed less than 0.2% of emissions, on average. During 2010, however, forests alone contributed to 69% of the total $CO_2$ emission from fires in Acre (Figure 3-7c), corresponding to 15.31± 2.10 $Tg.y^{-1}$ (Figure 3-7d).

By analyzing the social impacts, we observed up to 2500 respiratory morbidity cases during the second semester of all the analyzed years. In the normal climate years (2008, 2009, 2011, and 2012), the mean cases of respiratory illness were around 2711. Surprisingly, the lowest record of respiratory morbidity cases (2545 cases in total) was

found during 2010. Rio Branco, Cruzeiro do Sul, and Sena Madureira were the main municipalities in number of respiratory illness cases in all years.

Figure 3-7. The proportion of biomass loss (b) and CO2 emissions (c) by land use and land cover types and the total biomass loss (a) and total emissions(d) through the years analyzed.

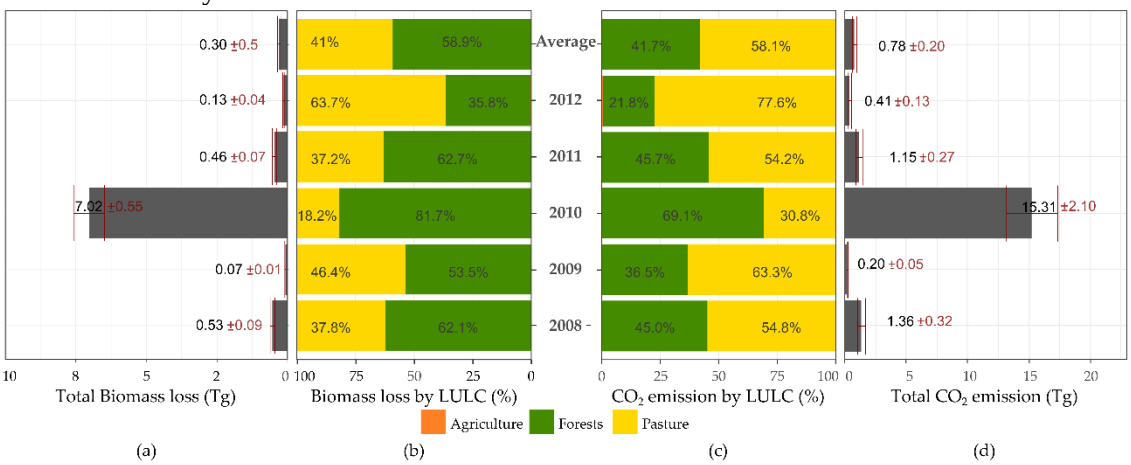


Source: From Author.

The relationship between respiratory morbidity cases and burned area during the extend dry season (Figure 3-8), suggests that Rio Branco is an outlier, with a higher amount of burned area and a high number of hospitalizations in the first three years analyzed. Meanwhile, Plácido de Castro, Senador Guiomard, and Acrelândia had an increase in burned area through the years, while their numbers of respiratory cases remained approximately the same. Contrarily, Cruzeiro do Sul persisted with almost the same number of hospitalizations and burned area through all the years analyzed.

After designing a linear regression where respiratory morbidity was the dependent variable and respiratory morbidity cases was the independent variable, modeled for each year (Figure 3-8), we observed a positive correlation coefficient ($r > 0$) more explicit for 2008 ($r = 0.64$, $r^2 = 0.42$, *p*-value = 0.0092), 2009 ($r = 0.72$, $r^2 = 0.52$, *p*-value = 0.0012), and 2010 ($r = 0.52$, $r^2 = 0.27$, *p*-value = 0.026) years. This result suggests that an increase in the burned area will lead to an increase in the number of hospitalizations. However, the quality of those models described by the determination coefficient ($r^2$), indicates that 2009 exhibited a better model fit than the others years. The 2008, 2009, and 2010 year models indicate that the burned area is relevant to explaining the respiratory morbidity cases, using a 5% significance level.

Figure 3-8. Correlation between respiratory morbidity and burned area by year analyzed, with the determination coefficient value ($r^2$), the correlation coefficient value (r), and the specific p-values.

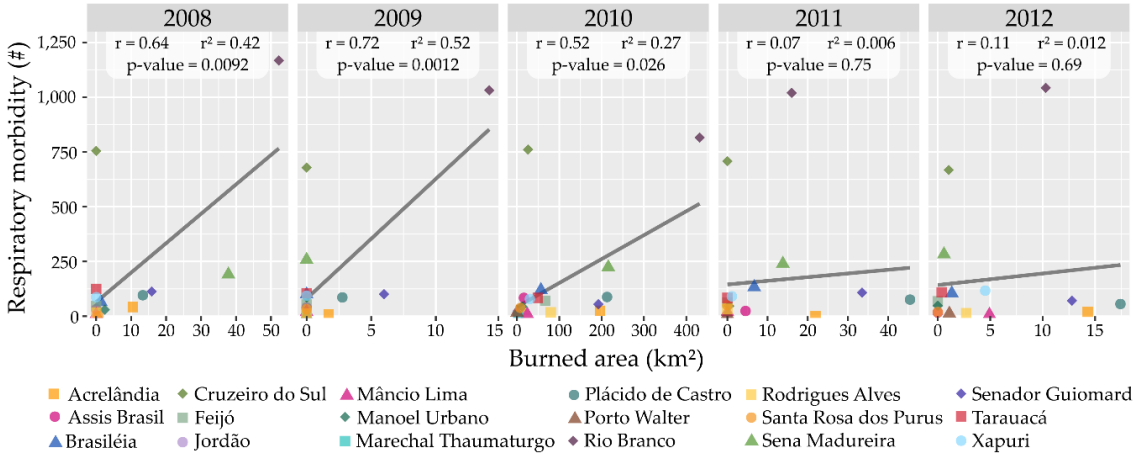


Source: From Author.

The fire-mediated economic losses in Acre between 2008 and 2012 are discriminated in Figure 3-9 and Table 3-11, where the values are specified by damage type, summarized with its total deviation and GDP equivalence. $CO_2$ emissions represented the greatest contribution to the total economic loss, ranging from 40% to 73%. Respiratory illness costs had the smallest contribution, representing up to 9.4% of all costs in 2009. In 2010, there was an increase of 8 percentage points in the $CO_2$ emission contribution for the total economic loss, compared to the average of the normal climatic years. Losses in propriety infrastructure (fences) represented 12% in 2010, the most representative year before 2012.

As expected, 2010 had the highest economic loss, corresponding to a total of US$ 243.36±85.05 million, representing around 7±2.45% of Acre's GDP for that year. Nevertheless, during normal climate years, the average loss was around US$ 16.03±3.27 million, representing 0.51±0.10% of the mean GDP.

Figure 3-9. Percentage of economic loss by type of damage (a), total economic loss (b), and GDP equivalence (c) by year.

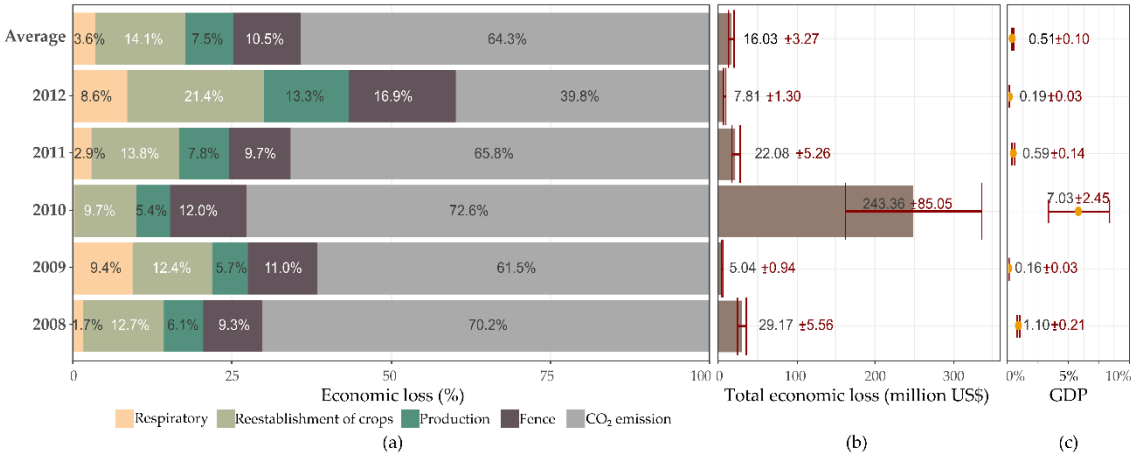


Source: From Author.

Table 3-11. Cost in millions of dollars of losses by fire in Acre state between 2008 and 2012, with a percent of total costs (%) and a related percent of total GDP.

| Type of Impact | 2008 | 2009 | 2010 | 2011 | 2012 | Average |
|---|---|---|---|---|---|---|
| Fence | 2.72(9.3%) | 0.55(11%) | 29.27(12%) | 2.14(9.7%) | 1.32(16.9%) | 1.68(10.5%) |
| Reestablishment | 3.70(12.7%) | 0.63(12.4%) | 23.63(9.7%) | 3.05(13.8%) | 1.67(21.4%) | 2.26(14.1%) |
| Production | 1.78(6.1%) | 0.29(5.7%) | 13.11(5.4%) | 1.72(7.8%) | 1.04(13.3%) | 1.21(7.5%) |
| CO2 emission | 20.49(70.2%) | 3.10(61.5%) | 176.77(72.6%) | 14.52(65.8%) | 3.11(39.8%) | 10.31(64.3%) |
| Respiratory | 0.49(1.7%) | 0.47(9.4%) | 0.57(0.2%) | 0.65(2.9%) | 0.67(8.6%) | 0.57(3.6%) |
| **Total** | **29.17± 5.56** | **5.04± 0.94** | **243.36± 85.05** | **22.08± 5.26** | **7.81± 1.30** | **16.03± 3.27** |
| %GDP | 1.10%± 0.21 | 0.16%± 0.03 | 7.03%± 2.45 | 0.59%± 0.14 | 0.19%± 0.03 | 0.5%± 0.10 |

Source: From Author.

## 3.4 Discussion

### 3.4.1 Spatio-temporal variability of fire dynamics

The eastern flank of Acre was the region with the greatest extent of burned area. This region is historically the epicenter for land use and land cover change, with up to 10% of forests burning twice between 1999–2010 (MORTON et al., 2013) and up to three times, when expanding the time-window from 1984 to 2016 (SILVA et al., 2018b), mostly occurring in Acre's frontier with Pando (Bolivia), Amazonas (Brazil), and Pucallpa (Peru).

The widespread occurrence of fires in 2010 is attributed to the severe drought that occurred in Amazonia as a consequence of the El Niño-Southern Oscillation (ENSO) phenomenon, intensified by the warming of the tropical North Atlantic Ocean (LEWIS et al., 2011; MARENGO et al., 2011). In 2010, the total area burned increased by 16 times in relation to the 2008–2012 average. Using the Burn Damage and Recovery (BDR) algorithm applied to MODIS and LANDSAT images, Morton et al. (2013) found that the total extent of burned forests in 2010 was 9.14 times greater in southern Amazonia than during the 2008–2009 mean. Silva et al. (2018b), applying the Burn Scar Index (BSI) to LANDSAT images in Acre state, found an increase of 166.9 times in the total burned forest area in 2010, when compared to the 2008–2012 mean. These increases were associated with the environmental conditions during severe drought years when fires rapidly spread into forest areas, a fact that does not occur during regular climate years (BRANDO et al., 2014). This statement is supported by the exacerbation of burn scars' occurrence in areas distant from roads and rivers and the total affected forests areas in 2010.

### 3.4.2 Fire occurrence and land tenure relationship

Pasture was the first LULC type burned more in all the regular climatic years. Usually, pasture management with fire during the dry season aims to eliminate accumulated dead material on the ground, which represents a physical barrier to the development of new plants, more palatability, and with a higher nutritive value (COSTA et al., 2011; COSTA, 2008). Furthermore, according to Costa (2008), in the northern Amazon, fire is a widespread practice for increasing pastures' productivity.

Observing at property scales, 8% of the large rural properties presented 52% of the burned areas while less than 2% of the small properties, where there is the prevalence of small producers and family farmers, accounted for 32% of the burnings. This indicates that fire is a widespread tool for management, independently of the land tenure.

Despite this, Soares-Filho et al. (2014) reported that, with the New Forest Code accession, the vegetation management within private properties becomes increasingly essential to mitigate global climate change effects, since about 53% of vegetation is located in these properties. In addition, with the possibility of delimitation and spatial location of properties and preservation areas in the SICAR system, environmental agencies have a

supporting tool to inspect forest management and protected areas in private properties, increasing law enforcement.

Currently, the three main fire-dependent activities in Acre are deforestation, undertaken by all classes of landholders (GODAR et al., 2014), subsistence agriculture by smallholders and pasture management, and recovery by small and medium cattle ranchers. Deforestation-related fires decreased with the reduction in deforestation (ARAGAO; SHIMABUKURO, 2010), a change which is part of a slowdown of the boom-and-bust dynamics of frontier expansion (WEINHOLD; REIS; VALE, 2015). In fact, the "bust" stage appeared to be replaced by the decoupling of agriculture and the rest of the economy from forest suppression and degradation, as evidenced by Weinhold et al. (2015), Tritsch and Arvor (2016), and Caviglia-Harris et al. (2016). In this new development paradigm, which is more adherent to the "industry life cycle" thesis (HALL; CAVIGLIA-HARRIS, 2013), the two other fire causes remain. The first is due to the still limited inclusion of smallholders in the formal economy, as they remain located mainly in remote government-administered settlements with low capacities to generate income and obtain funding (GUEDES et al., 2012). Secondly, barriers to income and funding, which limit capitalization of landholders, also contribute to perpetuating the low-input and extensive cattle ranching, which remains the rule in Amazon (SÁ; ANDRADE; VALENTIM, 2010).

The decrease in fires due to agricultural expansion and intensification is, in fact, a global trend, as argued by Andela et al. (2017) and endorsed for Western Amazonia by our results, where large proprieties decrease its contribution in 9 percentage points through the years, and additionally by the non-correlation between fires and the economic data of the agricultural sector after 2010 (Figure 3-10).

This detachment of fire as a management tool could be explained by the increased effectiveness of agricultural sustainability policy within the context of policies, such as the REDD+ for Early Movers (SILLS et al., 2014), the Sustainable Development Plan (BID, 2011), the farm certification program (AMARAL et al., 2018), the rural-environmental registry (SFB, 2018), the Integrated Plan for prevention and control of deforestation and fires (CEGDRA, 2011), Brazil's Low-Carbon Agriculture (ABC) Plan (MAPA, 2012), or even for a combination of them.

Figure 3-10. Correlation between GDP of the agricultural sector and burned area.

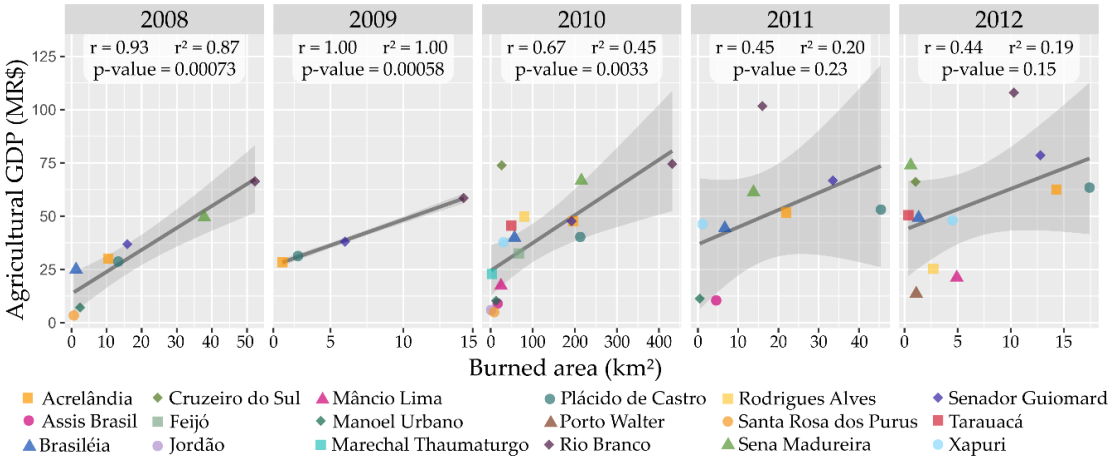


Source: From Author.

Most of those policies are addressed to private properties, however, governmental areas represented, on average, 1.2% of the total burned area in Acre, where Indigenous Lands are often found (~74%). Fire in these lands is part of several subsistence techniques of land clearing, agricultural management, hunting, planting, and religious rituals, being used with precaution and caution in all applications (GRAF, 2016; LEONEL, 2000; PIVELLO, 2011). Graf (2016) argues that fire use for deforestation and soil enrichment for those communities has been gradually eliminated in Acre, thanks to the inclusion of mitigation measures of the Environmental and Territorial Indigenous Management Plans (PGATIs) and through the formation of indigenous agroforestry agents (AAFIs) at these communities.

Another type of protected government area counted in this study were Conservation Units (CU). In Brazil there are two types, one that aims to preserve nature where only the indirect use of its natural resources is allowed, called Units of Integral Protection (UIP), and the other denominated Units of Sustainable Use (USU), that aim to make nature conservation compatible with the sustainable use of a portion of their natural resources and with human occupation. Each CU has their own groups. For UIP there are five types, ecological stations; biological reserves; national parks; natural monuments; and wildlife refuges. For USU, the groups are environmental protection areas; areas of relevant ecological interest; national forests; extractive reserves; wildlife reserves; sustainable development reserves; and private reserves of the natural patrimony (BRASIL, 2000).

In Acre, extractive reserves were the ones with the largest burning throughout the analyzed period (44.09 km², Table 3-9). In these areas, the traditional communities, whose subsistence activities are based on extractives, subsistence farming, and raising small animals, are allowed (BRASIL, 2000). The study of Torres et al. (2017), using a Brazilian firefighters database, revealed that the fire use for land clearing is the main cause of wildfires in the CUs. Incendiarism was the second recurrent cause of wildfires in CUs. With these two anthropogenic causes at the top, the authors showed that there is a strong human pressure on CUs, mainly on their borders. Allied to this, there is an existing agricultural pressure in this region of the Amazon as a whole, as it is now considered a new frontier for agricultural expansion.

### 3.4.3 Environmental, social, and economic impacts of fire

The impact of fire can be felt by different groups and at different scales (NELSON et al., 2013). Here, we look through five distinct components, $CO_2$ emissions, respiratory morbidity, infrastructure damages, future production losses, and crop reestablishment. Our analysis can be considered conservative because these five components are a small part of the whole impact and are at a low scale of what fire impact can influence.

Using deforestation rates given by PRODES (INPE, 2021b) as a baseline and the mean biomass value proposed by Salimon et al. (2011), the average biomass removed by deforestation in Acre between the 2008–2012 period was approximately 6.19±2.26 Tg. This is much higher than the average biomass committed by fire in the same period (0.30±0.5 Tg). However, the fire impacted more biomass (7.02±0.55 Tg) than deforestation (6.37±2.33 Tg) in 2010, due to the extreme drought. Thus, even though the emissions reduction by deforestation in Acre was about 85 Tg $CO_2$ between 2006 and 2010 (NEPSTAD et al., 2012), with the increasing probability of extreme droughts predicted due to climate change and the consequent collateral increasing of fires, the fire-related carbon emissions can substantially increase.

We did not find a clear temporal relationship between the number of cases of respiratory morbidities and the total area burned in each year. However, we found a strong relationship between these variables during the anomalous year. These results confront some of the studies already carried out for the Amazon (DE MENDONÇA et al., 2004; SMITH et al., 2014) or even for Acre (SILVA; SILVEIRA; SILVEIRA, 2008). This

divergence may be associated with other factors or a combination of factors, not accounted here, that could influence illness prevalence (such as vehicle pollution, and access to health assistance). The top three cities in the occurrence of respiratory illness (Rio Branco, Cruzeiro do Sul, and Sena Madureira) are the main centers of each microregion in Acre, being the most populated and developed (IBGE, 2021a). Hence, these cities are likely to concentrate all medical assistance for each region, inflating the amount of hospitalization, even while not showing a higher burned area.

The quantified fire-mediated impacts for the normal years amounted to 0.51±0.10% of the Acre`s GDP for the analyzed period. During 2010 these impacts represented 7.03±2.45% of the GDP, considering just a restrained part of the direct losses (fences, agriculture production, and $CO_2$ emissions) and indirect losses (respiratory illness). By conducting a more comprehensive assessment of direct and indirect impacts, these values will certainly be higher, with larger impacts upon the local economy. Brown et al. (2011) estimated that the economic, social, and environmental losses related to the 2005 burning events in Acre were to the order of US$100 million, which is equivalent to around 0.9% of the GDP. Additionally, De Mendonça et al. (DE MENDONÇA et al., 2004) calculated an economic loss related to 0.2 to 0.9% of the GDP for the Amazon from 1996 to 1999, considering the impact of fire on agriculture, forests, $CO_2$ emissions, and hospitalizations due to respiratory problems.

## 3.5 Conclusions

In five years, fire affected a total area of 2577 km², which represents around 2% of Acre's territorial area, or 1.6 times the area of São Paulo city. Just in 2010, as a consequence of the extreme droughts associated with El Niño and the subsequent warming of the Tropical North Atlantic, the total burn area was 2057 km². We demonstrated that drought effect on fire patterns favors spreading to places farther from the main means of ignition, such as roads and highways, entering protected areas (UC and IL), and areas with restricted use (APP and RL).

Interestingly, the pattern of use of fire in Acre has changed since 2010. The fire was closely linked to the agricultural sector, especially connected to large proprieties, as a tool for deforesting and also for pasture management. However, possibly due to some governmental policies, international pressure, and even the socioeconomic impacts of the

2010 fires, this relationship weakened after the 2010 drought. Additionally, during this later period, the number of properties that use fire as a tool for pasture management and subsistence has decreased.

Fire in traditional communities in the state is small compared to private proprieties, nonetheless, special projects and policies for these communities must continue and the existing ones should be shared with other communities, and even across the Amazon, to ensure minimum fire usage.

The impact of fire is more expressive than we anticipated, however, those five direct and indirect components that were calculated indicated an expressive influence on Acre's economy, representing 0.16±0.03% to 7.03±2.45% of the state's total GDP. The total $CO_2$ emission from fire can be more expressive than deforestation in extreme drought years, while infrastructure damages and production losses represented 27% to 52% of all fire costs.

Quantifying social fire impacts related to respiratory morbidity is complex. The difficulty to establish a robust diagnostic of cause and effect, with relation to fires and respiratory illness, introduces large uncertainties for defining the proportional contribution of these costs to the total economic loss estimates.

Our study showed that the economic impacts of fire can be large, especially in years of extreme drought. The state of Acre must take advantage of the National Policy on Climate Change (PNMC), instituted by Law 12,187/2009, which aims to encourage the development and improvement of actions mitigating greenhouse gas emissions in Brazil and to improve the formulation of environmental policies to restrain fire usage.

# 4 HOSPITALIZATION DUE TO FIRE-INDUCED POLLUTION IN THE BRAZILIAN LEGAL AMAZON FROM 2005 TO 2018

## 4.1 Introduction

Biomass burning in agriculture is, globally, a source of air pollution, and consequently, of morbi-mortality. The practice, which is more frequent in developing countries, especially China, India and Brazil (CASSOU, 2018), but also Indonesia (WATTS et al., 2019), has been evidenced as a source of respiratory illnesses and related hospitalizations (ARBEX et al., 2007; DO CARMO; ALVES; HACON, 2013; KUMAR; KUMAR; JOSHI, 2015, cap. 3; CHAGAS; AZZONI; ALMEIDA, 2016; SHELDON; SANKARAN, 2017; WATTS et al., 2019). Besides having thousands of lives impaired and eventually prematurely taken (REDDINGTON et al., 2015), the supply gaps of the national healthcare are widened and the human and physical resources are even more overloaded.

The Amazon biome is the region with the biggest amount of thermal anomalies of fire in Brazil (INPE, 2020). Historically, fires are set as part of the processes of deforestation, fallow and pasture management, but they may also run out of control and cause forest fires (ALENCAR; RODRIGUES; CASTRO, 2020). In addition to the fact that these events in the Amazon are mainly driven by humans, they are also boosted by climate extremes, such as the anomalous temperatures and droughts (ARAGÃO et al., 2007, 2018), that were stronger and more frequent over the years (1997/98, 2005, 2010, 2015/16).

These fire events release a massive load of pollutants in the atmosphere. Fire smoke is usually composed of primary pollutants, such as particulate matter (PM), carbon monoxide (CO), nitrogen oxides ($NO_x$), and non-methane organic compounds (NMOC), and some of them react to form secondary pollutants such Ozone ($O_3$) and onther secondary organic aerossols (SOA) (REISEN et al., 2015). When in contact with the human respiratory system, these components cause several negative consequences for the health. For instance, $CO_2$ exposure can induce a shortness of breath, cough, fatigue and can also lead to convulsions, coma and death depending on its concentration (PERMENTIER et al., 2017).

Since the process that connects pollution and health is a result of spontaneous social and atmospheric forces, and not a consequence of a controlled experiment randomly assigning pollution levels to locations, the available data for analysis is observational. It thus reveals variations of health measures, like hospitalizations, which are not only due to the variation of pollution. In this case, the econometric approach of quasi-experimental identification is useful, because under reasonable assumptions and after considering the variation of key variables, it manages to retrieve the random portion of pollution variation. This is exactly what the Instrumental Variable (IV)[4] technique does (WOOLDRIDGE, 2018), an it was used elsewhere to identify the effects of pollution on health (SHELDON; SANKARAN, 2017; DERYUGINA et al., 2019; HE; LIU; ZHOU, 2020). This approach is also applied here for the specific case of the Brazilian Amazon in the last two decades (2001-2020).

It should be highlighted that, in this chapter, fire is used as an instrumental variable to support the identification of the effect of pollution on hospitalizations, exploring the positive relationship these two variables generally exhibit (SHELDON; SANKARAN, 2017; GONÇALVES et al., 2018; HE; LIU; ZHOU, 2020). This also allowed, as an useful additional benefit, to account for fire's contribution to hospitalizations (HE; LIU; ZHOU, 2020). The latter was assessed both statistically, with results from the first-stage regression, and numerically, as the fraction of hospitalizations that would be avoided if fires were suppressed. Besides fire and following Deryugina et al. (2019) and Sheldon and Sankaran (2017), wind speed and wind direction were used as additional instrumental variables.

Despite having a huge literature branch that investigates the health consequences of Amazon fires, our contribution is original in addressing two key gaps. The first is the absence of an identification strategy that biases the available estimates of fire-induced pollution on health (that applies, for instance, to Do Carmo et al. (2013), Smith et al. (2014) and Machado Silva et al. (2020) ). Secondly, studies that cover the whole Amazon in long periods are rare, with most evidences belonging to Amazon states or smaller regions and to generally particularly fire-critical periods including one to a few

[4] An instrument variable is a proxy used to substitute the explanatory variable in the main model. Such variable needs to preserve the causal-effect context and the nature of the relationship among the explanatory and the response variables. In additional the IV must satisfy two statistical criteria: (1) it must be exogenous, that is, uncorrelated with the error term of the structural equation; (2) it must be partially correlated with the endogenous explanatory variable.(WOOLDRIDGE, 2018).

years (the case of De Mendonça et al. (2004), Carmo et al. (2010), Jacobson et al. (2014) and Machado-Silva et al. (2020)).

We use a dataset composed of municipal-level data of 805 Brazilian municipalities with four combinations among the three instrumental variables, four types of hospitalization diseases, three age groups, and 12 control variables. All data were monthly aggregated, totalizing 118,335 observations. Our estimates suggest a positive effect of fire in the hospitalization due to respiratory diseases in general and due to asthma in particular. Considering the total range of respiratory diseases, an increase in 1% of fire in the region leads to an average of 0.1383% in the hospitalization numbers, with higher levels of cases during the fire season (Aug-Oct)..

This chapter is structured in five sections, and firstly there is a brief introduction. The second section we describe the data used subdivided by its use in the model (instrumental variable, independent variable and control variable), then explain the way that we aggregated those data in municipality levels and lastly, how we performed the simulation of hospitalization atributable to fires. The third section presents the main results of the data behaviour for the region, the estimates of the econometrics model, the result of the simulation and one validity test. Fourth section introduces a discussion of the results, comparing them to the ones previously observed in the region, also pointing out some improvements in the model. Finally, the fifth section exhibits the main conclusion in the estimation of hospitalization counts due to fire-induced smoke in the Brazilian Legal Amazon over the past 20 years.

## 4.2 Material and methods

### 4.2.1 Study area

The study area comprises the Brazilian Legal Amazon (BLA), that covers approximately 5 million $km^2$ and includes the states of Acre, Amapá, Amazonas, Mato Grosso, Rondônia, Roraima, Tocantins, Pará and only the Maranhão's municipalities over the 44th Meridian (BRASIL, 2007). This area represents around 59% of the Brazilian territory (IBGE, 2020).

However, due to the availability of some data, we consider the full territory of all the states that are within the BLA (Figure 4-1), thus, we used 805 municipalities over the nine states of the BLA.

Figure 4-1. Municipalities within the nine states of BLA used in this study.

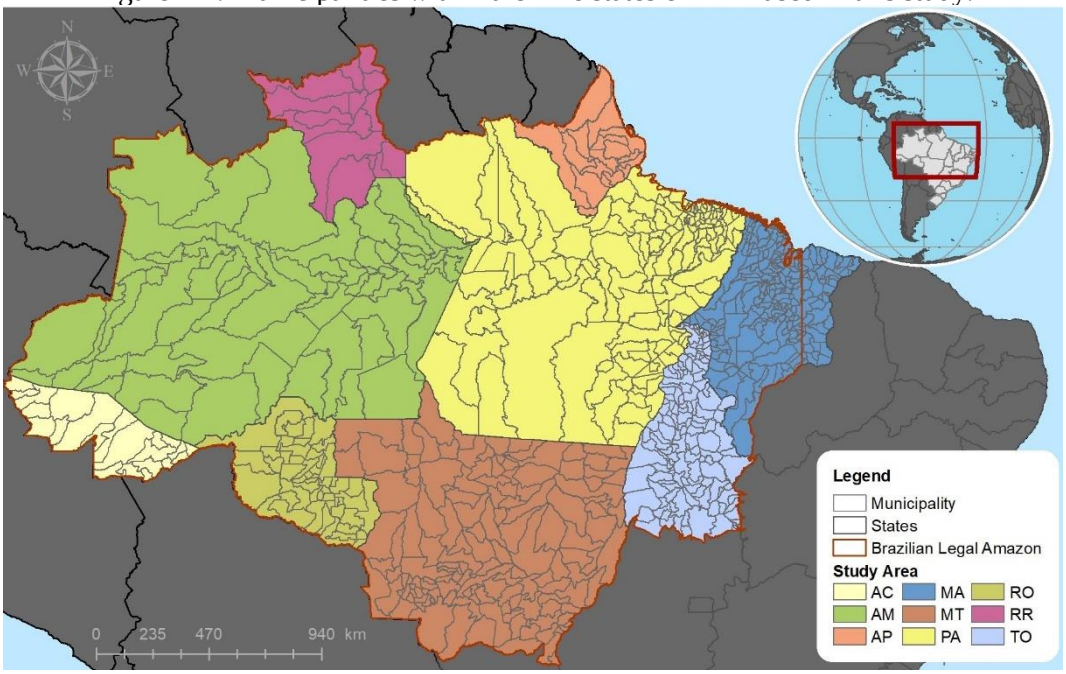


Data base from IBGE (2019).
Source:From Author.

### 4.2.2 Data

According to the econometric technique, three groups were organized: instrumental variables (IV), independent variables(IdV), and control variables (CtV) data (Table 4-1).

Table 4-1. Short description of the data, categorized by type.

| Variable | | | | Time | | | Spatial | | Source |
|---|---|---|---|---|---|---|---|---|---|
| **tp.** | **abr.** | **description** | **agg.** | **period** | **res.** | **agg** | **res.** | **agg.** | |
| IV | BA | Burned Area | Sum | 2000-2020 | d | m | 250m | mc | MCD64A1 |
| | TA | Thermal anomalies* | Sum | 2003-2020 | m | m | 250m | mc | MYD14A1 |
| | WDirec | Wind direction (degree) | Mean | 2001-2020 | m | m | 0.25° | mc | ERA5 |
| | WSpeed | Wind speed (m/s) | | | | | | | |
| IndV | AOD | Land Aerosol Optical Depth (AOD) | Mean | 2001-2020 | m | m | 1km | mc | MCD19A2 |
| | Hosp. | Hospitalization due to respiratory disease (Cap X), by location of residence, and age | Sum | 2001-2020 | m | m | - | mc | DataSUS |

Continues

Table 4-1. Conclusion.

| | | | | | | | | | |
|---|---|---|---|---|---|---|---|---|---|
| IndV | Asthma | Hospitalization due to asthma, by location of residence | Sum | 2001-2020 | m | m | - | mc | DataSUS |
| | Pneumonia | Hospitalization due to pneumonia, by location of residence | | | | | | | |
| | Bronchitis | Hospitalization due to bronchitis, by location of residence | | | | | | | |
| CtV | Pop | Estimated population | Sum | 1992-2019 | y | y | - | uf | DataSUS |
| | GDP | Gross domestic product in thousands of reais | Sum | 2002-2017 | y | y | - | mc | IBGE |
| | Chd_d | Infant mortality by location of residence | Sum | 01/2001-12/2018 | m | m | - | mc | DataSUS |
| | Crn_d | Chronic disease mortality By location of residence, which we considered the sum of the respiratory, cardiovascular, diabetes, and cancers mortality | Sum | 01/2001-12/2018 | | | | | |
| | Employe | Number of health professionals | Sum | 08/2005-12/2019 | | | | | |
| | Beds | Number of hospital beds | Sum | 10/2005-05/2020 | | | | | |
| | Faci. | Number of facilities | Sum | 08/2005 - 05/2020 | | | | | |
| | Temp | Mean, minimum and maximum temperature (kelvin) | Min Mean Max | 2001-2020 | m | m | 1km | mc | MOD11A2 |
| | Precp | Rainfall | Mean | 2001-2020 | m | m | 0.05° | mc | Chirps |
| | Road | Road density (m/m²) | | 2019 | - | m | - | mc | OSM |
| | Urb | Urban zones | Sum | 2001-2020 | y | y | 30m | mc | MapBiomas |
| | Cars | Fleet of Cars registered | Sum | 2005-2019 | m | m | - | mc | Denatran |

**Variable Tp** - Variable type data, among :IV (Instrumental variable data); IdV (Independent variable data), and; CtV (Control variable data); **Variable Abr.** – Abreviation; **Variable Agg.** – Aggregation method; **Time Res** - Is the time resolution of the data, as: d (daily); m (montly), and; y (yearly). **Time Agg.** – Is the time aggregation method used; **Spatial Res.**- is the spatial resolution of the source; **Spatial Agg.** – Is the spatial aggregation used, as by municipality (mc) or states (uf). * Thermal anomalies was used as instrumental variable only in the robustness procedures.
Source: From Author.

#### 4.2.2.1 Instrumental variable data

We use the MCD64A1-v6, product of burned area by Moderate Resolution Imaging Spectroradiometer (MODIS) of Terra and Aqua satellite, collected using the R package "MODIStsp" (BUSETTO; RANGHETTI, 2016). The MCD64A1 has a monthly periodicity, spatial resolution of 500 meters, and its data began in November of 2000. This product uses an association of surface reflectance with active fires, and an algorithm

that checks the temporal changes in the vegetation index (GIGLIO, LOUIS et al., 2015). Globally, it presented 99.7% of overall accuracy, with 40.2% commission error and 72.6% omission error (BOSCHETTI et al., 2019). In the Amazon region, it showed a great similarity to regional and supervised-based product, underestimating 2.9% of the total burned area, but detecting more fires in the north and northwest areas than in the southwest (PESSÔA et al., 2020).

For thermal anomalies, we use the collection 6 from the product MYD14A1 from Aqua MODIS, available on the BDQueimadas website (INPE, 2021a) . This product presents the active fire with date and quality indexes at a global scale, reproducing at 1 km of spatial resolution (GIGLIO, LOUIS; JUSTICE, CHRISTOPHER, 2015). This product is considered a "reference satellite" to *Progama Queimadas* from INPE, and it is the base for comparisons and trend analysis for all the Brazilian territory.

The wind data was obtained using the ERA5 monthly aggregate product, which combines model data with observations across the world, providing a global monthly product with 0.25 degrees spatial resolution (COPERNICUS CLIMATE CHANGE SERVICE, 2019). This product provides the U and V components of the wind, that we convert into wind speed and direction using the "rWind" package (FERNÁNDEZ-LÓPEZ; SCHLIEP, 2019).

#### 4.2.2.2 Independent variable data

Pollutant information was introduced by the Land Aerosol Optical Depth (AOD), gathered by the MCD19A2 version 6 data product and reported in blue band (0.47 $\mu$m). This product is a daily MODIS Terra and Aqua combined multi-angle implementation of atmospheric correction (MAIAC) at 1km spatial resolution (LYAPUSTIN, ALEXEI; WANG, YUJIE, 2018).

The measures of AOD reflect the sum of aerosols from natural and anthropogenic sources, such as emission from industries, vehicles, water vapor, dust and burned biomass (KUMAR, 2010). The product presents a high overall correlation with the ground measurements (≅ 95%) over South America, and is better over the forest, savanna, grassland, and cropland (MARTINS et al., 2017). Moreover, the AOD has been widely used to estimate highly dangerous pollutants for the human respiratory system with

considerable accuracy, such as the particulate matter (PM) (GUO et al., 2017; CHUDNOVSKY et al., 2013).

Hospitalization counts were gathered into TabNet (DATASUS, 2020), which is a governmental platform maintained by the DataSUS (*Departamento de Informaçoes do SUS*). We collect four different morbidities that are most related to the long exposure to fire pollution: disease of the respiratory system (ICD-10: X.[5]); Asthma (ICD10: J45-J46); Pneumonia (ICD-10: J12-J18); and Bronchitis (ICD-10: J20-J21).

This information was filtered by municipalities, place of residence and month of attendance. Due to the vulnerability of children and elderly people to fire pollution, we also collected the amount of hospitalizations caused by respiratory issues by age groups, totalizing 4 variables: small children ($\leq$ 4 years old), children (between 5 and 14 years old), elderly ($\geq$ 65 years old), and total (all age range).

#### 4.2.2.3 Control variable data

Estimated population data was collected from DataSUS portal (DATASUS, 2020), that compiles the yearly IBGE estimates produced to compatible data to the Brazilian legal provisions. This data is available yearly for each Brazilian municipality from 1992 until 2019.

Gross Domestic Product (GDP) is provided by the IBGE (IBGE, 2021b), and it is released yearly by municipality, in current prices and aggregated.

Infant Mortality and Chronic diseases are variables of the health level, as proposed respectively by Aquino et al. (2009) and Harris & Kohn (2018). The information was collected from DataSUS portal, filtering by municipality of residence and month of attendance. Infant mortality refers to the death of fetal and children under one year old. As Chronical disease, we considered four groups, like determined by Malta et al. (2014). These groups are: mortality caused by cardiovascular diseases (ICD-10: I00 to I99), cancer (ICD-10: C00 to C97), respiratory issues (ICD-10: J30 to J98), and diabetes (ICD-10: E10 to E14).

[5] Hospitalization code following the International Classification of Disease (ICD-10), where disease of the respiratory system were those between J00 and J99.

Other data used and related to the capacity of attendance were: the number of employees, the number of beds and the number of facilities. They were also obtained from DataSUS portal.

Weather information came from two different products. The temperature was acquired from MOD11A2, which provides an average 8-day of Land Surface Temperature with a 1 km spatial resolution (WAN, ZHENGMING; HOOK, SIMON; HULLEY, GLYNN, 2015).

The precipitation data came from CHIRPS (The Climate Hazards Group InfraRed Precipitation with Station data), which is a global rainfall dataset with 0.05° spatial resolution (FUNK et al., 2015). The product has a good performance either globally and locally, and particularly in the BLA its values explain 73% of the precipitation with a root mean square error (RMSE) below 15 mm (ANDERSON et al., 2018).

In order to infer about urban pollution, data related to road density, fleet of cars and urban zones were used. To generate road density, the road component was extracted from the total roads network provided by the Open Street Map (OSM, 2020) and the area of municipalities was provided by the IBGE. Fleet of cars was found on the DENATRAN website (MINFRA, 2020), which provides the number of registered cars by month and by municipality.

Lastly, urban density was measured using the MapBiomas product. This land use and land cover data are available annually from 1985 to 2018 with 30m of spatial resolution, based on Landsat images and produced using a pixel base classification and machine learning (MAPBIOMAS, 2021a; SOUZA et al., 2020).

### 4.2.3 Spatial aggregation

To the spatial data (BA, TA, Wind, AOD, Temperature, Precipitation, Roads and Urban zones) we used the *Google Earth Engine* to clip and aggregate them by municipality. Then, the exported tables were processed in the *RStudio* environment to merge all variables (spatially and non-spatially explicitly) into one single table compatible to *Stata* format.

It is worth mentioning that along 20 years of data, the municipalities boundaries suffered several legal updates, including the creation of new municipalities. To follow those changes, we used each annual current delimitation provided by IBGE to perform each clip and aggregation.

### 4.2.4 Empirical model

Let the hypothesis grounding data analysis, which is suggested by atmospheric science and epidemiological literature, be presented (CARMO et al., 2010; IGNOTTI et al., 2010; GONÇALVES et al., 2018). Once burnings of considerable size and number occur in a location, pollutants are released and transported through the atmosphere causing considerable appearance or exacerbation of respiratory illnesses. This process is a function of many variables. Fire emissions are, primarily, affected by the fuel type, the temperature of the fire and climatic conditions (URBANSKI; HAO; BAKER, 2008). In the atmosphere, fire pollution may be mixed with pollutants of vehicular or industrial sources, and is also affected by weather conditions (BERNARD et al., 2001). Finally, the number of hospitalizations is influenced by the number of inhabitants, their levels of health and income and the availability of health facilities and staff (CHAGAS; AZZONI; ALMEIDA, 2016; LIU; AO, 2021).

With that in mind, to evaluate the impact of fire-induced pollution on health, we follow the methodology proposed by (SHELDON; SANKARAN, 2017; DERYUGINA et al., 2019; ROCHA; SANT'ANNA, 2020; HE; LIU; ZHOU, 2020), who use the Instrumental Variable (IV), as an approach in which the wind is the exogenous source of variation used to identify the effect of pollution on respiratory morbidity – He et al. (2020) and Sheldon and Sankaran (2017) also adopt fire as a second instrument. The IV Method is based on the two-stage least squares estimator (2SLS) that corresponds to the Equation 4.1 and Equation 4.2 below, with "i" indexing spatial unit and "t" time period.

$$LogAOD_{it} = \alpha_0 + \alpha_1 IV_{it} + \alpha_2 \mathrm{CrV}_{it} + b_i + \varepsilon_{it} \quad (4.1)$$

$$LogHosp_{it} = \beta_0 + \beta_1 \widehat{LogAOD}_{it} + \beta_2 CrV_{it} + c_i + u_{it} \quad (4.2)$$

$LogAOD_{it}$ is the logarithm of atmospheric optical depth; $IV_{it}$ is a set of instrumental variables; $CrVi_t$ is the control variable vector; Log$Hosp_{it}$ , which is the logarithm of hospitalization count, is the independent variable; $\alpha_{it}$ and $\beta_{it}$ are time-invariant unobserved

heterogeneity terms; $\mathcal{E}_{it}$ and $u_{it}$ are the error of the model, $b_i$. and $c_i$. are unknown parameters.

Regarding the $IV_{it}$ vector, three instrumental variables were employed, burned area (Ba) in logarithmic form (LogBA), wind direction (WDirec) and wind speed (WSpeed). These were combined, either in original form or as interactions (denoted with "*"), into four alternative sets of variables. All of them included LogBA separately. The first and most comprehensive included the two interactions of burned area with the two wind measures (i.e.,Ba * WSpeed and Ba * WDirec). The second and third sets included only one of the possible fire-wind interactions (either Ba * WSpeed or Ba * WDirec). The fourth and least comprehensive did not include any interactions (only LogBA). The last three sets were used as potential alternatives to estimation in case the most comprehensive set was rejected in its validity by the tests employed. In this way, the least compreehensive was the last possible alternative in case the two double instrument sets were rejected.

Now regarding the $CrV_{it}$ vector, the control variables captured factors influencing supply and demand for health care. They were structured to indicate:

- Health level of the population, represented by infant mortality (Chd_d) (AQUINO; DE OLIVEIRA; BARRETO, 2009; BARUFI; HADDAD; PAEZ, 2012) and chronic disease mortality (Crn_d);
- Healthcare supply capacity represented by the number of health professionals (Emp), number of hospital beds (Beds) and number of health facilities (Faci);
- Sociodemographic factors, such as: estimated population (Pop), gross domestic product (GDP), urban zones (Urb), road density (Road) and fleet of cars (Cars);
- Weather, indicated here by: the temperature (Temp) and rainfall (Precp).

Those variables are crucial in estimation, once they address weather and socioeconomic confounders that could bias the estimation of the causal effect of pollution on hospitalizations. If these variables were not included, the factors that they capture would be left to the disturbance terms, thus creating omitted variable bias (WOOLDRIDGE, 2018).

The identification strategy was applied to the whole count of hospitalizations and to counts associated with specific ages and illnesses. Confounders, whose influence is

mitigated by the IV approach, may affect illness propensity in the form of viral, bacteriological and environmental factors varying across illnesses (POPE 3RD, 2000; NUNES; IGNOTTI; HACON, 2013). Therefore, by adopting alternative dependent variables, the performance of identification strategy was more broadly assessed, which was based on amounts of hospitalization due to asthma, pneumonia and bronchitis and as well as hospitalization of small children (aged 0 to 4), children (5 to 14) and elderly people (> 65).

The estimation was carried out on *Stata 14.1* program, with a balanced panel structure (at a monthly-municipal level) with fixed effects (state, year and month) and a heteroskedasticity-autocorrelation "robust" variance-covariance estimator. To check if the approach used was valid, the following testing sequence was adopted:

1 Generalized Hausman test for the null of consistency of the random-effects estimator (no omitted heterogeneity bias) against the alternative of consistenty of the fixed-effects estimator. Applying the "xtoverid" command from Schaffer and Stilman (2006);
2 Pollution exogeneity test for the null that ordinary least squares (OLS) would yield consistent estimates over the IV estimates, i.e., pollution is exogenous. For this, "dmexogxt" command from Baum and Stillman (1999) was applied;
3 Sargan's overidentification test for instrument validity which assumes validity under the null hypothesis that all instruments are valid, while rejection is interpreted as indicating that at least one of the instruments is not valid (CAMERON; TRIVEDI, 2009). For this, the "xtoverid" from Schaffer and Stilman (2006) command was used;
4 Tests for instrument weakness in the first stage, which was based on postestimation procedures with robust covariance matrix:
    a. Joint significance of the instruments (robust F test), with the test statistic compared to the rule-of-thumb value of 10, as proposed by Staiger and Stock (1997 apud; SHAO et al., 2019)[6];

[6] The IV rule of thumb is a practice in the econometric field when you are using the instrumental variable technique. That suggest a minimum value of test F, which is 10 (STAIGER; STOCK, 1997 apud; SHAO et al., 2019).

b. Stock and Yogo IV weakness test, which presumes homoscedastic errors in the instruments, and its null hypothesis is that the instrument is weak. This is rejected whenever the "minimum eigenvalue statistic" (CAMERON; TRIVEDI, 2009) exceeds the "critical value" of the (2SLS) estimator at 10% level.

When exogeneity was not rejected in step 2, OLS estimation was applied. Conversely, IV estimation was pursued, and for this, all four instruments were initially used. Then, if this set of instruments was not accepted in step 3, the list was piecewisely reduced until no instrument was deemed invalid or only one instrument remained.

### 4.2.5 Simulation: hospitalizations attributable to fires

In order to estimate the percentage of hospitalizations attributable to fires, the following procedure was pursued. It is important to have the corrections suggested by Wooldridge (2018, cap. 6) initially clarified, for models estimated with logarithmic forms, which were applied to end with predicted hospitalizations in non-logarithmic form. The predictions for the logarithm of hospitalizations were exponentiated, generating $\widehat{m}_i = exp(\widehat{logy_i})$; then a simple linear regression was run, with a null intercept, between the observed values (yi) and the predicted ones ($\widehat{m}_i$); finally, the slope of this regression was extracted, and this was considered the correction factor of the values ( $\breve{\alpha}_0$), which can also be described by the following equation (Equation 4.3).

$$\breve{\alpha}_0 = \left(\sum_{i=1}^{n} \widehat{m}_i y_i\right).\left(\sum_{i=1}^{n} \widehat{m}_i^2\right)^{-1} \tag{4.3}$$

The correction consisted of taking $\breve{\alpha}_0 \widehat{m}_i$ as the prediction. With this, the count of hospitalizations attributable to fires was calculated as the difference between hospitalizations predicted for the observed level of fires and for a counterfactual null fire level. This was pursued, as detailed in equations below, starting with the first-stage fire-pollution model (4.4.c and 4.4.e), then proceeding to the second stage pollution-hospitalization model (4.4.b and 4.4.d).

$$Hospitalizations\ attributable\ to\ fires \equiv \breve{\alpha}_0 \widehat{Hosp}_{it}^{0} - \breve{\alpha}_0 \widehat{Hosp}_{it}^{1} \tag{4.4.a}$$

$$\widehat{Hosp_{it}^{0}} = \widehat{\beta_0} + \widehat{\beta_1}\widehat{LogAOD_{it}^{0}} + \widehat{\beta_2}CrV_{it} \quad (4.4.b)$$

$$\widehat{LogAOD_{it}^{0}} = \widehat{\alpha_0} + \widehat{\alpha_1}IV_{it} + \widehat{\alpha_2}\mathrm{CrV}_{it} \quad (4.4.c)$$

$$Hosp_{it}^{1} = \widehat{\beta_0} + \widehat{\beta_1}\widehat{LogAOD_{it}^{1}} + \widehat{\beta_2}CrV_{it} \quad (4.4.d)$$

$$\widehat{LogAOD_{it}^{1}} = \widehat{\alpha_0} + \widehat{\alpha_1}.0 + \widehat{\alpha_2}\mathrm{CrV}_{it} \quad (4.4.e)$$

## 4.3 Results

### 4.3.1 Database behaviour

Despite having available data of the last two decades (2001-2020), some of them are not accessible, therefore, the time windows analysis is between August 2005 and December 2018. The main descriptive metrics of all data used is listed on Table 4-2. For the main variables (Burned area, AOD and Hospitalizations) we also presented the descriptive statistic spatially (Figure 4-2) and in a temporal way (Figure 4-3).

Table 4-2. Descriptive statistics of the data, subdivided by type and calculated at a municipality level and monthly.

| Type | Variable | Unit. | Mean | Std. Devia. | Min | Max |
|---|---|---|---|---|---|---|
| IV | BA | km² | 13.1 | 87 | 0 | 5,010 |
| | TA | # | 14.25 | 73.06 | 0 | 6,814 |
| | WDirec | degree | 1.39 | 1.02 | 0.002 | 7.72 |
| | WSpeed | m/s | 235.68 | 42.48 | 0.03 | 359.95 |
| IndV | AOD | - | 0.24 | 0.17 | 0.03 | 3.35 |
| | Hosp. | # | 20.62 | 56.31 | 0 | 1,676 |
| | Small Children | # | 7.98 | 31.31 | 0 | 1215 |
| | Children | # | 2.54 | 7.60 | 0 | 232 |
| | Elders | # | 3.61 | 8.46 | 0 | 210 |
| | Asthma | # | 3.10 | 10.42 | 0 | 424 |
| | Pneumonia | # | 11.34 | 33.39 | 0 | 1092 |
| | Bronchitis | # | 0.73 | 5.42 | 0 | 264 |
| CtV | Pop | # | 32,295 | 100,855 | 931 | 2,130,264 |
| | GDP | mil R$ | 463,997 | 2,493,686 | 5,606 | 73,200,000 |
| | Chd_d | # | 0.83 | 2.69 | 0 | 71 |
| | Crn_d | # | 0.53 | 2.34 | 0 | 72 |
| | Employe | # | 288 | 1,159 | 0 | 28,166 |
| | Beds | # | 65 | 267 | 0 | 5,099 |
| | Faci. | # | 24 | 91 | 0 | 1,999 |
| | Temp_max | K | 309.7 | 4.7 | 299.0 | 353.9 |
| | Temp_med | K | 303.6 | 3.3 | 290.6 | 320.0 |
| | Temp_min | K | 297.3 | 6.0 | 247.7 | 314.8 |
| | Precp | mm | 5.24 | 4.46 | 0.00 | 29.05 |
| | Road | m/m² | 4.65 | 14.41 | 0.01 | 242.00 |
| | Urb | % | 0.33 | 1.73 | 0.00 | 30.29 |
| | Cars | # | 6,780.07 | 29,523.87 | 1.00 | 689,937 |

IV (Instrumental variable data); IdV (Independent variable data), and; CtV (Control variable data).
Source: From Author.

Figure 4-2. Spatialization of the time series average for burned area, AOD and total hospitalizations, aggregated by municipalities.

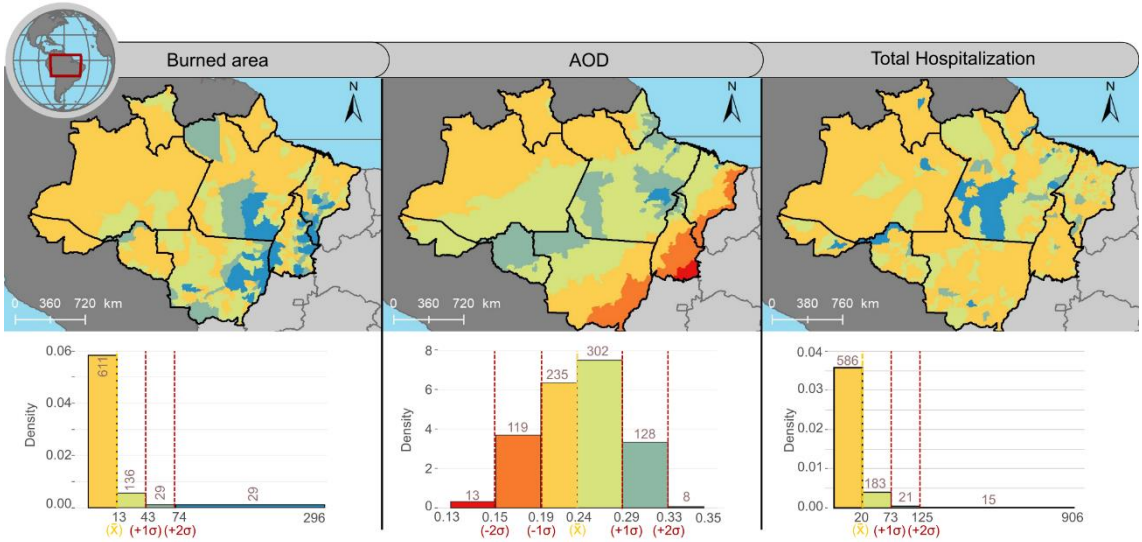


Note: The bar plot represents the histogram of the spatialized variable, where the bar shows the number of municipalities in each class, and the vertical lines exhibit the mean (yellow) and de first and second deviation (red).
Source: From Author.

Figure 4-3. Temporal variation in monthly average values for burned area, AOD and total hospitalizations.

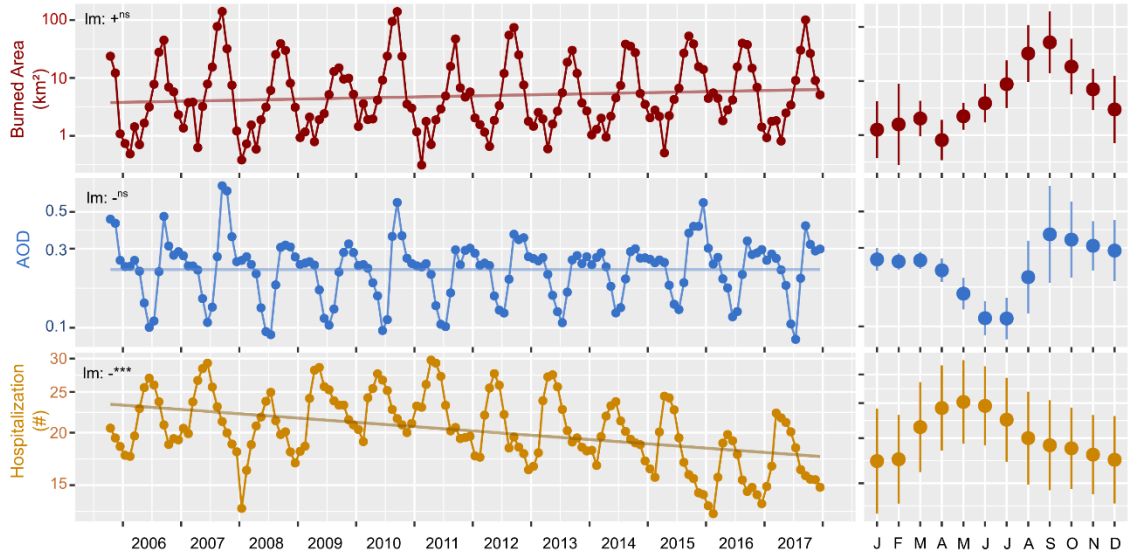


Source: From Author.

The average burned area by municipality is about 13 km² (± 87 km²), and the highest values were found on the triple border of Mato Grosso-Tocantins-Pará and in the border between Tocantins and Maranhão. The distribution of the values is asymmetrical for the region, with more municipalities with values below the time series average (2005-2018). Among the 805 municipalities that belong to the database, approximately 11.20% of the

municipalities (90 ± 88) have a monthly burned area above the average, while 88.80% (715 ± 88) of them have values below. Of those municipalities with values below the average, approximately 75% (538 ± 163) do not have values for burned area, but this feature varies throughout the year, reaching the maximum of 783 municipalities at the beginning of the year, and the minimum of 203 during the burning season.

On average, hospitalizations due to Pneumonia (11.34) are higher than Asthma (3.10) and Bronchitis (0.73). Considering their proportion among the total hospitalizations due to respiratory diseases, we have a contribution, respectively, of 55%, 15% and 4%. Thus, these illnesses together represent around 74% of all hospitalizations, while the other 26% are composed of other respiratory diseases such as pharyngitis, laryngitis and flu. The distribution of hospitalizations for respiratory diseases follows the asymmetric pattern, where the 15 municipalities with the highest values (over 2 deviations) are mostly in the state of Pará.

From the age group perspective, the average monthly contribution of the Small Children group represents approximately 39% of the total, while Children and Elders represent, respectively, 12% and 18%. Thus, the contribution of Small Children and Elders, together, represents more than half of those hospitalized monthly for respiratory diseases, emphasizing once again the vulnerability of these groups.

The AOD values vary between 0.03 and 3.35, with an average of 0.24 for the region. Its distribution follows a normal pattern, in which extreme values are found at the border of the BLA (less than 2 deviations) and in an area that goes from Rondônia to the northern border of Pará with Maranhão (greater than 2 deviations).

The variation of the main variables over the time (Figure 4-3) shows that the peaks between the variables are not the same. For the burned area, the average monthly values show two distinct peaks, one at the beginning of the year (Feb-Mar) and another at the end (Aug-Sep), the AOD values show a valley in the middle of the year (Jun-Jul) and the hospitalizations peak is in May.

The Figure 4-4 presents the monthly variation of the burned areas considering the wind speed and the prevailing wind direction. Between June and September, the period that covers the burning season in the region, there is the presence of winds coming from the

Northwest, and the average speed increases reaching the maximum between Aug-Sep, the peak of fire. Subsequently, the wind pattern returns to the Southwest direction, with winds that can reach up to 8 m/s.

Figure 4-4. Monthly variation in mean values of burned area (log) considering the predominant wind speed and meteorological direction for the BLA region.

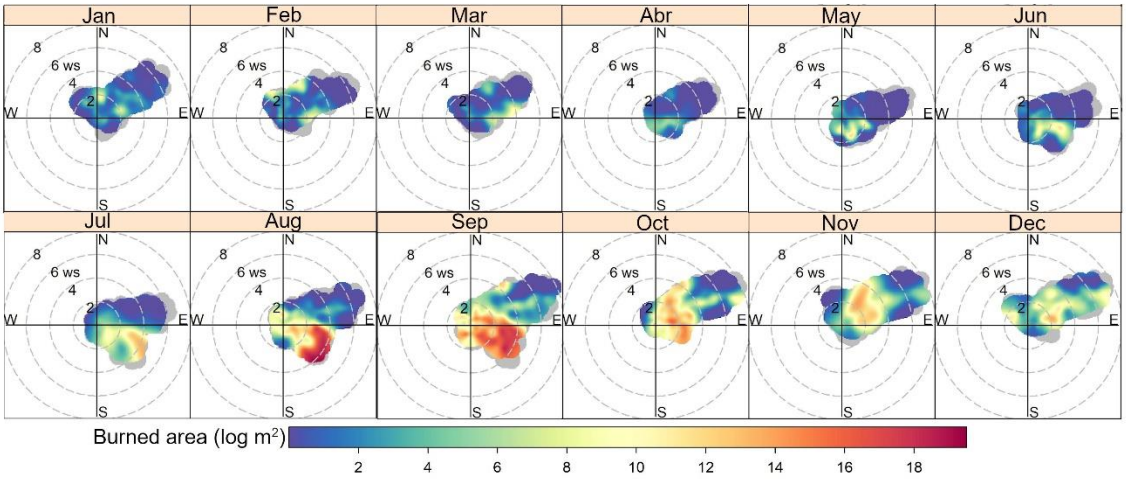


Source: From Author.

### 4.3.2 Econometrics estimates

A first and descriptive assessment of "weak instrument", that is, of the possibility that the instrument is not significantly related with pollution, is provided by the correlation between the instruments and the pollution (explanatory variable), and it is shown on Table 4-3. Only the logarithm of burned area (LogBA) did not exhibit a significant correlation with pollution, violating the instrument relevance requirement. Nevertheless, this is not a final evidence as it is biased by socieconomic and weather confounders that are addressed by the multivariate approach afterwards (see "weak instrument test" in table 4-4).

Table 4-3. Correlation between the instrumental variables and the explanatory variable.

| | LogBA | BaWSpeed | BaWDirec |
|---|---|---|---|
| AOD | $0.0023^{ns}$ | -0.0672*** | -0.0644*** |

Significance level: "***" p<0.001, "**" p<0.01, "*" p<0.05, "."p<0.1, "ns" not signifcant.
Source: From Author.

The Table 4-4 presents the results obtained with the estimator that was indicated by the four-step test procedure for each dependent variable. Detailed estimation results, also containing control variables and all the set of instruments (LogBA, BAWSpeed and

BAWDirec) and estimators (OLS, 2SLS, fixed effects and random effects) are presented in the APPENDIX A -.

Table 4-4. Summary of the best model fitted of the variation in the Aerosol Optical Depth (AOD) in hospitalization counts due to the thermal anomalies, presented by age and respiratory illness type.

| Disease | **Respiratory System** | | | | **Asthma** | **Pneumonia** | **Bronchitis** |
|---|---|---|---|---|---|---|---|
| Age | **All** | **Small children** | **Children** | **Elderly** | **All** | **All** | **All** |
| Estimator | IV | IV | IV | OLS | IV | IV | OLS |
| IV set | IVc01 | IVc04 | IVC04 | - | IVc01 | IVc04 | - |
| Pollution coefficient | 0.1383*** | -0.3381*** | -0.1815* | 0.00215*** | 0.0792*** | -0.1790$^{ns}$ | 0.0103** |
| IV exogeneity and validity tests | | | | | | | |
| Exog | 13.82*** | 20.9530*** | 7.6436** | - | 6.63** | 7.6513** | - |
| Overid | 1.20 ns | - | - | - | 3.56 ns | - | - |
| Weak Instrument tests | | | | | | | |
| Joint | 1103.36 | 252.589 | 252.589 | - | 1103.36 | 252.589 | - |
| Yogo: stat | 1445.95 | 282.652 | 282.652 | - | 1445.95 | 282.652 | - |
| Yogo: crit | 22.3 | 16.38 | 16.38 | - | 22.3 | 16.38 | - |
| Fixed effects | Y | Y | Y | Y | Y | Y | Y |
| Controls | Y | Y | Y | Y | Y | Y | Y |
| Obs. | 118,335 | 118,335 | 118,335 | 118,335 | 118,335 | 118,335 | 118,335 |

Notes: Estimator: IV is for instrumental variable two-stage least squares method; and OLS is for Ordinary Least Squares. IV Set is the possible instrumental combination: IVc01 is the Log_Ba plus the BaWSpeed and the BaWDirec; IVc02 is the Log_Ba plus the BaWSpeed; IVc03 is the Log_Ba plus the BaWDirec, and; IVc04 is only Log_Ba. "*Exog.*", computes a test of exogeneity for pollution based on a fixed-effect regression estimated via instrumental variables; "*Overid*" is the Sargan-Hansen statistic for instrument overidentification test. "*Joint*", for the joint significance test of the instruments in the first stage regression; "*Yogo: stat*", is the value of the Stock and Yogo test for instrument weakness; "*Yogo: crit*", is the table value for the Stock and Yogo test. Significance level: "***" p<0.001, "**" p<0.01, "*" p<0.05, "."p<0.1, "*ns*" not significant.
Source: From Author.

It should be noted that for all models tested, the value of the *Hausman* test indicated a significant difference between the coefficients generated by the fixed and random effects estimators, indicating consistency only for the first.

Among the four batch of instruments, the IV sets IVc01 (LogBa + BaWSpeed + BaWDirec) and IVc02 (LogBa + BaWSpeed) was the one that met all criteria in the four-step testing for a valid instrument (Section 4.2.4) for the total hospitalization dependent variable. However, according to the pre-defined testing order, the larger set, IVc01, was considered the main one for estimating the effect of pollution from fires on Total

hospitalizations for respiratory diseases in the BLA. According to the model, if the AOD increase 1% it causes an increase of approximately 0,1383% in the total of hospitalizations in the region, considering a regular increase of 1 SD (0.17) it will imply an increase of 2.35% in the hospitalizations.
Positive values, in addition to that presented for the Total hospitalizations, were also estimated for Asthma, whose estimates using the set of instruments IVc04 determined an increase of approximately 0.08% in hospitalizations for each rise of 1 % in AOD levels.

On the other hand, a negative coefficient was estimated for Small Children, Children and Pneumonia. For all of these models, the set IVc04 (LogBa) passed the four-step test for a valid instrument, indicating that each increase of 1% in AOD levels decreases the hospitalization of Small Children in 0.34% ($p<0.001$), 0.18% ($p<0.01$) in Children, and 0.18% ($p>0.1$) for Pneumonia. The last one presented a higher global significance (p-value), which indicates that changes in the Pneumonia's hospitalizations are not associated with the AOD.

For Elderly and Bronchitis equations, pollution was exogenous and thus OLS estimation was implemented, resulting in, respectively, 0.002% ($p<0.001$) and 0.0103% ($p<0.01$) effects on hospitalization.

### 4.3.3 Hospitalization attributable to fires

Based on the best set of instruments observed for each group of respiratory diseases, we perform the estimates of the hospitalizations. Thus, Figure 4-5 shows the average percentage of projected monthly hospitalizations for the Total Hospitalization and for Asthma, both using the set IVc01.

Total Hospitalization due to fires varies from 42 cases (0.25% in September) to minus 30 cases (-0.17% in November), with a positive monthly average only for the months of August (8 cases , 0.044%), September (3 cases, 0.014%) and October (3 cases, 0.020%). On the other hand, Asthma hospitalizations due to fires ranged from 4 individuals (0.115% in September) to minus 1 (0.03% in April), with a positive monthly average for the months of August (0.4 cases, 0.013%), September (0.3 cases, 0.007%) and October (0.2 cases, 0.007%).

Figure 4-5. Estimates of total hospitalizations and Asthma hospitalizations due to fires (%).

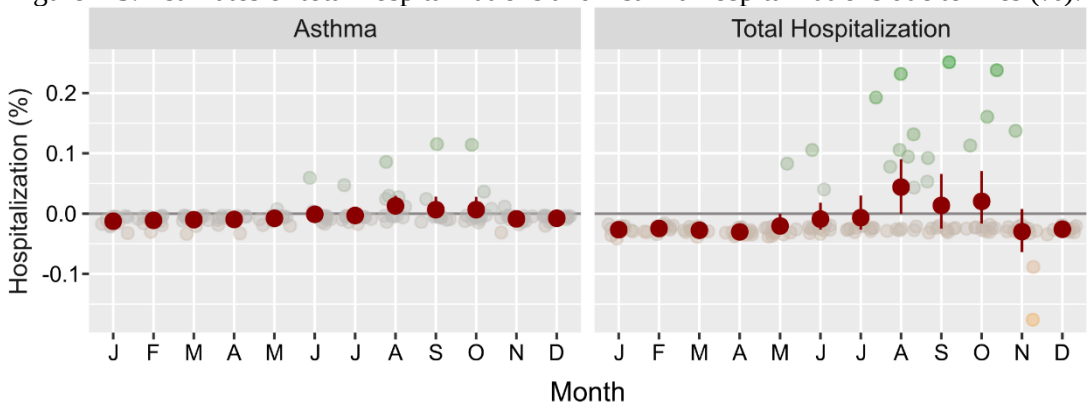


Source: From Author.

### 4.3.4 Robustness check

In order to verify the sensitivity of the effects and the general consistency of the results obtained, a robustness test was carried out by replacing the values of burned area for thermal anomalies. The correlation of the rebuilt instruments with the explanatory variable (AOD), is shown on Table 4-5, where all the new instruments presented positive and significant values.

Table 4-5. Correlation among the instrumental variables and the explanatory variable.

| | Log_TA | TaWSpeed | TaWDirec | Log_BA |
|---|---|---|---|---|
| AOD | 0.1672*** | 0.0323*** | 0.1002*** | 0.6892*** |

Significance level: "***" p<0.001, "**" p<0.01, "*" p<0.05, "."p<0.1, “ns” not signifcant.
Source: From Author.

The variation among the years and its average by month (Figure 4-6), show a similar seasonality as presented by the burned area, in which the count increases from May on, reaching its peak in Aug-Sep. However, the low peak of the beginning of the year (Feb-Mar) is not visible as observed for the burned area.

Figure 4-6. Temporal variation in average monthly values of thermal anomalies for the region.

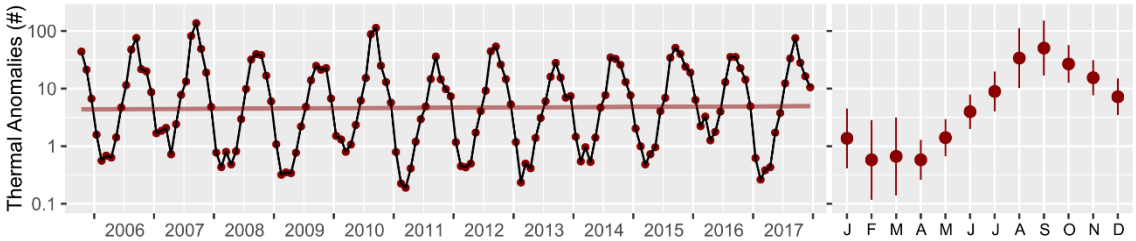


Source: From Author.

The Table 4-6 presents the best results obtained from each of the seven models analysed, using thermal anomalies as an instrumental variable, as well as their interaction with the wind direction and the wind speed. The use of this product returned negative results for all models in which method IV was satisfactory (Total, Small Children, Children, Elders, Pneumonia and Bronchitis), whereas for the only model estimated by the OLS method (Asthma) the effect of AOD on hospitalizations for respiratory diseases was positive.

Table 4-6. Mean effect of the variation in the Aerosol Optical Depth (AOD) on hospitalization due the thermal anomalies, presented by age and respiratory illness type.

| Disease | **Respiratory System** | | | | **Asthma** | **Pneumonia** | **Bronchitis** |
|---|---|---|---|---|---|---|---|
| Age | **All** | **Small Children** | **Children** | **Elders** | **All** | **All** | **All** |
| | | | | **OLS** | | | |
| AOD | 0.0443 *** (0.0072) | 0.0177 ** (0.0067) | -0.0061 ns (0.0051) | 0.0215 *** (0.0051) | 0.0265 *** (0.0060) | 0.059401*** (0.0069) | 0.0103 ** (0.0032) |
| OLS sig. | 2925.84 *** | 2114.69 *** | 1139.8 *** | 1460.89 *** | 1040.86 *** | 2391.69 *** | 677.16 *** |
| | | | | **2SLS** | | | |
| AOD | -0.0799 * (0.0333) | -0.2493 *** (0.0349) | -0.1250 *** | -0.0405 * (0.0190) | 0.0483 ** (0.0176) | -0.1237 *** (0.0351) | -0.0488 ** (0.0155) |
| 1S sig. | *** | *** | *** | *** | *** | *** | *** |
| 2S sig. | *** | *** | *** | *** | *** | *** | *** |
| Set of Instr. | 4 | 4 | 4 | 2 | 1 | 4 | 4 |
| Exogeneity and IV validity tests: | | | | | | | |
| Exog. | 20.71*** | 128.64*** | 38.12*** | 14.79*** | 3.06. | 49.23*** | 22.67*** |
| Overid. | - | - | - | 0.4 ns | 8.25* | - | - |
| Week Instrument tests: | | | | | | | |
| Joint | 2876.23*** | 2876.23*** | 2876.23*** | 2177.03*** | 2482.61*** | 2876.23*** | 2876.23*** |
| Yogo: stat | 4782.32 | 4782.32 | 4782.32 | 3915.95 | 4311.03 | 4782.32 | 4782.32 |
| Yogo: crit | 16.38 | 16.38 | 16.38 | 19.93 | 22.30 | 16.38 | 16.38 |

Notes: "*OLS sig.*", is the global significance calculated by the *Wald*; "*1s sig.*", stands for the global significance of test *F* for the first stage; "*2s sig.*" is the global significance *Wald* test for the second stage; "Set of Instr." is the order of the instrument set, where: 1 are LogTA + TaWSpeed + TaWDirec; 2 are LogTA + TaWDirec; 3 are LogTA + TaWSpeed; 4 is LogTA. "*Exog.*", computes a test of exogeneity for a fixed-effect regression estimated via instrumental variables; "*Overid*" is the Sargan-Hansen statistic for instrument overidentification test. "*Joint*", for the joint significance test of the instruments in the first stage regression; "*Yogo: stat*, is the value of the Stock and Yogo test for instrument weakness; "*Yogo: crit*", is the table value for the Stock and Yogo test. Significance level: "***" p<0.001, "**" p<0.01, "*" p<0.05, "."p<0.1. Blue-colored cells represent the best method fit for the model.
Source: From Author.

## 4.4 Discussion

The coeficcient (0.1383%) estimated for Total Hospitalization was tenfold larger than the one calculated by Rocha and Sant'anna (2020) for BLA[7], in which using the interaction between the wind direction and pollutants from neighboring municipalities as an instrumental variable, they found out that the increase of 17.3 μ/m³ (one standard deviation or 107% increased upon the average) in PM2.5 levels causes on average about 1.5% (0.95 hospitalizations per 100 thousand inhabitants) in total hospitalizations.

Additionally, the negative coefficient obtained for *Small Children* and *Children* is the opposite from the results previously found in the BLA by Carmo et al. (2010), Jacobson et al. (2014) and Rocha & Sant'anna (2020). It can be a reflex of the data used in the analysis, which present a difference peak between fire and hospitalization (which is in the humid season); and the measured impact is linked to the short-term response, while the pollution effect is accumulated over the time. Or as presented by Andrade Filho et al. (2013), some regions in the Amazon the hospitalizations due to respiratory diseases, especially in Children, are more associated with the humidity than the pollution aerosols.

For Elderly and Bronchitis the IV approach was not significant, being used the OLS method to obtain the estimates. This result is the opposite of those founded by Deryugina et al. (2019) and Rocha & Sant'anna (2020), which the IV method was able to estimated positive values for the Elderly and Bronchitis hospitalizations using the concentration of PM2.5 attributed to fires instead of AOD.

It should be noted that the estimates from OLS do not separate effects caused specifically by fires, so the effect related to AOD may include other sources of aerosol emissions, such as deserts, oceans, forest, industry and fossil fuel burning (LENOBLE; REMER;

[7] The authors used: monthly data of PM2.5, a reanalysis product from CAM (Copernicus Atmosphere Monitoring Service) with spatial resolution of 12.5 km and obtained through the SISAM (portugues acronymun to Environmental Information System Integrated to Health) platform; Hospitalization data were obtained from SUS focusing on the total number of hospitalizations for respiratory diseases in children (age less than or equal to 5 years) and the elderly (over 60 years), all normalized per 100 thousand inhabitants; Thermal anomalies are gathered from MODIS/Acqua obtained in the INPE platform; Wind direction data were obtained from the product ERA-Interim, which is a global atmospheric reanalysis with a spatial resolution of 12.5 km, also available in SISAM platform; Control data were, precipitation (CPC/NOAA), relative humidity (ERA-Interim) and temperature (ERA-Interim), all available in SISAM. The data were grouped for each 772 municipalities of BLA, covering the period from January 2010 to December 2019, where they structured a balanced panel, with fixed effects.

TANRÉ, 2013). Specially in BLA, the amount of AOD can be influenced by: dust coming from the Sahara desert (BEN-AMI et al., 2010); water particles coming from Oceans (FISCH; MARENGO; NOBRE, 1996); pollutants from urban zones, industry and from the fossil fuels burning (SHRIVASTAVA et al., 2019); and biogenic aerosols from the forest (ARTAXO et al., 2009).

The low coefficient estimate for the hospitalization groups reflects on hospitalization counts for the region, which are below from those already estimated by other authors using a similar methodology for the Amazon region (DE MENDONÇA et al., 2004; MENDONÇA; SACHSIDA; LOUREIRO, 2006). However, the model follows the fire seasonality in BLA, when the peak of estimates is from July to November, mainly the pattern of the states with the largest contributions in burned area of the region (MT, RO, TO).

The difficulty to establish a clear cause-effect of fire-pollutants in hospitalizations is also revealed by a description of data. At first, when considering only the spatial distribution of the main variables (Burned Area, AOD and Hospitalizations for respiratory diseases), a positive relationship between, from one side, burned area, and, from another side, pollution and hospitalizations, is only observed in the South-Centre of Pará, while for the other regions with a large burned area, AOD and Hospitalizations are low. Despite these spatial patterns presenting few regions with higher concomitant values of pollutants, fire and hospitalization seem to be prevalent, because it was also indicated by Souza et al. (2020) analyzing the relationship between deforestation, hot spots, pollutants (PM2.5) and hospitalizations of indigenous people from the BLA.

Hospitalization data is also limited. It only includes the patient who remains at the hospital under supervision for a period equal or longer than 24 hours (BRASIL, 2002). In these cases, care and clinical diagnoses for patients with mild symptoms are excluded. As a result, the number of patients related to fire exposure accounted may be underestimated, since out-patients are ignored. Or, in another perspective, the required level of exposure to the pollutant for a person to be hospitalized is higher than in cases of outpatient visits, whose information is not easily available through the health systems.

The wind analysis follows the patterns presented by Gatti et al. (2014) and Cassol et al. (2020) for the Amazon region, including the dispersion of aerosols, in which there is a change in the predominant wind direction at the beginning of the fire season. This factor can spread and direct smoke plumes to neighbouring municipalities and other Amazonian countries, making a transboundary issue exemplified by the study of Sheldon & Sankaran (2017). In this way, neighbourhood factor can be a complement for further analysis, as assessed by some authors (JACOBSON et al., 2014; RANGEL; VOGL, 2019; ROCHA; SANT'ANNA, 2020). This factor consists of taking the amount of fire and then the pollution produced by each neighbouring municipality into account, by using spatial weight matrix to describe the dependency among the municipalities. This new approach will improve the data outside and inside the fire season.

This difficulty to establish a good estimate among all variables (age and illness group) and pollution, continues through the robustness check. In five out of seven dependent variables, the sign of estimates differed when based on burned area and on thermal anomalies.

It shows that besides the substantial correlation between point and areal fire detections (0.95; Figure 4-7), their statistical behaviour is not similar enough regarding the relationship between pollution and hospitalizations. Even with the higher frequency of point detections by the TA product (GIGLIO et al., 2020), the correlation with BA at low levels (less than 5 thousand $km^2$), specially between February and April (Figure 4-7), leads to a disarrangement in the early peak of burned area that matches the increasing stage of hospitalizations (Figure 4-3 and Figure 4-6). This may have favoured the appearance of negative estimates in the robustness check, due to the appearance of a well-defined valley.

Figure 4-7. Correlation of monthly values of thermal anomalies and burned area, for all-time series and monthly.

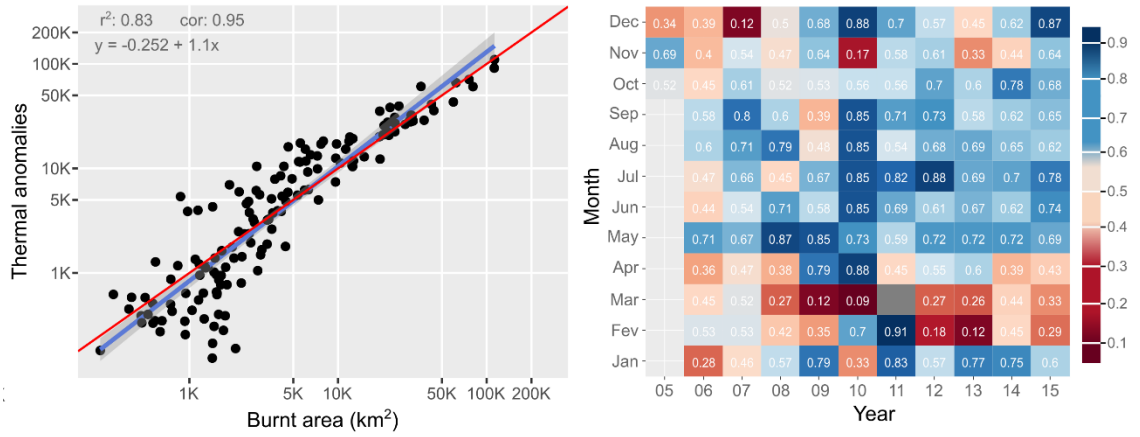


Source: From Author.

## 4.5 Conclusion

In this chapter, we estimate the hospitalization attributable to fire-induced pollution in the Brazilian Legal Amazon (BLA) using a balanced panel structured in a monthly-municipal level, with available data from the last twenty years (2005-2018). Our strategy was based on capturing this influence by increasing the possible connections that fire-pollution has in different ages and illnesses, applying an instrumental variable method with a set of instruments that relies on wind speed and direction, over three classes of diseases and four age group. Thus, contributing to expand the evidence of hospitalizations due to fire-induced pollution and primarily by considering the effect in the whole BLA and using a long time series.

In general, among the seven hospitalization variables evaluated, four variables (Total, Elderly, Asthma, Bronchitis) were significantly positive, one (Small Children) significantly negative and the others (Children and Pneumonia) were not significant. Thus, demonstrating that there is a positive effect of pollutants on the levels of hospital admissions for respiratory diseases in the BLA.

Estimates of total hospitalizations based on the IV model indicated that during the fire season (Aug-Oct), hospitalizations caused by pollutants generated by fire per municipality are 5 individuals on average, resulting in approximately 4 thousand for all BLA territory.

The observed effects were not consistent when applying the robustness test, in which the burned area was replaced by thermal anomalies, showing a fragility of the estimates of the causal-effect of fire and hospitalizations. Therefore, it is essential to make new estimates considering other pollutant indicators, neighborhood effects, time lag of variables, or even downscaling the time aggregation to capture inter-montlhy peaks.

# 5 TWO DECADES OF FIRE IMPACTS IN THE BRAZILIAN LEGAL AMAZON

## 5.1 Introduction

Anthropogenic fires are observed across all the Brazilian territory, mostly as agricultural burnings for land preparation, varying by the scale of production, mechanization and modernization degrees (EMBRAPA, 2000). The National Institute for Space Research (INPE, 2020) monitors the fire condition and demonstrates that among all Brazilian phytogeography domains, the Tropical Forest (Amazonia) and the Savannah (Cerrado) are the most exposed to fire along the years, representing, in average, 49% and 31% respectivetly, of all fires in Brazil.

Historically in the Amazon region, the use of fire is a cultural and basic practice related to the human activities (DA MOTTA et al., 2002). Due to these antropogenic features, the three main kinds of fires in the region are: the deforestation fire, the agricultural manage fire, and the wildfire caused by the lack of control of one of the previous types (ALENCAR; RODRIGUES; CASTRO, 2020).

As the benefit of using fire is proven in a short term, the losses are higher for all society, either directly, such as: human lives loss (AHRENS; EVARTS, 2020), burning production (DE MENDONÇA et al., 2004), damaging infrastructure (DIAZ, 2012), reducing biodiversity (BARLOW et al., 2003; BRANDO et al., 2014; SILVA et al., 2018a), affecting cultural resources (RYAN et al., 2012), or indirectly: such as changing the climate (ANDREAE et al., 2004; GONÇALVES; MACHADO; KIRSTETTER, 2015), increasing the hospitalizations rates due to respiratory problems (DERYUGINA et al., 2019; ROCHA; SANT'ANNA, 2020), reducing tourism (BOUSTRAS; BOUKAS, 2013), promoting species migration (NOLASCO, 2006; PAOLUCCI et al., 2017), and affecting aerial and terrestrial transport of people and goods (ANDERSON et al., 2011).

In addition to the fact that in the Amazon these events are mainly human driven, they are also boosted by climate extremes, such as anomalous temperatures and droughts (ARAGÃO et al., 2007, 2018), with increased intensity during the most recent drought events (1997/98, 2005, 2010, 2015/16). Only during the last five years of this decade, the Amazon region faced two large-scale fire events, one in 2015/16, associated with the El

Niño, and the other more recently in 2018/2019, associated with an increase in the deforestation and weakening of environmental protection (ARAGÃO et al., 2018; BRANDO et al., 2020), with several local, regional and global scale impacts.

Thus, to quantify and understand the process related to the fire patterns, such as size, frequency, intensity, seasonality and extent, it is extremelly useful to plan mitigation strategies, control measures and if necessary, suppression actions. Moreover, by performing such diagnosis, it is possible to predict fire patterns and inform managers and governmental institutions, identifying the environmental and human exposure and vulnerabilities to fires (ARCHIBALD et al., 2013).

The assessment of the impact of fire in a region is complicated by the complex feedback chain propagating impact across multiple scales and stakeholders (NELSON et al., 2013). One solution is to decompose impacts according to a conceptual classification criteria, which is commonly applied to quantify environmental disasters. In this context, we can split the impact into Material, Human and Environmental damages (DE CASTRO et al., 2003).

To communicate the importance of the fire threat to different social actors, it is necessary to estimate the size of the associated damage (DA MOTTA et al., 2002). Monetary quantification is adopted here mainly for being a pragmatic and dimensionally rigorous way to convert qualitatively different impacts into a single number, which is also useful as basis for estimation of environmental compensation mechanisms (MENDELSOHN; OLMSTEAD, 2009; KUMAR et al., 2013).

This chapter uses a 20-year set of fire data (2001-2020) to analyze its pattern and impacts over the Brazilian Legal Amazon (BLA), aiming to answer three major questions: (Q1) What are the main patterns of the burned area in the BLA?; (Q2) What is the potential magnitude of the fire impact over those 20 years?; (Q3) What are the effects on national and international environmental targets?

## 5.2 Material and methods

### 5.2.1 Study area

There are many delimitations of the Amazon region, like phytogeographic, climatic, hydrological, and political (Figure 5-1). In this chapter the political delimitation, known as Brazilian Legal Amazon (BLA) was used. The BLA consists of the states of Acre, Amapá, Amazonas, Mato Grosso, Rondônia, Roraima, Tocantins, Pará and west of Meridian 44° of Maranhão (BRASIL, 2007). This region represents 60% of the Brazilian territory, which is around 5 million km² (IBGE, 2021a).

Figure 5-1. Different delimitation of the Amazon, with focus on the Brazilian Legal Amazon.

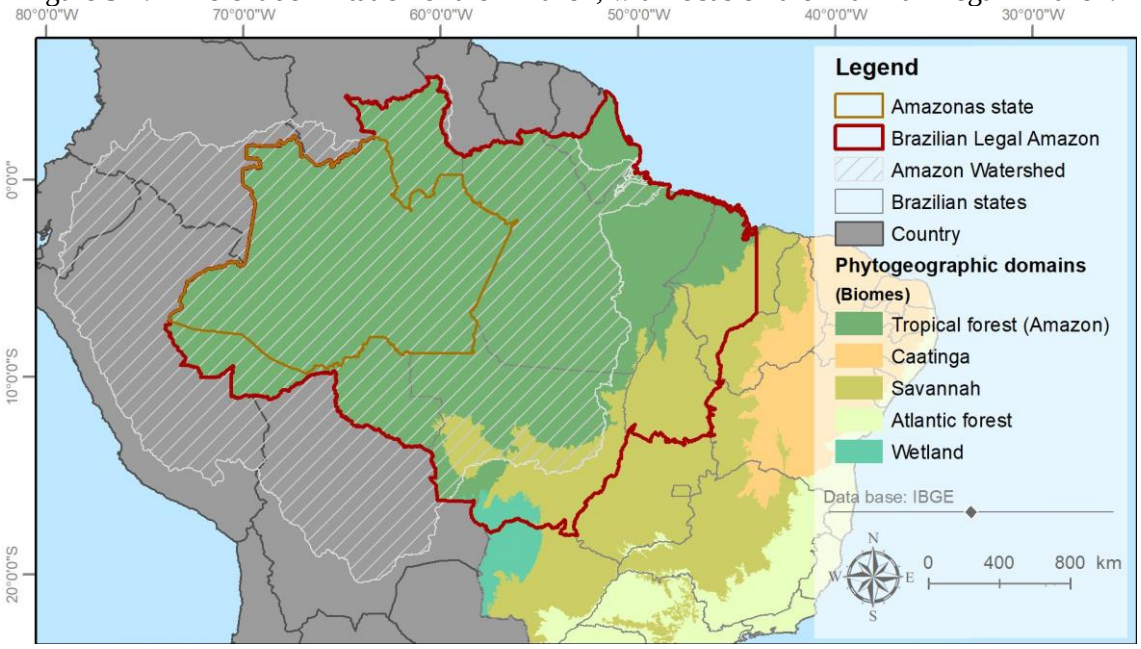


Source: From Author.

The BLA has three phytogeographic domains: 90% of Amazon (Rainforest), 7% of Cerrado (Savannah) and 3% of Pantanal (Wetland). Around 24% of its population is situated in rural areas (IBGE, 2021a). The economy is based on services, except in the states of Amazonas and Mato Grosso, where the industrial sector and the agricultural sector, respectively, are the most representative. All region contributes an average of 8.45% to the Brazilian GDP (SUDAM, 2016).

### 5.2.2 Spatial dataset

#### 5.2.2.1 Burned area

We use the Moderate Resolution Imaging Spectroradiometer (MODIS Terra e Aqua) burned area product MCD64A1-v6. This product has a monthly periodicity, spatial resolution of ~500 meters, and its data started in November of 2000. It uses an association of surface reflectance with active fires, and an algorithm that checks the temporal changes in the vegetation index (GIGLIO, LOUIS et al., 2015). Globally this product presented 99.7% of overall accuracy, with 40.2% commission error and 72.6% omission error (BOSCHETTI et al., 2019). In the Amazon region, this product showed a great similarity to regional and supervised-based product, detecting more fires in north and northwest areas than southwest (PESSÔA et al., 2020). Therefore, the results presented in this study can be considered conservative.

#### 5.2.2.2 Land use and land cover

The land use and land cover data used were the collection 5.0 of MapBiomas (MAPBIOMAS, 2021a). This product is based on Landsat images and machine learning procedures over a pixel base classification, generating an annually product with ~30m of spatial resolution from 1985 to 2019.

The classes used, are the 7 main types aggregated form the 31 MapBiomas level-2 classes (Table 5-1) plus the "Old-growth" and "Secondary Forest" class derived from the main Forest using the methodology proposed by Nunes et al. (2020) and Silva Júnior et al. (2020) from information between 1985 to 2019. The classified LULC map of 2019 was replicated to expand the analysis until 2020.

Table 5-1. Reclassification of MapBiomas' collection 5 of land use and land cover classes.

| MP_ID | MapBiomas C5 Class | New Category |
|---|---|---|
| 1 | Forest | Forest |
| 2 | Natural forest | Forest |
| 3 | Forest formation | Forest |
| 4 | Savanna formation | Forest |
| 5 | Mangrove | Forest |
| 9 | Forest plantation | Forestry |
| 10 | Non forest natural formation | Natural Field |
| 11 | Wetland | Natural Field |
| 12 | Grassland | Natural Field |
| 32 | Salt flat | Natural Field |

Continues

Table 5-1. Conclusion.

| MP_ID | MapBiomas C5 Class | New Category |
|---|---|---|
| 15 | Pasture | Pasture |
| 14 | Farming | Agriculture |
| 18 | Agriculture | Agriculture |
| 19 | Temporary crop | Agriculture |
| 39 | Soybean | Agriculture |
| 20 | Sugar cane | Agriculture |
| 41 | Other temporary crops | Agriculture |
| 36 | Perennial crop | Agriculture |
| 21 | Mosaic of agriculture and pasture | Agriculture |
| 31 | Aquaculture | Agriculture |
| 29 | Rocky outcrop | Other |
| 13 | Other non-forest formations | Other |
| 22 | Non vegetated area | Other |
| 23 | Beach and Dune | Other |
| 24 | Urban infrastructure | Other |
| 30 | Mining | Other |
| 25 | Other non-vegetated area | Other |
| 27 | Non observed | Other |
| 26 | Water | Water |
| 33 | River, Lake and Ocean | Water |

Mp_ID is the identification number of each MapBiomas classes.
Source: From Author.

#### 5.2.2.3 Land tenure

Information related to Land Tenure was provided by Imaflora through the Agricultural Atlas of 2018 (FREITAS et al., 2018). This product gathered information of all different territorial types respecting legal determination of each land category in one national map.

Imaflora's product organizes and adjusts overlapping features, both within each category and between categories. The hierarchy used within each feature is based on the removal of invalid and duplicated geometries, in addition to prioritizing more reliable geometries, either by the demarcation stage (in the case of indigenous lands and public forests), registration date (as in the case of properties of INCRA) or by the registration system (properties of INCRA, SIGEF/SNCI).

The hierarchy between categories is premised on "[...] the reliability of the available information, considering the recognition of rights and domain over land and the possibility of future change in the current occupation" (FREITAS et al., 2018, p. 8). Thus, the authors emphasize that this prioritization is not based on an order of environmental importance or the right to land, but on the legal security of law, the accuracy of geospatial information, the possibility of receiving overlap and the possibility of changing domains.

With this methodology, it was possible to map and reconstruct the land tenure of 82.6% of the Brazilian territory, more precisely 91% in the BLA[8].

Following the descriptions of each land tenure class of the IMAFLORA product, the three public classes were allocated to the "Not Designated" class. The classes "Undesignated land from Terra Legal Program", "Undesignated public forests" and "Public properties at INCRA system" do not have a specific destination and are characterized by governmental agencies as "not intended". In this way, these classes together with the category of "No information" were named "Not designated".

Table 5-2. Class of land tenure available in the IMAFLORA product, with the indicative of category and group.

| Description | Category | Group |
|---|---|---|
| Without information | Not Designated | - |
| Undesignated land from Terra Legal Program | Not Designated | - |
| Undesignated public forests | Not Designated | - |
| Public properties at INCRA system | Not Designated | - |
| CAR premium | Private | Properties at CAR system |
| CAR poor | Private | Properties at CAR system |
| Private properties at INCRA system | Private | Properties at INCRA system |
| Private properties from Terra Legal Program | Private | Properties at Terra Legal program |
| Rural settlements | Public | Rural settlements |
| Communitarian lands | Public | Rural settlements |
| Military areas | Public | Military areas |
| Quilombola lands | Public | Quilombola lands |
| Homologated indigenous land | Public | Indigenous lands |
| Non-homologated indigenous land | Public | Indigenous lands |
| Full protection conservation unit | Public | Conservation Units |
| Sustainable use conservation unit | Public | Conservation Units |
| Water bodies | Urban, Water | - |
| Transportation network | Urban, Water | - |
| Urban areas | Urban, Water | - |

Source: Adapted from Agricultural atlas (2018) and Freitas et al. (2018).

#### 5.2.2.4 Biomass

The biomass values for each LULC class were obtained based on the Biomass_CCI product (European Space Agency-ESA), and on the LULC classes of MapBiomas previously reclassified.

For the studied region, the version 2 available for 2010, 2017 and 2018 with a spatial resolution of 100 meters and on a global scale was used. This product utilizes a repository of Synthetic Aperture Radar (SAR) images from the C-band (Envisat ASAR for 2010 and

[8] We make this account by clipping the values to the BLA region. The full result are specify in Table B-1.

Sentinel-1 for 2017-18) and L-band (ALOS-1 PALSAR-1 for 2010 and ALOS-2 PALSAR-2 for 2017-18) to estimate the forest structure parameters and subsequently the biomass value. The larger range in the characteristics for the years 2017 and 2018 leads this set to improve estimates in areas close to the tropics and in regions with low biomass (SANTORO; CARTUS, 2021).

To minimize errors within each LULC class, the average of the biomass was calculated for the three years of data, thus obtaining the values presented in Table 5-3.

Table 5-3. Average biomass values by LULC class extracted from the Biomass_CCI product.

| Class | Biomass (Mg/ha) |
|---|---|
| Old growth | 223.28 (±73.5) |
| Secondary Forest | 110.03 (±36.7) |
| Forestry | 59.86 (±22.4) |
| Pasture | 24.73 (±8.18) |
| Natural fields | 26.85 (±9.15) |
| Agriculture | 7.32 (±2.4) |

Source: From Author.

#### 5.2.2.5 Ecosystem services

Monetary information of silvicultural production was obtained through the ecosystem service products estimated by Strand et al. (2018). The products use marginal economic value estimation models based on spatially explicit local and regional data to estimate average annual income values. These incomes reflect the marginal value of ecosystem services (US$ $ha^{-1}$ $yr^{-1}$) that would be lost with each additional hectare of forest removed.

Among the products available, the following were chosen to compose the total value for the Forest class: the annual income estimates in sustainable wood production (Timber), the average economic return in rubber production (Rubber), and the average income in Brazil Nut extraction (Nuts).

All these products were built for the Amazon biome. Thus, it was necessary to carry out a complete data collection for municipalities that are outside the biome but included within the study territory. For this purpose, the average value for each municipality within the biome was initially aggregated. Then, a spatial interpolation based on a neighborhood matrix was applied (GOLGHER, 2015). Neighbors were defined as municipalities either sharing boundaries with or within 1 km of the reference municipality. The matrix was

used to replace the missing values of the municipalities outside the biome for the average value across neighbors inside the biome. Relying on the structure of neighboring links in the matrix, the interdependence of municipalities (the fact that each one is a neighbor of its own neighbors) was the basis for multiple interactions of replacement in two stages. In the first, all missing values were replaced starting with municipalities closer to those in the biome. Undesirably, the average assigned to each municipality accounted only for neighbors that were closer to the biome along the particular direction in which the replacement process was feasible. That was clearly biased and corrected in the second stage by iterating replacement until municipalities' values became fixed with arbitrary precision ($<10^{-5}$).

#### 5.2.2.6 Political boundaries

The political-administrative division of the BLA territory was obtained from the Brazilian Institute of Geography and Statistics – IBGE website. The product is compatible with the 1:250,000 scale and represents the current situation of state and municipality boundaries (IBGE, 2021c).

Along 20 years, the number and area of municipalities, as well as the political boundaries of some states have changed. Therefore, the statistical information for each state was used based on the official boundaries provided by IBGE for each year.

### 5.2.3 Non-explicit spatial datasets

Data on total hospitalizations for respiratory diseases were obtained from the TabNet portal (DATASUS, 2020), filtering the values by respiratory diseases (ICD-10: X), municipalities, place of residence and month of treatment. The data comes from the SUS' Hospital Information System, managed by the Ministry of Health, in which every hospital unit (public or private) associated with SUS sends information on carried out hospitalizations. The total number of admissions in the period and the total hospitalization cost were also used.

The rate of hospitalizations resulted from an increase in pollutants derived from fire in the region was obtained from the estimates presented in Chapter 4 of this thesis, in which the calculation was performed by using the Instrumental Variable method.

Other data that are not spatially explicit and were used in the process of monetarily quantifying are described in Section 5.2.4.4.

### 5.2.4 Data analysis

#### 5.2.4.1 Fire pattern

First the MCD64A1 product was clipped to the AMZL region and set as a binary – fire affected areas and not affected areas. After, in order to determine the total amount of burned area, the raster map was converted to a vector and changed its projection of World Geodetic System (WGS84) to South America Albers Equal Area Conic. This procedure is fundamental to guarantee the value of each burned area in a metric scale.

The Recurrence and Frequency of fires in the region was calculated using all monthly burned area product layers from January of 2001 to December of 2020. The frequency of fires represents how many times the same area was burned in the period, with the maximum possible value of 240, considering the total number of months in the period. The recurrence represents the amount of fire events in the mentioned years, with a maximum value of 20.

To determine trends in the period, we use three different approaches. First a regular Linear Model (LM), second a Maan-Kendall test (MK), and third a Season Maan-Kendall (SMK). The LM was used because it is a simple index and is highly disseminated both within and outside the scientific community. The MK test is a non-parametric analysis used to track trend in time series (HIPEL; MCLEOD, 1994, cap. 23). Finally, the SMK, which is a modification of the MK test, was used because it considers seasonality in the data and also looks up trends in individual months (HIPEL; MCLEOD, 1994, cap. 23; POHLERT, 2020).

The fire season was defined as the contiguous month that comprehended more than or equal 80% of all burned area (ARCHIBALD et al., 2013).

Related to the fire size classes, the aggregation proposed by Heinselman (1978 apud; COVINGTON; MOORE, 1994) was adopted. This method is based on seven classes of the USDA-Forest Service Wildfire, which are merged into four: patches smaller than 99 acres (≤40 ha) are identified as “Small”; while patches between 100 acres and 999 acres

(40 to 404 ha) are considered as “Medium”; in turn patches between 1000 acres and 9999 acres (404 to 4,046 ha) are identified as “Large”; and finally patches larger than 10,000 acres (≥ 4,046 ha) are classified as “Very Large”.

#### 5.2.4.2 Clustering years

In order to determine similar years and behaviors over time, two forms of grouping were carried out: the first refers to the establishment of groups based on the data, and the second part dividing the time series into four groups of five years each.

In this way, years with similar characteristics were initially grouped using the evolution of fire in the intra-annual period. Thus, firstly, it was used the Dynamic Time Warping (DTW) technique to determine the similarity between the data series. After, the Multi-Dimensional Scale (MDS) algorithm was used to reduce the dissimilarity matrix in a pair of coordinates and determine the groups, using the Hierarchical method. The entire process was carried out on the RStudio platform, using the “dtw” (GIORGINO, 2009) and “MASS” (VENABLES; RIPLEY; VENABLES, 2002) libraries.

From a temporal perspective, the series was divided into groups of 5 contiguous years, obtaining 4 groups. In this step, a distinction of normal climate years and anomalous ones was not made. Within each group, the characterization of the fire regime was carried out based on Archibald et al. (2013) methodology, obtaining the values for the following parameters: average monthly area, maximum annual area, minimum annual area, average size of burned areas, average number of events, number of months describing the burning season, number of months with fire anomalies, and number of affected municipalities per year. The groups were submitted to the *Wilcoox* test for comparison between means to obtain similar groups and verify disaggregation within the series.

#### 5.2.4.3 Fire impacts

To determine the fire impact over different land cover, first we downscaled the burned area to the same resolution of LULC maps, and then performed a monthly intersection between them, preserving the reference of each year. All procedures were based on a pixel level. The same procedure was applied to extract burned areas over different types of land tenure.

The extraction of these data supported the quantification of economic impacts, whether in the agricultural sector (Agriculture, Pasture and Natural Field classes) or in the forestry sector (Forestry, Old growth and Secondary Forests), which will be described in section 5.2.4.4. This same strategy supported the estimates of environmental damage by quantifying gross carbon dioxide emissions for each category.

For the "Forest" and "Forestry" classes, we used the fire loss equation (Equation 5.1), proposed by Anderson et al. (2015) and updated by Pêssoa et al. (2020) to estimate the amount of committed carbon emissions. The equation considers a biomass density gradient, in which places with lower biomass have greater carbon loss due to fire, and in forest formations, due to the microclimate generated within the canopy, there is a reduction in fire intensity and susceptibility, causing partial loss of biomass. In this way, the value of committed carbon in tons per hectare was quantified by subtracting the value of the final biomass in relation to the initial biomass and applying the conversion factor of 1,835 to retrieve the carbon dioxide (Equation 5.2). For the other classes (Agriculture, Pasture and Natural Field), the total conversion of biomass into carbon was considered, thus only the conversion factor was applied to the total biomass committed.

$$Bf = 0.05 * Bi^{1.47} \quad (5.1)$$

$$CO_2 = 1.835 * (Bi - Bf) \quad (5.2)$$

*Bf* is the total aboveground biomass after a fire in $Mg.ha^{-1}$, *Bi* is the initial biomass in $Mg.ha^{-1}$, and $CO_2$ is the total carbon dioxide committed in $MgCO_2.ha^{-1}$.

Immediate emissions were quantified using the total biomass aboveground and the conversion factor to Standing biomass and Surface litter, followed by the complete combustion factors, indicated by Van Der Werf et al. (2017) for South America. The values were quantified only for forest classes (Primary Forest, Secondary Forest and Forestry) due to their long-term stay in the atmosphere.

It is worth mentioning that vegetation growth rates for none of these classes were considered, nor the variation in emissions due to the repetition of fire in the same area. Thus, biomass values were applied each month in relation to each land use affected by the fire, and the total carbon loss in the year reflects a base value for quantifying the total

annual loss. The committed biomass loss was calculated for purposes of biomass quantification, but it was not included in the annual scale valuation analysis.

#### 5.2.4.4 Monetary damages

To access the total monetary damage caused by fire in the BLA region, a microeconomic approach was used. The technique chosen is based on the revealed preference methods, that are useful in gathering values using existing or surrogates markets (OECD, 2006).

Related to production damage, for the "Old growth" class, the digital map produced by Strand et al. (2018) of potential net revenue related to the extraction of wood and non-wood products was used.

Considering that from a certain age "Secondary forests" can provide ecosystem services similar to "Old growth", an age threshold was established for each type of wood and non-wood product. Thus, rubber extraction was considered from 10 years old, because the production of latex in commercial plantations stabilizes at this age (MORAES; MORAES; MOREIRA, 2008; PEREIRA; LEAL; CASTRO, 2003); Brazil nuts extraction for forests older than 12 years old (MÜLLER et al., 1995); and the extraction of commercial wood from 25 years old, due to the minimum time for the cutting cycle in Sustainable Forest Management Plans (PMFS) in the BLA, regulated by the Normative Instruction n°.05/2006 (MINISTÉRIO DO MEIO AMBIENTE, 2006).

For the "Natural field" and "Pasture" classes, production loss and restoration values were not used, since in most pastures in the region, management and conservation practices are not frequently parts of the agriculture. However, the cost of leasing new pastures for animal exploitation was accounted for a period of 90 days, a period equivalent to the regrowth of vegetation (TOWNSEND; COSTA; PEREIRA, 2012), a proxy for the impact of fire on pasture. These values were obtained on *Fundação Getúlio Vargas* data portal (FGV IBRE, 2021) by selecting the states that compose the region.

The leasing data series is part of the free data set, however discontinued by the Foundation since 2014. In this way, to expand the series until 2020, we used variations in the price of live cattle, since it is common to use this index to estimate the land lease value (PEREIRA et al., 2020). Thus, live cattle prices were extracted from the historical series of the Center for Advanced Studies in Applied Economics – CEPEA (CEPEA, 2021).

For the “Agriculture” class, initially the main agricultural crops (annual and perennial) were determined based on the value of production and harvesting area, reported by the Municipal Agricultural Production survey (PAM- IBGE) (IBGE, 2021d). Then, it was found out that soybean and corn are the foremost crops in the BLA, representing together 67% of all production and 78% of total harvest area, between 2001 and 2019. In possession of this information and the calendar for the Northern region made by the Ministry of Agriculture, Livestock and Supply (MAPA), an annual production system was set up. The months from October to May are intended to soybeans and the ones from June to September are designed to corn.

Once the agricultural calendar of the region was set up, the net income was quantified based on estimates of production costs and total income for each crop over the period. The cost values were obtained from the website of the National Supply Company – CONAB (CONAB, 2021b), separating the total operating cost for the total. Income was calculated from average production estimates for both crops (CONAB, 2021a) with prices paid to the producer (CONAB, 2021c), both made by CONAB.

In certain years, corn production has a negative net income value, mainly due to expenditure on pesticides, fertilizers, and machinery. This happens because the accounting data provided by CONAB assumes high technology, overestimating the regional average cost, given the heterogeneity in the adoption of technology in the region, including small producers that do not use mechanization or agrochemicals (ALVES; MODESTO JÚNIOR, 2020; BÖRNER; MENDOZA; VOSTI, 2007; CAVIGLIA-HARRIS, 2018; FONTES; PALMER, 2018). In this way, it was assumed that when a corn crop that produces a negative profit is burned, the loss will be null rather than negative. This reasoning not only allows the mitigation of excessive cost, which is one of the causes of negative values for profit, but also it is consistent with the economic concept of sunk cost, which is understood as comprising irreversible expenses at the time the decision is taken (VARIAN, 2010, sec. 20.6), like those imposed by the fire. In fact, the expenditure on land preparation (including mechanization and agrochemicals) becomes irrecoverable soon after it is carried out. Therefore, the economically adequate measure of damage is, in the particular case, the unrealized profit. In such cases that this would be negative, there is, therefore, no damage.

In order to quantify the total number of hospitalizations because of smoke generated by fires in the region and the amount spent on the treatment of respiratory diseases, the monthly percentages of hospitalizations due to fire-smoke pollutants calculated in Chapter 4 were applied to all time series used in this chapter.

The values per ton of carbon dioxide emitted correspond to the equilibrium price of the European Union Emissions Trading System (EU-ETS), the largest and oldest carbon trading system in the world, obtained from the World Bank portal (THE WORLD BANK, 2021). It was considered only prices from the third phase of the EU-ETS (2013-2020), the most recent, and, thus, less subjected to the influence of market failures that were gradually repaired along the existence of the scheme. Carbon taxes were ignored for being regulated prices, thus not reflecting the actual marginal cost of carbon abatement (GOULDER; SCHEIN, 2013; MEADOWS; VIS; ZAPFEL, 2020). The period between 2018-2020 was excluded because of market functioning amendments, including approval of a cancellation mechanism in 2018[9] (CARLÉN et al., 2019; HINTERMAYER, 2020) and the market stability reserve introduced in 2019[10] (CARLÉN et al., 2019; EUROPEAN COMMISION, 2021), which increased the carbon price in an over threefold larger average.

In this way, the average value between 2013-2018 was attributed to the year with the smallest difference and subsequently monetarily corrected (inflated and deflated) for the rest of the time series using the Harmonized Index of Consumer Prices (HICP) index of European Union inflation provided by the European Commission via the EUROSTAT portal (EUROSTAT, 2021).

The final value of the damage by emissions was quantified only for immediate emissions from the combustion process of the forest classes, since these LULC classes present, once burned, a potential long-term contribution to climate change in relation to other classes,

[9] In 2018, the cancellation mechanism, a "quantity-based instrument", was approved to be implemented in 2023, consisting in cancelling allowances in the reserve exceeding the allowances exchanged in the previous year (CARLÉN et al., 2019; HINTERMAYER, 2020). This could have had an anticipated effect on price.

[10] In 2019, the market stability reserve was introduced (CARLÉN et al., 2019; EUROPEAN COMMISION, 2021), resulting "on higher and more robust carbon prices and helped to ensure a year on year total emissions reduction of 9% in 2019, with a 14.9% reduction in electricity and heat production and a 1.9% reduction in industry", and could have been anticipated in 2018 by traders thus anticipating price increase (anticipatory behaviour is assumed by (HINTERMAYER, 2020).

in which the rapid growth of vegetation removes carbon emissions generated during the burning from the atmosphere.

The values of forest products (timber and non-timber) together with the carbon values were available in dollars, and using the exchange rates provided by the Institute for Applied Economic Research (IPEA, 2021), they were converted into reais throughout the time.

Finally, to obtain the magnitude of the monetary damage caused by fire over these 20 years, the values obtained were converted into percentages equivalent to the Gross Domestic Product (GDP), obtained from the IBGE portal for Brazil (IBGE, 2021e) and for AMZL through the grouping of the municipalities that are part of the region (IBGE, 2021f).

It should be noted that to obtain comparable values within the series, the final value of monetary damage was corrected to current prices (January 2021) through the IPCA index (Extended Consumer Price Index) provided by IBGE for the entire series (IBGE, 2021g).

### 5.2.5 Uncertainty

The uncertainties measurement involves the propagation of the variance (σ) of the variables used and the equations that follow it. For this, the uncertainty propagation equations presented by Vuolo (1996, cap. 8) and explained in Table 5-4 were used, especially for the following situations: sum of variables (Equation 5.3); product between variables (Equation 5.4); product of a constant (Equation 5.5).

Table 5-4. Used expressions for uncertainty propagation.

| Initial equation | Expression to determine the uncertainty | Eq. |
|---|---|---|
| $w = x + y$ | $\sigma_w^2 = \sigma_x^2 + \sigma_y^2$ | (5.3) |
| $w = x.y$ | $\left(\frac{\sigma_w}{w}\right)^2 = \left(\frac{\sigma_x}{x}\right)^2 + \left(\frac{\sigma_y}{y}\right)^2$ | (5.4) |
| $w = a.x$ | $\sigma_w = \lvert a \rvert . \sigma_x$ | (5.5) |

Source: Adapted from Vuolo (1996).

## 5.3 Results

### 5.3.1 Fire pattern in the BLA

Figure 5-2, the graph on the left shows the history of monthly burned area in the BLA between 2001 and 2020, in which the monthly average was 10,271 km², approximately the size of Três Lagoas, a municipality of Mato Grosso do Sul. The three highest values were registered in 09/2007 (112,016 km²), 09/2010 (110,641 km²) and 09/2017 (79,565 km²), whilst the lowest values were registered in 02/2002 (196 km²), 01/2002 (225 km²) and 02/2005 (234 km²).

Figure 5-2. Monthly and total annual variation of the burned area between 2001 and 2020 (left) and monthly average values (right).

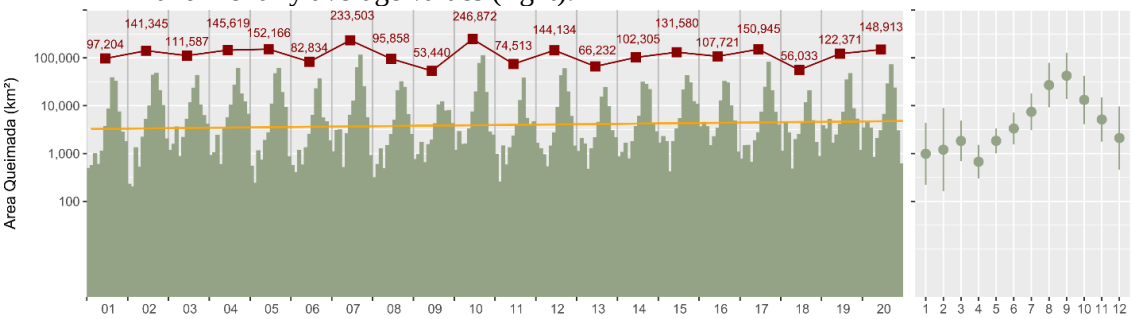


Note: The bars represent the monthly total of burned area, where the yellow line shows the linear trend of this data; the graph of lines and dots at the top represent the annual accumulated, and; the graph on the right represents the average value of the burned area and its variation over the months.
Source: From Author.

In relation to the annual burned area (graph of points in Figure 5-2), we found an average of 123,259±51,262 km², which is close to the size of England (130,000 km²). The years with the highest records of accumulated area were 2010 (246,872 km²) and 2007 (233,503 km²), while the smallest areas were observed in the years of 2009 (53,440 km²) and 2018 (56,032 km²).

No significant trends were found over the total annual burned area values, using both Linear and Mann-Kendall tests. On the other hand, the analysis of the monthly totals showed an increase in the levels of burned area using the non-parametric analysis (Mann-Kendall). Thus, the monthly trends are presented in Figure 5-3, and a significant increase in burned areas was identified in the months of January, February and March.

Figure 5-3. Trend in burned area at a monthly scale for the BLA region.

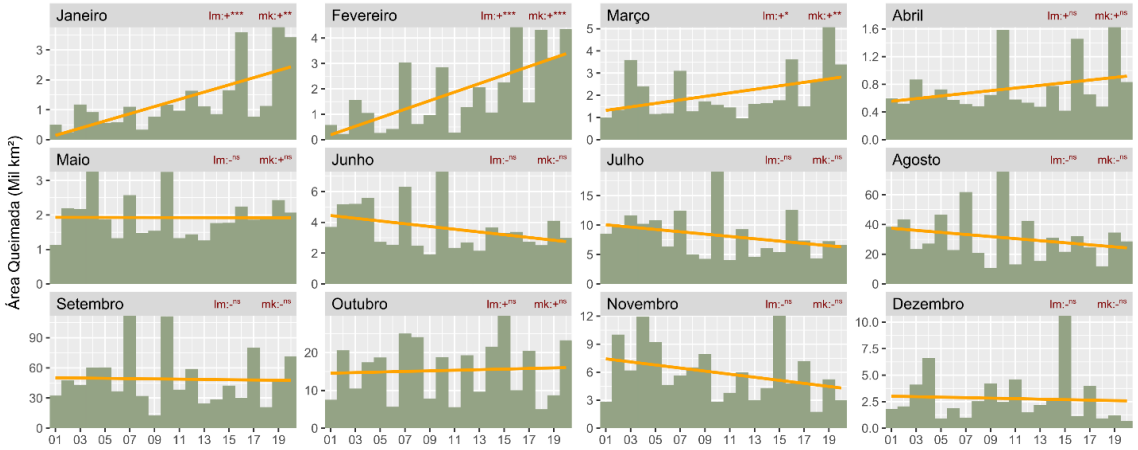


Note: the yellow line represents the linear trend of the data. The trend can be positive (+) or negative (-) and is obtained through: linear trend (lm) and Maan-kendal (mk). Significance levels: "***" p<0.01, "**" p<0.05 and "*" p<0.1.
Source: From Author.

The temporal pattern of fire existing in the BLA (Figure 5-2 right) is characterized by its onset in February-March, with a small peak in the burned area values which together represents approximately 3.54% (±2.08p.p) of the annual burned area. The month of April, in turn, registered the lowest value in the series, with an average of 736±370 km², representing about 0.65% (±0.32p.p) of the total area affected by fire annually. Since then, the series shows an increase in the values of burned area, reaching the maximum in August-September (average of 39,858 km²), which can represent up to 80% of the annual burned area. The year is ended with a decrease in the values until the cycle is restarted.

Over this 20-year period, there is an increase of 1.5% (p<0.1) in the magnitude of the minimum monthly values, while the average and maximum monthly values are statically stable (Figure 5-4 left). However, anomalous events[11] showed an increase in their recurrence over these 20 years (Figure 5-4 right), in which half of the series (2002, 2003, 2004, 2007, 2010, 2015, 2016, 2018, 2019 and 2020) presented at least one month above 80% of the data. Among these anomalous events, the year of 2010 stands out, when half of the months were characterized as a positive anomaly of the burned area, then the years of 2004 and 2016, in which 1/3 of the months were characterized as positive anomalies.

[11] Anomalous events are events that deviate from the average of the data. In this study, they are months whose burned area value is greater than 80% of all burned areas recorded in that month, considering the last 20 years.

Figure 5-4. Trend in annual maximum, mean and minimum values (left), and monthly burned area anomalies (right).

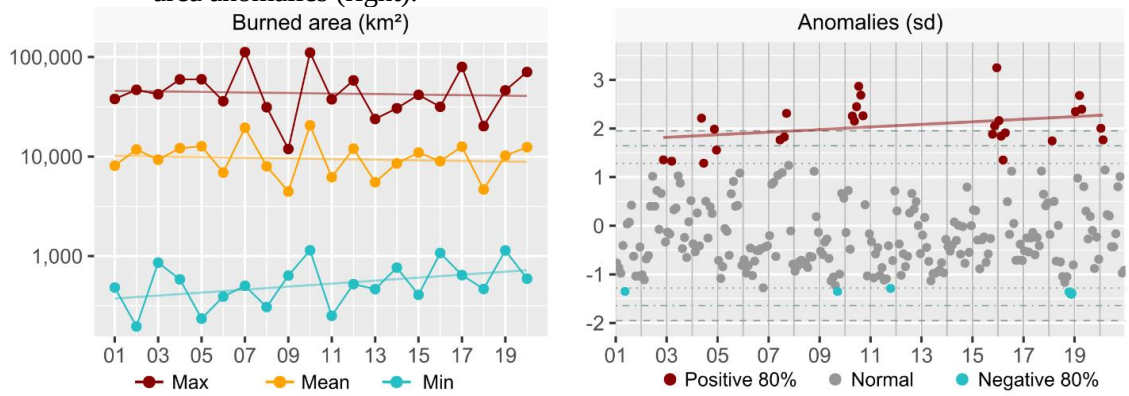


Note: On the left plot red dots represents an descriptive statistic over the total monthly burned area, where red is the maximum, yellow the average and blue the minimun. On the right plot, each dot represents an anomaly of the total monthly burned area, where the greater (red) and the lower values (blue) were highlighted. Lines, in both plots, representes the Linear trend over the respective colored values.
Source: From Author.

The months characterized as fire season for the BLA region and its states are presented in Figure 5-5. Predominantly, the months of August, September and October represent the fire season for the BLA region. This pattern is also observed for the states of MA, MT, PA, RO and TO. A variation without the month of October is found for the states of AC and AM. However, for the state of Amapá (AP) the months with the highest occurrence of fires are October and November, and for the state of Roraima (RR), the peak is in January, February and March.

Figure 5-5. Percentage of monthly fire by year, highlighting the fire season for the Brazilian Legal Amazon (BLA) and for each state covered by it.

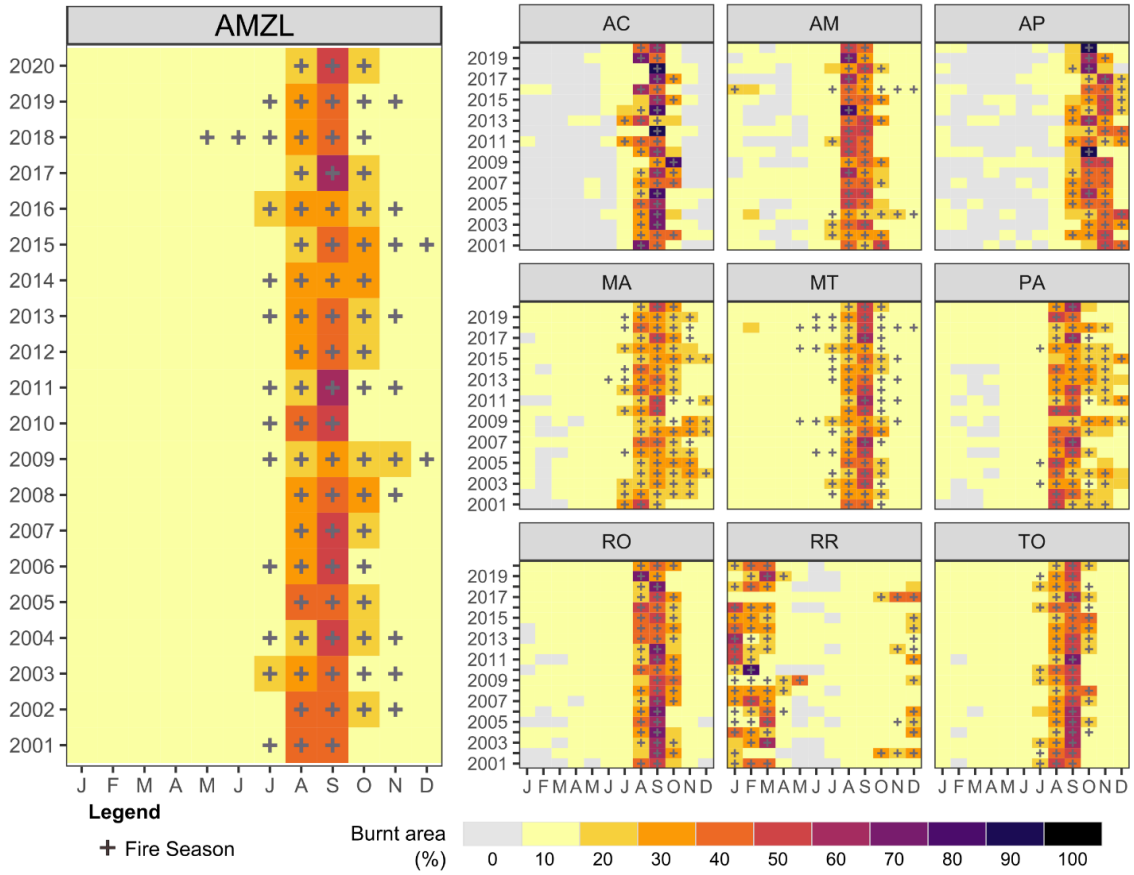


Source: From Author.

Among the nine states that are part of the BLA, the order of average contribution is: MT, TO, MA, RR, PA, AP, RO, AM and AC. However, the contribution levels throughout the year vary (Figure 5-6), such as between the months of January and April, when the contribution of RR is greater than that of TO, but this dynamic is inverted in the following months, when the values of TO remain high (around 30%) while the ones of RR cease. MT in turn has a high average contribution value throughout the year, but its highest percentages are found until May, a divergent peak from the fire season for the state.

During the analyzed period, considering a linear trend, there was an increase in the contribution of TO in the total burned area values for the BLA, and in contrast the state of AC recorded a decline in burned area values (Figure 5-6). However, from a seasonal perspective, the states that showed a positive and significant trend were: RO, AC, RR, PA, TO and MA, while a negative trend was observed only in MT.

Figure 5-6. Contribution (%) of each state in the total burned area for the BLA, presented in monthly and annual values.

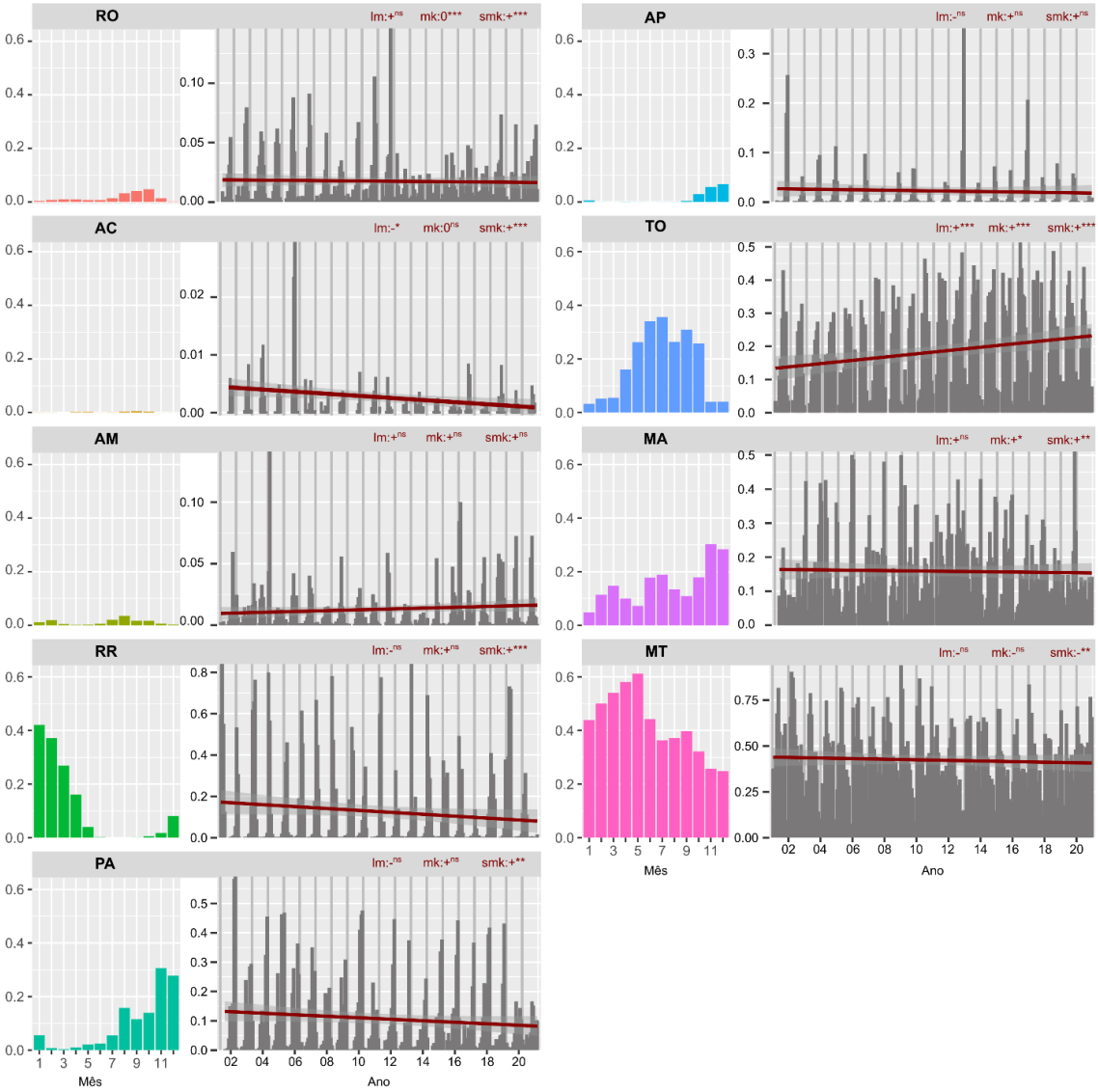


Note: the red line represents the linear trend of the data. The trend can be positive (+) or negative (-) and is obtained through: linear trend (lm), Maan-kendal (mk) and Maan-kendal considering seasonality (smk). Significance levels: "***" p<0.01, "**" p<0.05 and "*" p<0.1.
Souce: From Author.

In the last 20 years, about 2,465,176 km² have already been affected by fire in the region, but considering the total extension between new and overlapping areas, the region presented 17% (≈ 840,163 km²) of its total area affected by fires (Figure 5-7), almost the size of the state of Mato Grosso. Of this total, 346,956 km² burned only once, while 493,206 km² burned more than once. Of the areas hit more than once by fire, approximately 17% only burned two years in a row, 0.34% was affected for ten consecutive years and the areas that fire has always been used represent approximately

67 km² (less than 0.01% of the total already burned). These areas where there has always been fire are located in the border between the states of MA and TO, and between TO and MT, more specifically in the municipalities of Campinápolis-MT, Barra do Garças-MT, Ribeirão Cascalheira-MT, Paranatinga-MT, Canarana -MT, Formoso do Araguaia-TO, Goiatins-TO and Balsas-MA.

Figure 5-7. Spatial distribution of frequency and recurrence of burned areas in the Brazilian Legal Amazon.

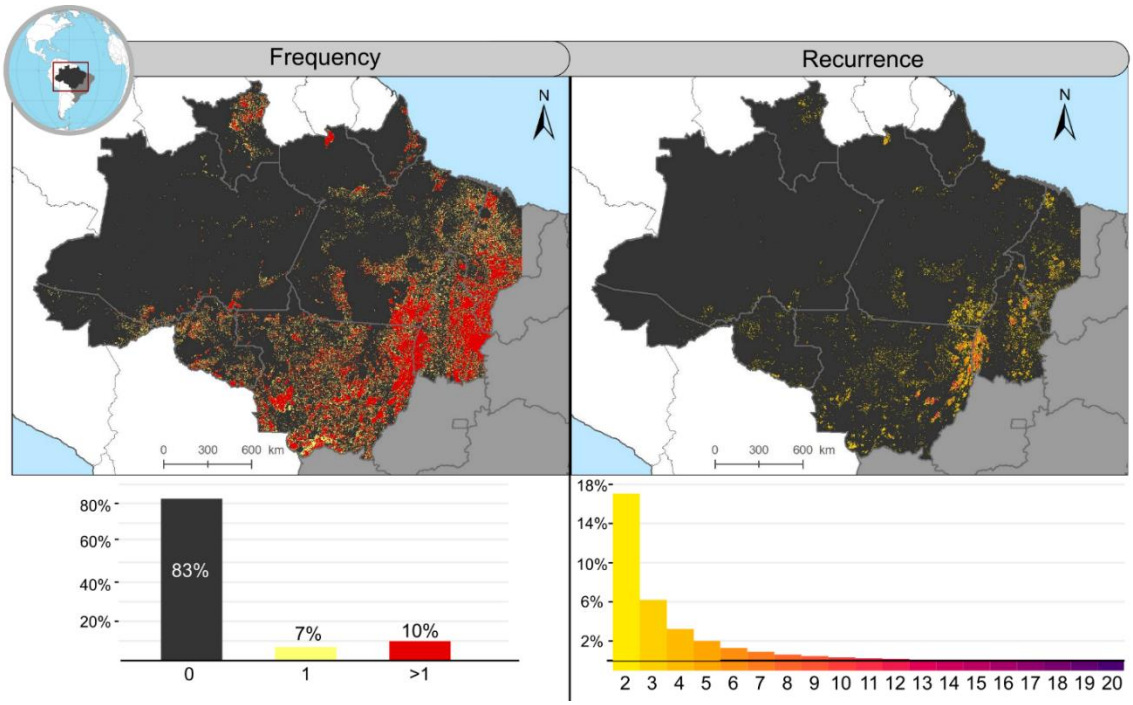


Source: From Author.

The proportion of new burned areas (36%) is low compared to the occurrence of fire in previously affected areas (64%). Monthly, (Figure 5-8) the new burned areas have their lowest values in the middle of the year (Jun-Jul), later they show a growth following the period of burning in the region (Aug-Oct) reaching their maximum at the beginning of the year (Jan-Feb). On the other hand, the proportion of old areas affected has grown in March, reaching its maximum between June and July.

Figure 5-8. Variation in the proportion of new burned areas and previously affected ones over the analyzed period and per month.

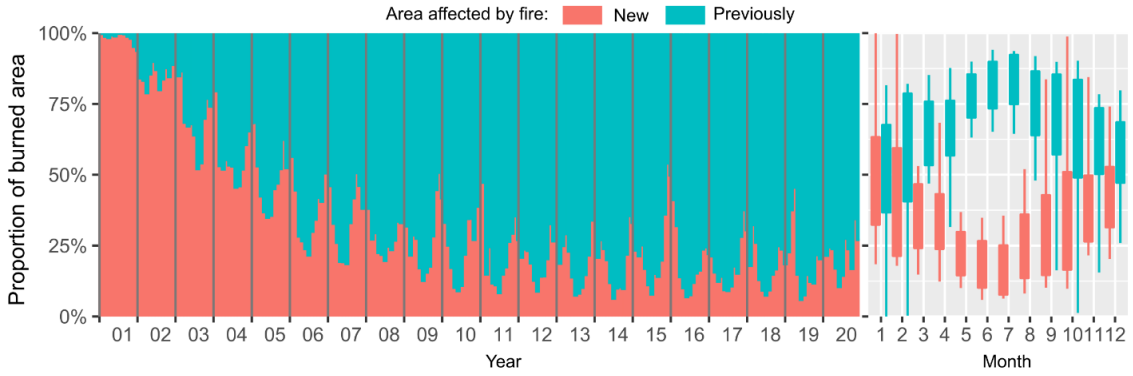


Source: From Author.

Figure 5-9 presents the proportion of events according to size classes. Events of low extension (Small class) are the majority in the region, which annually represent about 80%. “Large” and “Very Large” events together represent an average of 1.5% of the total in terms of fire-affected area contribution. The months with the highest concentration of “Large” events are the months from June to September, when there is a reduction of almost 10 percentage points in the amount of “Small” events.

Figure 5-9. Variation of events by size class occurred per month (first row) and per year (second row) in the BLA.

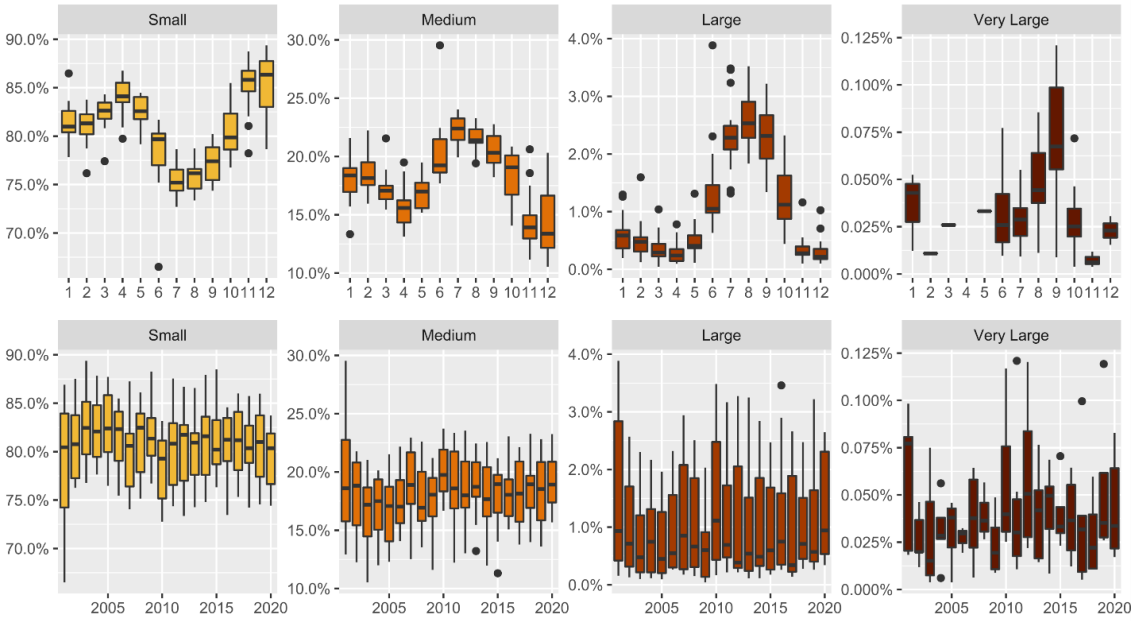


Size classes where: Small are patches smaller than 40 ha; Medium are patches between 40 and 404 ha; Large are burned areas between 404 and 4,046 ha, and; Very Large are patches with an area greater than 4,046 ha.

Source: From Author

### 5.3.2 Clustering years

At first, years with similar characteristics in relation to fire seasonality can be grouped into four categories (Figure 5-10): group 1 (C1) is composed of the extreme years with the largest annual burned area, which are 2010 and 2007; group 2 (C2) are the years with high values, consisting of the years 2020, 2019, 2017, 2015, 2012, 2005, 2004 and 2002; group 3 (C3) is the intermediate values, which are composed by the years 2016, 2014, 2008, 2006, 2003 and 2001; the last group (C4) are the years with the lowest values (2018, 2013, 2011 and 2009).

Figure 5-10. Groups of similar years in relation to the accumulated total and its variation over the months.

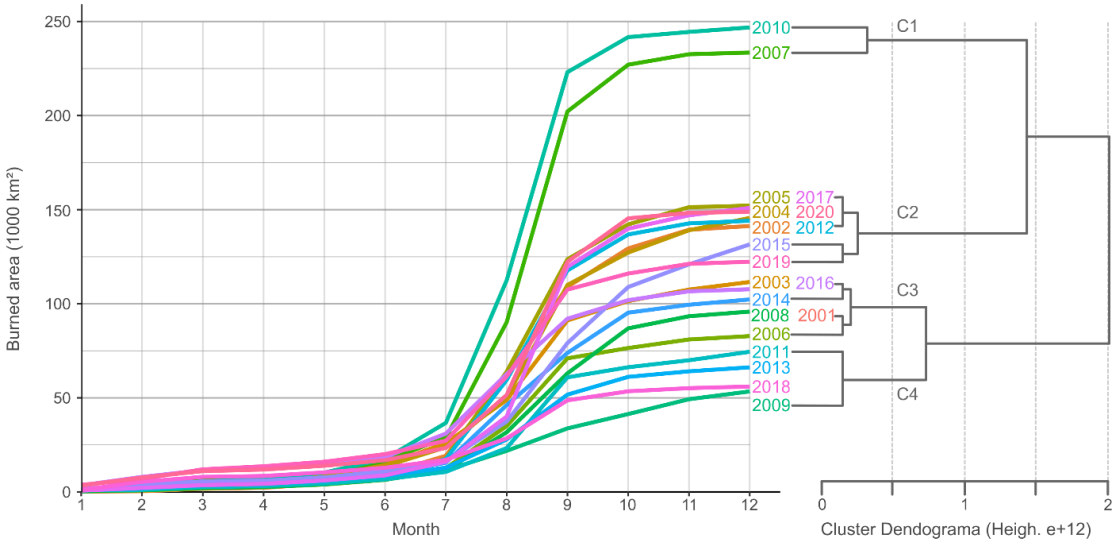


Note: Groups determined using the DTW to verify the dissimilarity in the series, the MDS to reduce the dimensions, and cluster hierarchization for groupings.
Source: From Author.

Under the temporal perspective, which divided the series into 4 periods, we did not find significant differences at 5% (Table 5-5) regarding to: annual burned area; maximum monthly burned area; minimum monthly burned area; average annual amount of patches; percentage of patches by size; number of months within the fire season; number of months with anomalies and number of municipalities affected annually.

However, divergences were found in the monthly scales for: monthly total area, for February; average amount of patches, in January and February; and for the average number of affected municipalities, in February and March. The last group (G4: 2016 to

2020) presented the highest and significantly divergent values from the other groups, especially compared to the first one (G1: 2001 to 2005).

These changes are also detected in relation to the damage, as in: the annual average of LULC affected by fire, especially in the Agriculture, Pasture and Forestry classes; the annual average of land tenure affected by fire, which the Urban class shows a decrease in the area; and in the equivalence of monetary damage in relation to the Brazilian GDP.

Table 5-5. Mean values for each variable used in the characterization of fire, as well as the significance (p.value) of the Kruskal-Wallis test for comparison between means, separated by group of years.

| VARIABLE | | G1 2001-2005 | G2 2006-2010 | G3 2011-2015 | G4 2016-2020 | p.value |
|---|---|---|---|---|---|---|
| Annual burned area (km²) | | 129,584 | 142,501 | 103,753 | 117,197 | 0.6975 |
| Maximum monthly burned area (km²) | | 49,270 | 60,379 | 38,381 | 49,679 | 0.6075 |
| Minimum monthly burned area (km²) | | 471 | 596 | 482 | 783 | 0.2989 |
| Monthly total area (km²) | Jan | 658 | 763 | 1,221 | 2,515 | 0.0535 |
| | Feb | 710[(a)] | 1,551[(a)] | 1,362[(a)] | 3,533[(b)] | 0.0218 |
| | Mar | 1,866 | 1,737 | 1,457 | 3,220 | 0.1447 |
| | Apr | 651 | 750 | 546 | 1,001 | 0.2621 |
| | May | 2,109 | 2,012 | 1,492 | 2,091 | 0.1566 |
| | Jun | 4,433 | 4,080 | 2,779 | 3,096 | 0.2608 |
| | Jul | 10,086 | 9,345 | 5,749 | 7,505 | 0.1520 |
| | Aug | 35,308 | 38,010 | 24,246 | 25,848 | 0.5319 |
| | Sep | 48,020 | 60,379 | 37,818 | 49,236 | 0.6975 |
| | Oct | 14,758 | 16,101 | 17,030 | 13,314 | 0.8964 |
| | Nov | 7,955 | 54,30 | 5,759 | 4,319 | 0.4515 |
| | Dec | 3,032 | 23,44 | 4,294 | 1,518 | 0.1940 |
| Amount of patches (#) | Annual | 3,762 | 3,663 | 2,831 | 3,062 | 0.4476 |
| | Jan | 352[(a)] | 444[(a)] | 631[(ab)] | 1,303[(b)] | 0.0288 |
| | Feb | 359[(a)] | 838[(a)] | 854[(ab)] | 1,778[(b)] | 0.0263 |
| | Mar | 1,061 | 1187 | 940 | 1,743 | 0.1130 |
| | Apr | 478 | 451 | 393 | 660 | 0.1884 |
| | May | 1,143 | 831 | 889 | 1,149 | 0.1581 |
| | Jun | 1,478 | 1,284 | 1,124 | 1,174 | 0.8040 |
| | Jul | 2,728 | 2,170 | 1,459 | 1,781 | 0.0605 |
| | Aug | 8,474 | 7,935 | 5,172 | 6,218 | 0.3934 |
| | Sep | 10,717 | 13,063 | 7,599 | 9,603 | 0.5760 |
| | Oct | 5,226 | 5,067 | 4,911 | 3,939 | 0.6075 |
| | Nov | 4,292 | 3,191 | 2,907 | 2,347 | 0.2773 |
| | Dec | 2,452 | 1,365 | 2,887 | 966 | 0.1331 |
| Percentage of patches by size class (%) | small | 81.50% | 80.63% | 80.54% | 80.39% | 0.3569 |
| | medium | 17.49% | 18.29% | 18.41% | 18.48% | 0.2711 |
| | large | 1.01% | 1.06% | 1.07% | 1.13% | 0.6509 |
| | very large | 0.03% | 0.04% | 0.04% | 0.04% | 0.6674 |
| Number of months within the fire season (#) | | 4.00 | 4.00 | 4.40 | 4.40 | 0.8571 |
| Number of months with anomalies (#) | | 1.40 | 2.00 | 0.80 | 2.40 | 0.4610 |

Continues

Table 5-5. Conclusion.

| VARIABLE | | G1 2001-2005 | G2 2006-2010 | G3 2011-2015 | G4 2016-2020 | p.value |
|---|---|---|---|---|---|---|
| Number of municipalities affected annually (#) | Annual | 255 | 252 | 244 | 252 | 0.92 |
| | Jan | 108 | 110 | 127 | 133 | 0.6697 |
| | Feb | 54$^{(a)}$ | 77$^{(a)}$ | 77$^{(a)}$ | 127$^{(b)}$ | 0.0228 |
| | Mar | 77$^{(a)}$ | 90$^{(a)}$ | 87$^{(a)}$ | 121$^{(b)}$ | 0.0111 |
| | Apr | 87 | 91 | 89 | 111 | 0.3124 |
| | May | 152 | 151 | 143 | 175 | 0.0592 |
| | Jun | 223 | 216 | 213 | 228 | 0.8714 |
| | Jul | 317 | 294 | 257 | 280 | 0.0866 |
| | Aug | 448 | 429 | 379 | 409 | 0.1385 |
| | Sep | 527 | 512 | 488 | 488 | 0.4573 |
| | Oct | 509 | 498 | 470 | 442 | 0.4556 |
| | Nov | 342 | 335 | 326 | 305 | 0.7819 |
| | Dec | 220 | 225 | 269 | 207 | 0.5856 |
| Annual average of LULC affected by fire (%) | Agriculture | 18.11$^{(a)}$ | 25.45$^{(ab)}$ | 27.98$^{(b)}$ | 28.87$^{(b)}$ | 0.007 |
| | Natural Field | 31.42 | 32.70 | 32.91 | 30.23 | 0.643 |
| | Pasture | 20.59$^{(a)}$ | 16.32$^{(ab)}$ | 13.42$^{(b)}$ | 13.97$^{(b)}$ | 0.008 |
| | Forestry | 0.01$^{(a)}$ | 0.02$^{(a)}$ | 0.03$^{(ab)}$ | 0.05$^{(b)}$ | 0.036 |
| | Old growth | 24.51 | 21.22 | 21.01 | 21.83 | 0.374 |
| | Secondary Forest | 4.76 | 3.82 | 4.24 | 4.44 | 0.345 |
| Annual average of land tenure affected by fire (%) | Private | 60.35 | 60.86 | 60.32 | 59.76 | 0.917 |
| | Public | 26.33 | 26.31 | 26.98 | 26.73 | 0.9775 |
| | Not Designed | 12.20 | 11.89 | 11.87 | 12.64 | 0.8617 |
| | Urban | 1.11$^{(a)}$ | 0.94$^{(ab)}$ | 0.82$^{(b)}$ | 0.87$^{(b)}$ | 0.0231 |
| Total $CO_2$ immediate emission ($TgCO_2$) | | 799.58 | 937.55 | 663.27 | 729.68 | 0.9016 |
| Equivalence of monetary damage in relation to Brazilian GDP (%) | | 0.94%(a) | 0.41%(ab) | 0.21%(b) | 0.28%(b) | 0.0171 |

Note: Equal letters within parentheses represent the similarity between the means.
Source: From Author.

### 5.3.3 Fire impacts

The proportion of LULC classes derived from the reclassification of the MapBiomas product can be seen in APPENDIX B - Figure B-1, where it is verified that the forest class (Old growth and Secondary) represents 75% of the total of the Brazilian Legal Amazon region in 2020. If we analyze the classes impacted by fire over the last 20 years (Figure 5-11), the class “Old growth” was the most affected (38.73%), followed by “Natural Field” (30.21%), “Pasture” (19.74%), “Agriculture” (6.47%), “Secondary Forest” (4.62%), “Water” (0.3%), “Others” (0.09%) and “Forestry” (0.01%).

During this period, there was an increase in the average levels of the burned area for the “Agriculture” and “Forestry” classes, while for the “Pasture” class there was a decline and for the others the trend was not significant.

Figure 5-11. Summary of fire impacts on the LULC over the last 20 years: A - is the fire trend in each LULC class; B - is the LULC map for the year of 2019; C – is the average annual of each class affected by fire; D – historical percentage of each class affected by fire.

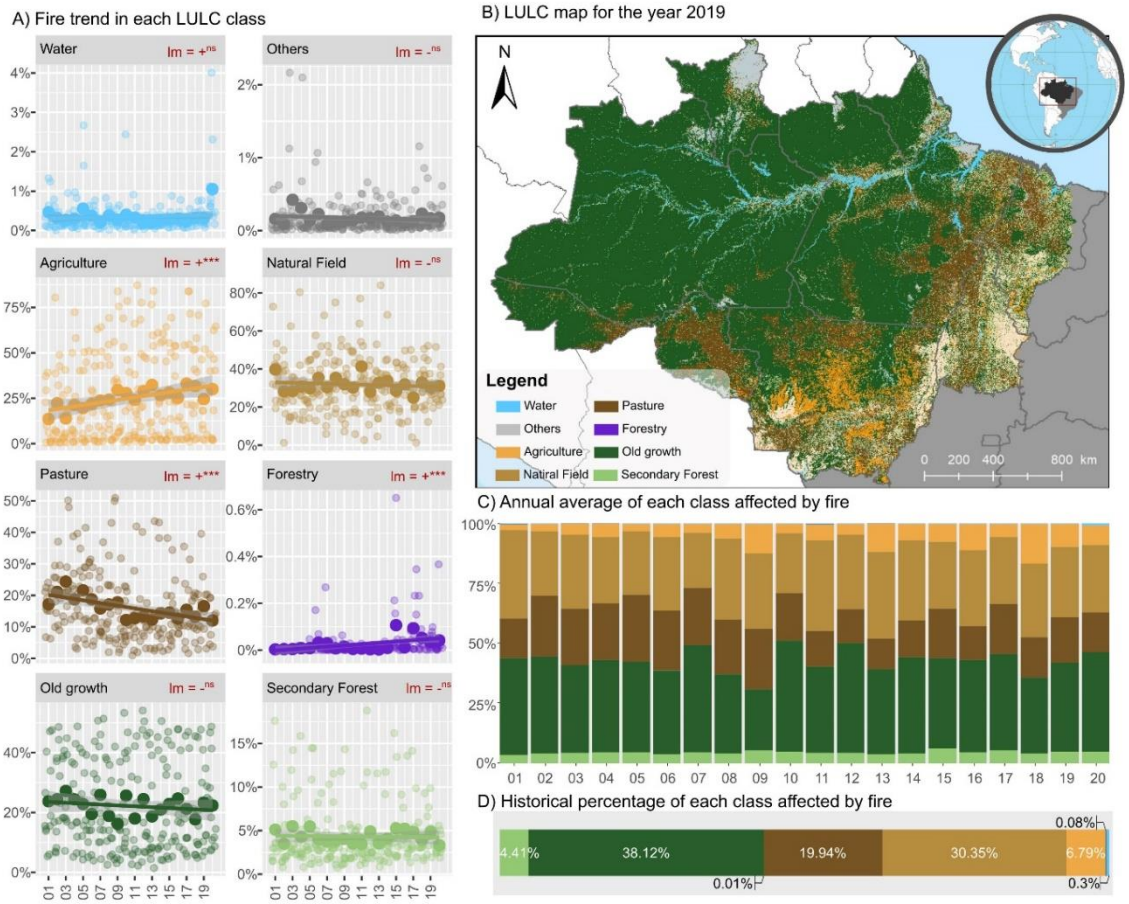


Source: From Author.

From the legal perspective of land tenure (Figure 5-12), we find that historically "Private" areas are the most affected, accounting for 60.3% of all fires, followed by "Public" (26.6%) and "Not Designated" areas (12.2%), in which didn't show a trend over the 20 years analyzed. In turn, the "Urban" areas, which are "Urban", "Highways" and "Water" classes, present a significant downward trend over the years, however this class has a low contribution to the total affected area, around 0.9%.

Figure 5-12. Summary of fire impacts on land tenure: A – distribution map of land tenure in the BLA region; B – trend in burned area by land tenure class; C – annual average of burned classes; D - average of Public class affected by fire per year.

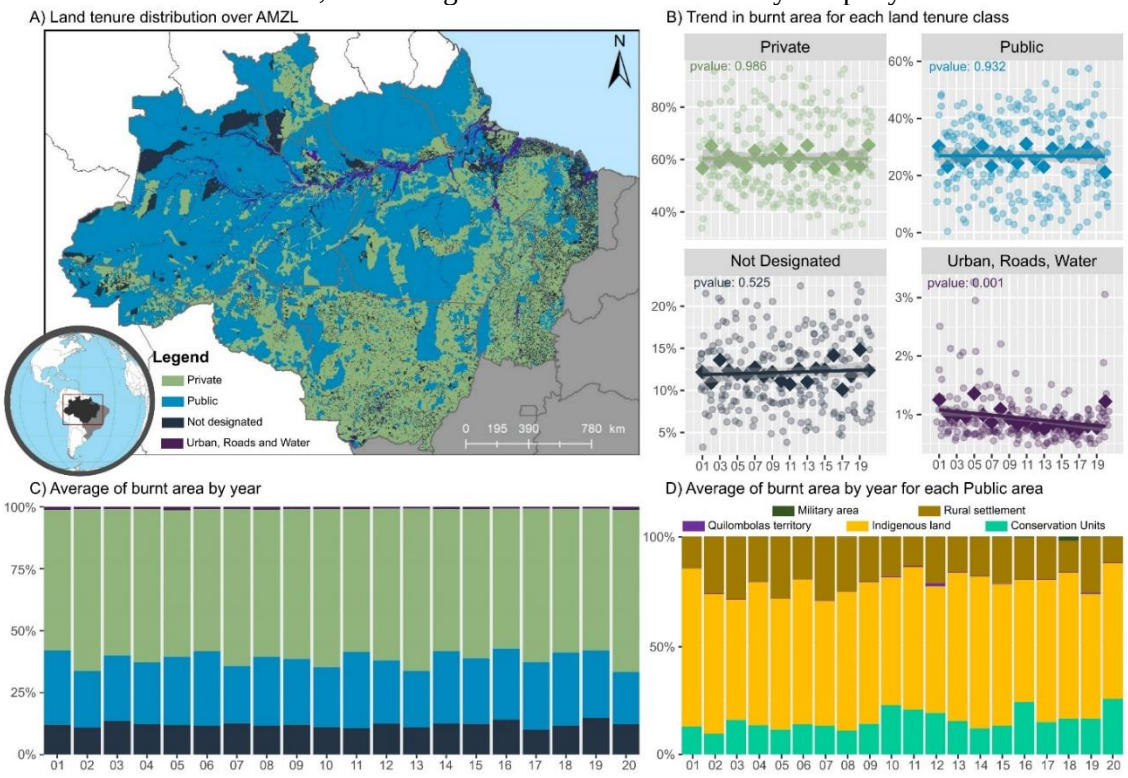


Source: From Author.

The average number of hospitalizations resulting from fire in the region (Figure 5-13) is approximately 98 hospitalizations annually. There is also a low value for the year 2020, however these values may be associated with the lack of updating of the system by the municipal and state health agencies during the COVID-19 pandemic.

Figure 5-13. Estimate of the number of hospitalizations for respiratory diseases over the last 20 years.

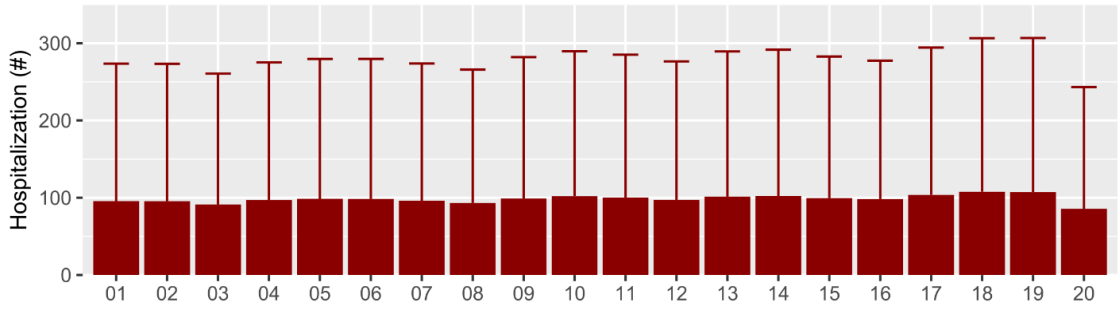


Source: From Author.

The estimated carbon dioxide values for the region during the analyzed period are presented in Figure 5-14. The bars represent the monthly values, the points the annual accumulated values and the dashed line the average annual value for the period. Both from gross and immediately emission.

When it comes to gross emissions, the region, on average, is responsible for 1,092 $TgCO_2$ annually, with average monthly contributions of 92 $TgCO_2$. While the immediately emission, here accounted only from the forest physiognomies (Old growth, Secondary Forest and Forestry classes), it is observed monthly contributions in the order of 65 $TgCO_2$ and an annual average of 782 $TgCO_2$.

Figure 5-14. Estimates of carbon dioxide emission (Tg $CO_2$) per month over the 20 years analyzed under the committed and immediate form.

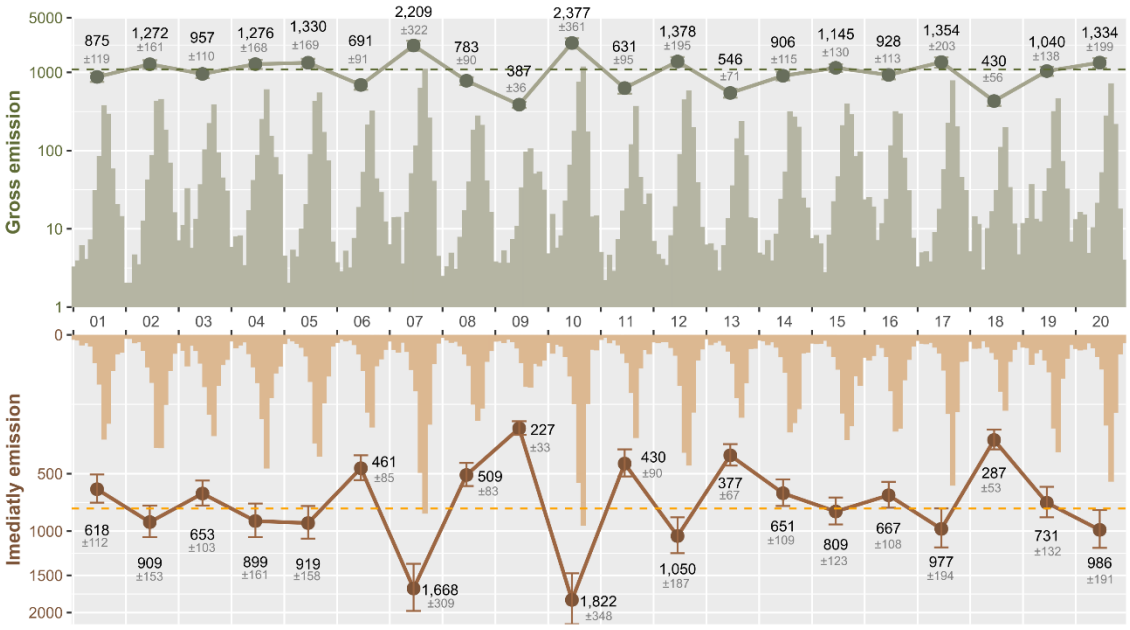


Note: The bars represent the monthly values, the dots represent the accumulated annual values and the dashed line the average annual value for the period. Gross emissions represent the total $CO_2$ that can be emitted immediately and later with the decomposition process. Immediate emissions refer to the total $CO_2$ emitted by the complete combustion of biomass from the forest classes (Old growth, Secondary Forest and Forestry).
Source: From Author.

### 5.3.4 Monetary quantification

The total damage over these 20 years sums around R$ 541 billion (Figure 5-15). The years of 2002 (R$ 59.91 ± 11.41 billion), 2007 (R$ 49.31 ± 9.02 billion) and 2004 (R$ 48.07 ± 8.38 billion) were the ones that accumulated the largest monetary damage

over the period. The total damage ratio represented an average 6.28%±1.1p.p of AMZL's GDP, ranging between 18.89%±3.60p.p (2002) and 1.27%±0.21p.p (2018), while for Brazil's GDP the damage represented an average of 0.46%±0.08p.p ranging between 1.31%±0.25p.p (2002) and 0.11%±0.02p.p (2018), as it is seen in Figure 5-16. Environmental damage, accounted here only for the $CO_2$ emission, corresponded to the largest fraction of the total damage, followed by material damage (accounted by loss of agroforestry production) and human damage (values for hospital admissions).

Figure 5-15. Total monetary damage caused by fire over the last 20 years in the BLA region, discretized by damage category.

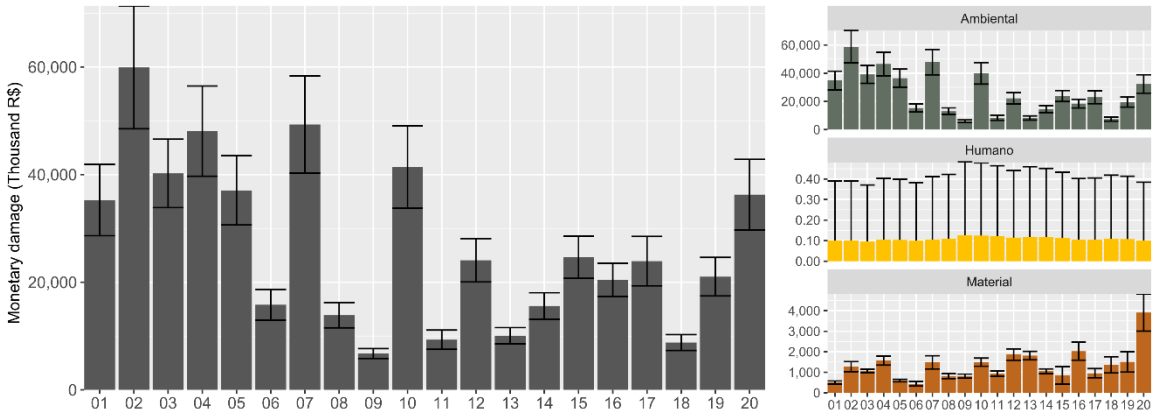


Note: Values corrected to current prices (January 2021) through the IPCA index provided by IBGE (2021b).
Souce: From Author.

Figure 5-16. Ratio between total fire damage and GDP in the region over the time series.

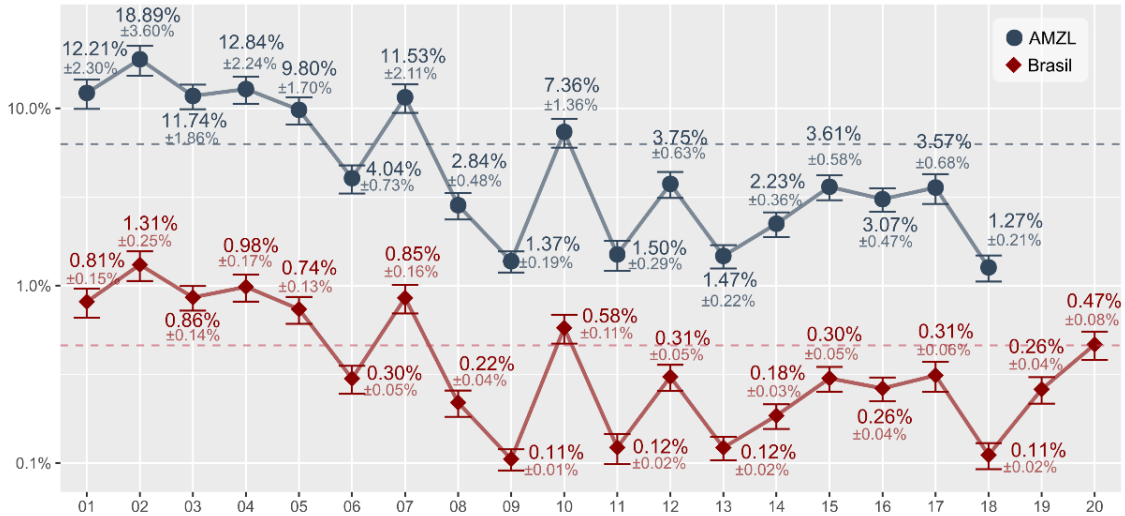


Source: From Author.

## 5.4 Discussion

### 5.4.1 The main patterns of the burned area in the BLA

The total burned area values are similar to those provided by global monitoring platforms, such as the GWIS -Global Wildfire Information System[12], (GWIS, 2021), which has one of its bases the MCD64A1 burned area product, with territorial and global analysis. In an annual comparison, maximum variations of 4% were obtained, mainly explained by the different methodologies for quantifying the total area. In comparison with national burning monitoring platforms, such as BDQueimadas (INPE)[13], the values presented in this study show the same high and low trends that occurred for the Amazon biome, but on average 40% higher.

Usually, optical satellite images only capture forest fires when the crowns of the trees are directly or indirectly affected. This technical limitation excludes other types of fires, such as the ground fires or understory fire, which do not have enough strength to be detectable by the satellite or to reach the canopy to the point to cause a detectable impact on the crown (CHUVIECO et al., 2019). Consequently, global fire products are often not accurate in detecting and estimating the total burned area in regions of dense forest cover (GIGLIO et al., 2009), such as the Amazon. Therefore, it is important to consider that all estimates derived from burned area products are potentially underestimated.

Among the 20 years analyzed, a negative linear trend was found in the monthly and annual burned area, but not significantly. This decrease pattern is also identified on a global and continental scale within the period from 2003 to 2015, based on burned area data using the MCD64A1 (ANDELA et al., 2017), in which the authors determined a significant decline of 1.15% per year globally and 1.4% per year for South America. In a longer series (2001 to 2016), but with hotspot data, Earl and Simmonds (2018) determined a significant 10% decline for the Amazon region. Both works are supported by the fact

[12] Data are available by states, thus the comparison were made by summarizing the total values of the nine states that are part of the BLA (AC, AM, AP, PA, MA, MT, RR, RO, TO).
[13] The AQ1Km product is built from MODIS data collection 6 from the concomitant AQUA and TERRA satellites, with low spatial resolution (1 km), and is made available by Biome, in this way the comparison was performed only with data for the Amazon biome.

of having a strong link between deforestation and fires, with the latter showing a large reduction in the period between 2011 and 2016.

However, there was a separation of these processes throughout the course of the Action Plan for Prevention and Control of Deforestation in the Legal Amazon - PPCDAm, (ARAGÃO et al., 2018; LIBONATI et al., 2021). Thus, this initial relationship, which would be leading to a negative trend until mid-2016 (Figure B-5), currently becomes non-significant and in positive parts due to the increase in the levels of burned area at the end of the series (Figure 5-2) and mainly by increasing trends in the first four months of the year (Figure 5-3). The full evolution is presented in the Appendix B.1.

Regulation and restrictions policies about the use of fire in states that have the greatest contribution in the total BLA's burned area, such as those in the state of Mato Grosso (MATO GROSSO, 2019, 2020, 2021), may be conditioning the trend in the BLA to be stable. However, it was found that even with these restrictions on controlled burning, as in the case of Tocantins (TOCANTINS, 2018, 2019, 2020), there was an increase of 10 percentage points in the contribution to the BLA's total burned area (Figure 5-6), leading to believe that these restrictions are not enough to prevent such growth or that other forms of fire, not subject to the mentioned restrictions, have become more relevant.

Repeated use of fire in the same place could be a sign of a specific land management practice, such as slash-and-burn agriculture. As pointed out by Costa (2008), fire is a widespread practice for increasing pastures and productivity in the northern Amazon. This practice has a high probability to create uncontrolled burning that reaches other areas, especially forests, due to the high flammability of grassland. The place with the highest frequency and recurrence of fire (Figure 5-7) is located in the middle-east of Mato Grosso, south-west of Tocantins and south of Maranhão, where the agriculture is expanding (FREITAS; MACIENTE, 2015), besides being the centre of the so-called "Arc of Deforestation".

Mato Grosso is also pointed out as the top state with repeated fires by Morton et al. (2013), in the study of forest fires between 1999 and 2010[14]. The authors found that the maximum frequency of repeated burning was five years, whereas our study points some places out

[14] The authors use fire patches greater than 50 ha to account the fire frequency in the Amazon region.

where they burn every year. These differences are linked to the size of the spots used in each methodology and the time series analysis.

Despite the reduction in the cost of agricultural land preparation due to the use of fire, repeated burning can trigger negative effects in the physical, chemical and biological soil properties (SANTÍN; DOERR, 2016), reflecting in more effort in the crop management. In the physical attributes, frequent burning increases the bulk density, decreases the hydraulic conductivity and the water conducts macroporosity (MAGOMANI; VAN TOL, 2019). Related to the chemical soil attributes, the effects are into changing carbon and nitrogen storage and also reducing decomposition rates of the organic matter (PELLEGRINI et al., 2020).

Regarding to forests, repeated burning causes impoverishment of biodiversity in forest ecosystems (NASI et al., 2002) and even when due to natural causes, they can reduce the height and diameter of vegetation in new regrowth (MEDEIROS; MIRANDA, 2005). Thus, the recurrence of fires can lead to drastic changes in the structure and composition of the forest, generating a sequence of transforming effects after each fire event (BARLOW; PERES, 2008).

Most areas affected by fire (64% of events) are in regions that have already suffered at least once from this type of phenomenon. Thus, when considering fire as a strategy for opening new areas and for agricultural expansion, the values presented are similar to those found by Aragão et al. (2008), in which the authors determined that approximately 60% of fire in the BLA region during 2005 was in deforested areas.

### 5.4.2 The magnitude of fire impact over 20 years

Approximately 17% (≈ 840,163 km²) of the BLA has already suffered from fire over 20 years, the land size is approximately equal to Mato Grosso state. This value is not far from those presented by the MapBiomas-Fogo project, which using Landsat images, determined that between 2001 and 2019 approximately 10% of the Amazon biome was damaged by fire, while approximately 18% of Brazil's territory was already impacted by this event (MAPBIOMAS, 2021b).

Among the main LULC, "Old growth" is the most affected class in the region, a fact linked both to the lack of fire control in agricultural areas and the consequent incidence

in this land cover, as well as to the use of fire in the expansion of areas. However, the alert is given in areas of the "Agriculture" class, where there has been a significant increase in its contribution over the years, leaving 13.6% in 2001 and reaching the 30% mark in 2020. This fact is evidenced by the significant difference between the beginning of the series (G1: 2001-2005) and the end (G4: 2015-2020), Table 5-5. However, due to the characteristics in the construction of the use and coverage product, fire may have been used to open new agricultural areas or for handling an existing crop, and this methodology cannot be used to separate them.

Thus, if we consider that the BLA has already burned at least 17% of its territory in the last 20 years and that fire affects an average of about 123,259 km² per year, approximately 36% (44.373 km²) of these are in a new area. Also, considering that out of the 5 million km² that the region covers and following the MapBiomas classification that only 2% are areas without vegetation, we can infer that if these rates remain constant, in approximately 46 years we will have burned half of the region and in 92 years the entire legal Amazon will have been affected by fire.

The responsibility for fire mostly rests with private properties, where an average of 60.3% (Figure 5-12) of all the fire is in this kind of territory, even though they only cover 30.69% of the region (Table B-1). Within public responsibility, the areas with the highest incidence are: Indigenous Lands (TI: 63.11%) followed by Rural Settlements (Aru: 20.52%), Conservation Units (UC: 15.71%), Quilombolas (Qu: 0.39%) and Military Areas (ArM: 0.28%).

Among these, the UCs, ArM showed a positive trend in the burned areas and is significant at 5% (Figure B-2). On the other hand, ARu showed negative trends in the occurrence of fire along the years, but significant only at 10%. Finally, TI and Qu did not present a significant trend in the burned area along the analyzed years.

Even without an established trend over the years, TI are the territorial units that suffer from the increase in illegal activities that threaten their delimitation and the safety of those who live there (FELLOWS et al., 2021), this factor may be leading the high levels of area burned during the entire period. However, it is good to mention that the delimitation of land tenure by the IMAFLORA is static over time, thus it is not possible to separate the

use of fire before the approval of public lands. On the other hand, according to Veríssimo et al. (2011), the greatest increase in the extension of indigenous lands was in two periods prior to the data series used in this study, one in 1990/1994 and the other in 1995/1998. Therefore, most of the fires that occurred inside the TI was an attempt for invasion and illegal appropriation of land, like the work presented by Fellows et al. (2021), in which 83% of all TI in the Amazon region suffered from cases of invasion using fire and deforestation.

Among these illegal activities, land grabbing is an integral part of Brazilian land tenure history (MARTINS, 1994 apud; TORRES; CUNHA; GUERRERO, 2020), especially in the Amazon region where it is closely linked to the expropriation of traditional people and communities. During the process of recognition of Indigenous territories, the lack of official boundaries motivates a wave of invasions that expect to have legal rights over the TI area due to breaches and flexible regulations in the current law (TORRES; CUNHA; GUERRERO, 2020). Or in newly created UCs that suffers a pressure for occupation or for implementation of economic activities (agriculture, logging and mining) that are not consistent with the preservation class or legal activity within the buffer zone (DUARTE; SILVA; CERQUEIRA; et al., 2019).

This pressure is also perceived in the classes that are still in process to have a recognized destination, in the case of "Not Designated" category, which grouped "Public properties", "Public Forest", "Undesignated land" and areas without a legal information. This category shows a high stability along the years (average 12.2%±1.1p.p of all fire registered), however it presented two big events in the last 5 years, one in 2019 (15%) and other in 2016 (14%). This was also sensed in the work by Alencar et al. (2020), using thermal anomalies, in which they found that 30% of all fire in 2019 occurred in the "not designated forest" and "without information" classes, assigning those values to the increase in illegal occupation of these territories without official records.

Translating all these damages over the years into monetary values, we saw that Environmental damage has the greatest influence in this quantification. This component shows large fluctuations over these 20 years, in which the first quarter of the series (2001 to 2005) is strongly related to emissions from the "Pasture" and "Forest" classes, which

are the greatest potentials for emissions. However, this pattern is changed at the end of the first decade for a bigger contribution of emissions by the "Agriculture" class.

This relation follows the pattern of deforestation in the region that was strongly linked to the fire at the beginning of the 21st century, and after the deforestation started to decrease (ARAGÃO et al., 2018; LIBONATI et al., 2021). This relation induces high values in normal climate years, like the ones registered in 2004, which present monetary values similar to drought years (2002, 2005 and 2007) in the same decade.

The second decade is characterised by smaller values at the beginning with a gradual increase, reaching in 2020 the same levels of 2002-2004. In this second half, the value added by the Material component is highlighted in relation to the first half, while the Environmental component follows the pattern of lower emissions due to the change in the LULC. However, both components (Environmental and Material damages) are influenced by the combination of inflation and the dollar price, associated with this combination, the profit on soybean production in 2020 was three times higher than in previous years, and with that, there was a significant increase in this year in relation to the others, impacting not only this class but also the total damage.

The average annual damage in the BLA is around R$ 27.1 billion per year (~US$ 5.22 billion)[15]. If an average of 123,259 km² burns per year, it implies that each km² burned refers to a damage of R$ 219,778. The annual damage is two time greater than those estimated by De Mendonça et al. (2004), which indicate a damage of R$ 11.5 billion per year (maximum of R$ 22.79 billion and minimum of R$ 0.41 billion)[16]. The authors also predicted values above R$ 40 billion in years of severe droughts. Similar to the values presented in this chapter, the total damage was mainly influenced by the $CO_2$ estimate.

These damages compared to the Brazilian Gross Domestic Product are on average 0.46%±0.08p.p, and for the BLA region it is approximately 6.28%±1.1p.p. This value is greater to that found by De Mendonça et al. (2004) which is around 0.2% and 0.9% in relation to the region. However, it is noteworthy that in this study we focused on three

[15] Considering the exchange rate of US$1 as R$5.16, exchange value in earlier 2021 (IPEA, 2021).
[16] The authors estimate the annual costs, in 1998, of approximately US$ 90 to US$ 5,055 million, reaching US$ 9 billion in El Niño years. To bring it to the same period that are in this chapter (January of 2021), we convert the values to reais using the 1998 exchange rate by (IPEA, 2021) and then uses the IPCA index by (IBGE, 2021g), making the values comparable whith those founded in this chapter.

out of the various components that fire can interfere and also on a single scale of impact, the regional one. Thus, the values presented here, regarding the multidimensionality of the damage, omit some components (eg, loss of biodiversity, impacts on land and air transport, and tourism).

Although fires have a significant impact on the economy of a region, the available budget by the federal government for fire control and management in the BLA is around US$ 3.1 million per year, about 1% of the entire budget allocated for the Ministry of the Environment (MORELLO et al., 2020), a value that is 1,683 times lower than the average annual damage. This available value represents, by the indices and values found here, the equivalent of the annual damage of an area of approximately 70 km² (7,000 hectares), same amount that on average impacts 4 municipalities in a year. Considering that the BLA has 772 municipalities and along these 20 years, around 674 (87%) municipalities were impacted by fire every year (Figure B-3), the budget allocated to control and manage all territory is very low.

The budget allocation is primarily for firefighting and suppression actions in detriment to prevention and control actions, such as the creation and maintenance of monitoring systems; brigade training; community support, and environmental education (MORELLO et al., 2017b). Adopting only suppression measures is trying to mitigate damage that has already been caused and they do not allow society to change its habit, either by introducing production practices with less impact (including for example, low-carbon agriculture (MAPA, 2012), no-till system, agroforestry systems) or by having environmental education for sustainability. Within this context, it is essential to develop a management system that encompasses a broader structure through the integration of actors, researchers, monitoring entities at a federal and a state level, with agencies of education, communication, training, prevention and response at lower levels (State and Municipal) in order to deal with this phenomenon that is directly linked to human activities (ANDERSON et al., 2019).

### 5.4.3 Side effect of fire in national and international environmental targets

After years of degradation and exploration of the BLA's environmental matrix, the effects of the use of fire are already felt in milestones and guidelines for environmental protection and conservation, in internal policies or in established international agreements.

In a national context, analysis of forest cover through the years indicates that the percentage of forest cover (Old growth and Secondary Forest) for the BLA region (Figure B-1) is below that one established by law, regarding protection of forest resources. This value is lower than the 80% established for Legal Reserve, according to the New Brazilian Forest Code (BRASIL, 1998, cap. IV, 2012). Considering a region that has 7% of its territory made up of strict protection Conservation Units (Table B-1), and that, in addition to legal reserve areas and the presence of permanent preservation areas is mandatory, the value allocated for the protection of forests is way less than what is required by law.

However, the percentage to be destined varies according to the predominant phytophysiognomy of the place. Thus, properties within the Amazon biome must make 80% of their territory available for this purpose, while in properties within Savannah formations this value is 35%, and in other phytophysiognomies this value drops to 20% (BRASIL, 2012). Performing these separations based on the delimitation of Brazilian biomes according to IBGE (Figure B-1), it was found that the value of forest cover within the Amazon biome from 2018 onwards is below that one required by law, and in 2020 it represented 1.2% less than the required only for the Legal Reserve item, a liability of 6,217 $km^2$. These values can be much higher, since after the consolidation of the New Brazilian Forest Code many properties were granted amnesty, removing the responsibility for restoration or compensation (SOARES-FILHO et al., 2014).

Another guideline found is the negligence or low effectiveness of policies to regulate the use of fire in emerging states, such as the one found for the state of Tocantins, which presented an increase of 10p.p in its contribution to the total burned in the AMZL region. This increase in the contribution may, at first, be related to the decrease in the contribution of other key states. However, throughout the series, the absolute values for this state showed an upward trend (Table B-2), especially when considering the seasonality of the data.

Within the category of reduction of greenhouse gas (GHG) emissions, the carbon dioxide estimates made by the National Emission Registry System - SIRENE (MCTIC, 2019)[17]

[17] Among the possible methods to quantify emission from burned areas are: the burning of agricultural residues for the agriculture sector, which is based on the area planted with sugarcane; and the burning associated with deforestation, within the Land Use Change sector, in which it is accounted from the remaining dry matter in the field after a vegetal extraction.

do not consider those from forest fires, neglecting the entire effect that fire has contributed to the pollutant load. Our estimates point to an emission load up to 2,377±361 $TgCO_2$ in extreme years, which can be gradually release in 30 years (SILVA et al., 2020). In an immediate way, it is quantified that in extreme years, around 1,822±348 $TgCO_2$ is emitted, its represents 6 times greater than the total computed for the category of "Land Use Change" for the whole year of 2010 by SIRENE. The non-incorporation of these immediate issues and over 30 years, leads to underestimating and sometimes generating unrealistic rates, which at first can create a feeling of a completed goal, but there is much to be done ahead.

If these estimates were included in the national accounts, only the immediate emission from fires in forest formations in the BLA region would contribute, on average, to an 50% increase in values, reaching 152% in years of extreme drought (for example, in 2010), reflecting on average 31% in the contribution with a maximum of 60% (Figure B-4).

One of the first targets for regulating the reduction of greenhouse gas emissions, as a result of an international commitment, was the institutionalization of the National Policy on Climate Change (PNMC), governed by Law N°. 12,187 of 2009 and regulated by Decree N°. 9,578 /2018. It predicts a reduction between 1,168 $TgCO_2eq$ and 1,259 $TgCO_2eq$ of emissions by 2020. However, considering the immediate emissions from forest formations only for the BLA region, this target was not achieved, thus when considering fires in other Brazilian regions, this scenario is even worst

After this initiative, and still following the guidelines taken during the United Nations Framework Conventions on Climate Change (UNFCCC), Brazil implemented the Determined National Contribution (NDC) in 2016, and in 2020 an update was made (BRASIL, 2020; UNFCCC, 2021), which undertakes, among other measures, a 37% reduction in greenhouse gas by 2025 and 43% by 2030, based on the estimate in 2005. Considering the estimates presented in this chapter and the extrapolation of official data for 2020[18], the reduction rates are in 14%. This shows the need to adopt stricter measures

[18] The national estimate provided by the SIRENE (MCTIC, 2019) is only until 2016. For the remaining years, we use the trend in each category to extrapolate, with exception for the lad use change category that we use the correlation of it with deforestation rates provided by Terrabrasilis (INPE, 2021b).

to restrain the increase in the emissions levels by the main contributors to GHG, which currently are the LULC changes and forest fires that are not totally accounted for.

It should be noted that these estimates are including only the immediate emission by completely combustion of forest and only for the BLA region. It is not taking into account the gradual degradation of the burned matter, which is released over a 30-year period (SILVA et al., 2020), nor other regions, like the entire Savannah, which is the second biome with the highest records of fire in Brazil (INPE, 2020), or the contribution of anomalous events from other regions that face irregular fire events, such the ones occurred in the Wetland biome in 2020 (PLETSCH et al., 2021) that presented an expressive impact, demonstrating that the guidelines and national measurements must be revised over the years, in order to properly include those effects.

## 5.5 Conclusion

This chapter quantified the damage caused by fire over 20 years in the Brazilian Legal Amazon, highlighting its main components, temporal trend, and geographic distribution. Geoprocessing methods, statistical and economic analysis were combined in an innovative way, generating a satisfactorily broad understanding of the multidimensionality of the impact caused by fire. Worryingly, the results revealed a sizeable damage that is not following a decreasing trend, which is a call for a more effective policy.

The region has burned areas throughout the year, with a monthly average of 10.271 km², mostly consisting of small patches up to 40 ha. The fire season is concentrated between the months of August and October, when there is an increase in large (404 to 4,046 ha) and very large (≥ 4,046 ha) patches, the same period in which most of the affected areas have already suffered from some burnings in previous months/years. In total, approximately 840,163 km² of the area have already been burned, this is the equivalent of 17% of the total area of the BLA. The recurrence of fire in the region is high, with emphasis on agricultural expansion zones (MT, MA and TO) where burning was recorded every year.

Burned areas presented an increasing trend in the minimum area per month; in the occurrence of anomalous months; and in the burned area of the first months of the year.

Compared to previous years, the years from 2015 to 2020 already showed evidence of changes in the fire pattern at the beginning of the year (January and February), especially regarding to the increase in the burned area, the increase in the number of events during the month, and in the number of municipalities that are affected.

The impact of this phenomenon over the years is represented by the equivalent damage of an average of 6.28%±1.1p.p. per year of the BLA's GDP, 0.46%±0.08p.p per year of the Brazilian GDP. The first 10 years of the series showed the highest damages, however, there is an increase in the damage again in relation to the last 3 years of the series. The Environmental component ($CO_2$ emissions) is the largest fraction of the total damage and its estimate can destabilize national and international short and long-term reduction targets.

The monetary quantification presented in this chapter is limited firstly by the burned area product and its specificities; later by the quantity, type and scale of components affected by fire chosen, and finally by the microeconomic approach used in the monetary quantification which is based on established or surrogate markets. Therefore, supporting more studies over the other components affected by fire, including different scales, can provide more information about the real impact of fire in a region. Besides this, adopting other and more accurate burned area products or including information of fire power levels will refine the impact caused by the fire and expand the perception of its magnitude. Then, with a common methodology, it will be possible to incorporate monetary quantification in a monitoring system, enabling new perspectives of risk assessment and impact of fire.

# 6 GENERAL DISCUSSION

Chapter 3 presented the quantification of the damage caused by fires in the state of Acre, west of the Legal Amazon, between 2008 and 2012. From five impacts, subdivided into three groups, it was possible to determine the total damage caused during this period, with emphasis on years with extreme droughts (2010).

In this case study, the increase in fire events in a year of extreme drought was evident, mainly due to the determination of burned areas farther away from the main sources of fire propagation in the region (roads and rivers). These effects were reflected in the total damage that occurred during these climatically anomalous years, reaching up to 16 times greater compared to normal ones.

Within this chapter, the introduction of a more robust methodology for quantifying $CO_2$ is highlighted, through the insertion of a remaining carbon stock after a burning event, being considered for the subsequent burning months, describing in a better perspective the effect that recurrent burns have on total emissions.

One of the limitations found in this chapter was a non-identification of a clear relationship between the number of respiratory cases and the total burned area. However, estimates made with the OLS method do not separate the specific effects of fire. In addition, the performed analysis did not consider the existing chain of events to link burned area and respiratory hospitalization, among other aspects such as variables that can control demand and supply of this cause-effect chain.

Due to this lack of relationship using the initial data series of Chapter 3, which accounted for only 5 years, Chapter 4 was built with more improved techniques to estimate hospitalizations attributable to pollution of burned areas within a larger data series.

Thus, Chapter 4 is based on the premise that once fires of considerable size and number occur in one location, the load of pollutants released and transported to populated areas will cause considerable onset of respiratory diseases (CARMO et al., 2010; IGNOTTI et al., 2010; GONÇALVES et al., 2018). This effect is different between vulnerable groups, either because of the difference in age or by type of corelated disease.

Therefore, this relationship was estimated through the application of the instrumental variable method under a balanced panel at a municipal and monthly level of data. Therefore, a positive effect was found between fire-pollutants and the number of hospitalizations due to respiratory diseases, with the main emphasis on the 65-year-old age group and the group of diseases related to Asthma and Bronchitis. This positive effect was previously found by other studies with similar methodological strategies (CARMO et al., 2010; JACOBSON et al., 2014; DERYUGINA et al., 2019; ROCHA; SANT'ANNA, 2020).

This new methodology indicated that during the burning season (Aug-Oct) approximately 4,000 people are hospitalized for some respiratory-related disease in the BLA region. However, new estimates must be carried out in order to incorporate other related events, such as the effect of other pollutant sources; the weight that neighboring municipalities can exert both on the load of pollutants and also on the hospitalizations counts, and the effect of the lag between fire and hospitalization values.

In the Chapter 5 it was applied the initial methodology provided for Chapter 3 with the updated hospitalizations rate found in Chapter 4 for the entire Legal Amazon region, but using a 20-year time scale (from 2001 to 2020), also including the description of the fire occurrence pattern throughout the months and its evolution during the data series.

At first, there was no significant tendency in the increasing in burned areas in the time series, as shown by Andela et al. (2017) and Earl & Simmonds (2018) in which this characteristic is mainly explained by the existing fluctuation between deforestation and fire. However, there was an increase in the minimum monthly burned area, and in the frequency of anomalies in burned months, especially during the last years.

Agricultural activities were highlighted both in the local context (Chapter 3), where the "Pasture" class was the most affected by fire, and in the regional context (Chapter 5) where the "Agriculture" class presented the largest increase (17 percentage points) throughout the series. It indicates that the BLA still has fire as a recurrent agricultural practice.

This dynamic is also notable from the perspective of territorial responsibility, in which most of the burned areas were found in private areas (60.3% in BLA and 98.4% in AC).

Considering the public management areas, Indigenous Lands have a relevant role in the amount of burned area, and this is due more to the fact that indigenous territories suffer from the increase in illegal activities, such as “land grabbing” (FELLOWS et al., 2021), than the use of fire as an agricultural practice or religious ritual (LEONEL, 2000; PIVELLO, 2011; GRAF, 2016).

The damages occurred during these 20 years when compared to the Brazilian Gross Domestic Product (GDP) it is equivalent to an average of 0.46%±0.08p.p while for the BLA region these values are close to 6.28%±1.1p.p.. Within the state scale (Chapter 3), damages in normal climate years are equivalent to approximately 0.51%±0.10p.p of Acre's GDP, and in anomalous years it can represent 7.03%%±2.4p.p. However, the real magnitude of these values are higher, since this thesis only counted few components impacted, not considering others impacts such, biodiversity reduction; habitat changes; species migration; decrease in tourism; losses of cultural assets; change in the hydrological cycle; change in the soil properties; phycological traumas; car accidents; or infrastructure losses.

Finally, the recurring erosion of BLA's environmental matrix over the time begins to be felt, among other aspects, in milestones and guidelines for the protection and conservation of the environment, whether in non-compliance with the Forest Code (BRASIL, 2012) or in an incompatibility with the goal of reducing greenhouse gas emissions ratified by law, first by the National Policy on Climate Change – PNMC (BRASIL, 2009), which foresees reductions until 2020, and later with the low reductions conquered until now, but still far from those established in the Paris Agreement, through the Nationally Determined Contribution - NDC (BRASIL, 2020; UNFCCC, 2021).

# 7 CONCLUDING REMARKS

This thesis provided support to understand the extent, the magnitude and the damage caused by the use of fire in the Brazilian Legal Amazon during the last 20 years, which can subsidize the planning of public investments, policies and mitigating measures to decrease the region vulnerability to fires.

The region is affected by fire throughout the year, with a monthly average of 10,271 km², with the fire peak between the months of August and October, presenting small differences between the fire regimes in the Northern states than in the Southern ones, where the initial months are gaining greater proportions.

The change in the way of quantifying the rate of hospitalizations due to respiratory illnesses, obtained in Chapter 3 and Chapter 4, improved the estimates in addition to contributing to the understanding of the relationship between fire-induced smoke in hospitalization due to respiratory illness in the BLA region. These estimates indicated a positive effect of pollutants on hospitalization levels for the region, and it can be estimated that around 4,000 people are hospitalized annually during the fire season.

Fire has a complex and interconnected chain of direct and indirect effects that can make the study of its impact challenging. A few items, such as those used in this thesis (losses in agroforestry production, carbon dioxide emissions and hospitalizations for respiratory diseases) can cause great harm, which for the whole BLA was found, on average, the equivalent to 6.28%±1.1p.p. of GDP reaching a maximum of 18.89%±3.6p.p. In some cases, these damages are much greater, with a maximum recorded of 7.03% of GDP as observed in Acre, during anomalous dry years.

## REFERENCES


AGÊNCIA NACIONAL DE ENERGIA ELÉTRICA - ANEEL. **Dados estatísticos de transmissão**. Available from: https://www.aneel.gov.br/fiscalizacao-da-transmissao-conteudos/-/asset_publisher/agghF8WsCRNq/content/dados-estatisticos-da-transmissao/656808?inheritRedirect=false. Access on: 24 Dec. 2020.

AHRENS, M.; EVARTS, B. **Fire loss in the United States during 2019**. NFPA - National Fire Protection Association, 2020.Available from: https://www.nfpa.org//-/media/Files/News-and-Research/Fire-statistics-and-reports/US-Fire-Problem/osFireLoss.pdf.

ALBURQUERQUE, I. et al. **Análise das emissões brasileiras de gases de efeito estufa e suas implicações para as metas de clima do Brasil 1970-2019**. Observatório do Clima, 2020. Available from: https://seeg-br.s3.amazonaws.com/Documentos%20Analiticos/SEEG_8/SEEG8_DOC_ANALITICO_SINTESE_1990-2019.pdf. Access on: 6 July 2021.

ALENCAR, A.; RODRIGUES, L.; CASTRO, I. **Amazônia em chamas: o que queima e onde**. Brasília: Instituto de Pesquisa Ambiental da Amazônia, 2020. Available from: https://ipam.org.br/wp-content/uploads/2020/08/NT5-pt-final.pdf. Access on: 7 Jan. 2021.

ALMEIDA, C. A. et al. High spatial resolution land use and land cover mapping of the Brazilian Legal Amazon in 2008 using Landsat-5/TM and MODIS data. **Acta Amazonica**, v. 46, n. 3, p. 291–302, 2016.

ALVARES, C. A. et al. Köppen's climate classification map for Brazil. **Meteorologische Zeitschrift**, v. 22, n. 6, p. 711–728, 2013.

ALVES, R. N. B.; MODESTO JÚNIOR, M. S. **Roça sem fogo**: da tradição das queimadas à agricultura sustentável na Amazônia. Brasília - DF: Embrapa, 2020.

AMARAL, E. F. et al. **Inventário de emissões antrópicas e sumidouros de gases de efeito estufa do estado do Acre**: ano base 2014. Rio Branco: EMBRAPA-AC, 2018.

Available from: http://www.bdpa.cnptia.embrapa.br/consulta/busca?b=ad&id=1105534&biblioteca=vazio&busca=1105534&qFacets=1105534&sort=&paginacao=t&paginaAtual=1.

ANDELA, N. et al. A human-driven decline in global burned area. **Science**, v. 356, n. 6345, p. 1356–1362, 2017.

ANDERSON, L. O. et al. Counting the costs of the 2005 Amazon drought: a preliminary assessment. In: MEIR, P. et al (Ed.). **Ecosystem services for poverty alleviation in Amazonia**. [S.l.]: ESPA, 2011.

ANDERSON, L. O. et al. Detecção de cicatrizes de áreas queimadas baseada no modelo linear de mistura espectral e imagens índice de vegetação utilizando dados multitemporais do sensor MODIS/TERRA no estado do Mato Grosso, Amazônia brasileira. **Acta Amazonica**, v. 35, n. 4, p. 445–456, 2005.

ANDERSON, L. O. et al. Detecção de cicatrizes de áreas queimadas baseada no modelo linear de mistura espectral e imagens índice de vegetação utilizando dados multitemporais do sensor MODIS/TERRA no estado do Mato Grosso, Amazônia brasileira. **Acta Amazonica**, v. 35, n. 4, p. 445–456, 2005.

ANDERSON, L. O. et al. Development of a point-based method for map validation and confidence interval estimation: a case study of burned areas in Amazonia. **Journal of Remote Sensing & GIS**, v. 6, n. 1, 2017.

ANDERSON, L. O. et al. Disentangling the contribution of multiple land covers to fire-mediated carbon emissions in Amazonia during the 2010 drought: drought, fire, and C emission in Amazonia. **Global Biogeochemical Cycles**, v. 29, n. 10, p. 1739–1753, 2015.

ANDERSON, L. O. et al. Modelo conceitual de sistema de alerta e de gestão de riscos e desastres associados a incêndios florestais e desafios para políticas públicas no Brasil. **Territorium**, n. 26, n.1, p. 43–61, 2019.

ANDERSON, L. O. et al. Vulnerability of Amazonian forests to repeated droughts. **Philosophical Transactions of the Royal Society B: Biological Sciences**, v. 373, n. 1760, p. 20170411, 2018.

ANDRADE FILHO, V. S. et al. Aerossois de queimadas e doencas respiratorias em criancas, Manaus, Brasil. **Revista de Saúde Pública**, v. 47, n. 2, p. 239–247,. 2013.

ANDREAE, M. O. et al. Smoking rain clouds over the Amazon. **Science**, v. 303, n. 5662, p. 1337–1342, 2004.

AQUINO, R.; DE OLIVEIRA, N. F.; BARRETO, M. L. Impact of the Family Health Program on infant mortality in brazilian municipalities. **American Journal of Public Health**, v. 99, n. 1, p. 87–93, 2009.

ARAGÃO, L. E. O. C. et al. Interactions between rainfall, deforestation and fires during recent years in the Brazilian Amazonia. **Philosophical Transactions of the Royal Society B: Biological Sciences**, v. 363, n. 1498, p. 1779–1785, 2008.

ARAGÃO, L. E. O. C. et al. Spatial patterns and fire response of recent Amazonian droughts. **Geophysical Research Letters**, v. 34, n. 7, L07701, 2007.

ARAGAO, L. E. O. C.; SHIMABUKURO, Y. E. The incidence of fire in Amazonian forests with Implications for REDD. **Science**, v. 328, n. 5983, p. 1275–1278, 2010.

ARAGÃO, L. E. O. E C. et al. 21st Century drought-related fires counteract the decline of Amazon deforestation carbon emissions. **Nature Communications**, v. 9, n. 1, p. 1–12, 2018.

ARAGÃO, L. E. O. E C. et al. Assessing the influence of climate extremes on ecosystems and human health in southwestern Amazon supported by the PULSE-Brazil Platform. **American Journal of Climate Change**, v. 5, n. 3, p. 399–416, 2016.

ARBEX, M. A. et al. Air pollution from biomass burning and asthma hospital admissions in a sugar cane plantation area in Brazil. **Journal of Epidemiology & Community Health**, v. 61, n. 5, p. 395–400, 2007.

ARCHIBALD, S. et al. Defining pyromes and global syndromes of fire regimes. **Proceedings of the National Academy of Sciences**, v. 110, n. 16, p. 6442–6447, 2013.

ARTAXO, P. et al. Aerosol particles in Amazonia: their composition, role in the radiation balance, cloud formation, and nutrient cycles. In: KELLER, M. et al. (Ed.). **Amazonia and global change**. [S.l.]: AGU, 2009. p. 207–232.

AVILA-DIAZ, A. et al. Assessing current and future trends of climate extremes across Brazil based on reanalyses and earth system model projections. **Climate Dynamics**, v. 55, n. 5–6, p. 1403–1426, 2020.

BACCINI, A. et al. Tropical forests are a net carbon source based on aboveground measurements of gain and loss. **Science**, v. 358, n. 6360, p. 230–234, 2017.

BANCO CENTRAL DO BRASIL - BCB. **Cotações e boletins**. Available from: https://www4.bcb.gov.br/pec/taxas/port/ptaxnpesq.asp?id=txcotacao. Access on: 9 July 2018.

BANQUE INTERAMÉRICAINE DE DÉVELOPPEMENT - BID. **BR-L1289:** the Acre Sustainable Development Program (PDSA-II). Available from: https://www.iadb.org/fr/project/0?projectNumber=2928/OC-BR;BR-L1289. Access on: 30 Sept. 2018.

BARLOW, J. et al. Clarifying Amazonia's burning crisis. **Global Change Biology**, v. 26, n. 2, p. 319–321, 2020.

BARLOW, J. et al. Large tree mortality and the decline of forest biomass following Amazonian wildfires. **Ecology Letters**, v. 6, n. 1, p. 6–8, 2003.

BARLOW, J.; PERES, C. A. Fire-mediated dieback and compositional cascade in an Amazonian forest. **Philosophical Transactions of the Royal Society B: Biological Sciences**, v. 363, n. 1498, p. 1787–1794, 2008.

BARUFI, A. M.; HADDAD, E.; PAEZ, A. Infant mortality in Brazil, 1980-2000: a spatial panel data analysis. **BMC Public Health**, v. 12, n. 1, p. 181, 2012.

BAUM, C. F.; STILLMAN, S. **DMEXOGXT**: stata module to test consistency of OLS vs XT-IV estimate. Boston College Department of Economics, 1999. Available from: https://ideas.repec.org/c/boc/bocode/s401103.html. Access on: 26 Oct. 2020

BEN-AMI, Y. et al. Transport of North African dust from the Bodélé depression to the Amazon Basin: a case study. **Atmospheric Chemistry and Physics**, v. 10, n. 16, p. 7533–7544, 2010.

BERNARD, S. M. et al. The potential impacts of climate variability and change on air pollution-related health effects in the United States. **Environmental Health Perspectives**, v. 109, Suppl 2, p. 199–209, 2001.

BOONE KAUFFMAN, J.; CUMMINGS, D. L.; WARD, D. E. Fire in the Brazilian Amazon 2: biomass, nutrient pools and losses in cattle pastures. **Oecologia**, v. 113, n. 3, p. 415–427, 1998.

BÖRNER, J.; MENDOZA, A.; VOSTI, S. A. Ecosystem services, agriculture, and rural poverty in the Eastern Brazilian Amazon: interrelationships and policy prescriptions. **Ecological Economics**, v. 64, n. 2, p. 356–373, 2007.

BOSCHETTI, L. et al. Global validation of the collection 6 MODIS burned area product. **Remote Sensing of Environment**, v. 235, e111490, 2019.

BOUSTRAS, G.; BOUKAS, N. Forest fires' impact on tourism development: a comparative study of Greece and Cyprus. **Management of Environmental Quality: An International Journal**, v. 24, n. 4, p. 498–511, 2013.

BRANDO, P. et al. Amazon wildfires: scenes from a foreseeable disaster. **Flora**, v. 268, p. 151609, 2020.

BRANDO, P. M. et al. Abrupt increases in Amazonian tree mortality due to drought-fire interactions. **Proceedings of the National Academy of Sciences**, v. 111, n. 17, p. 6347–6352, 2014.

BRASIL. CÂMARA DOS DEPUTADOS. **Lei Complementar n°124, de 3 de Janeiro de 2007**: institui, na forma do art. 43 da Constituição Federal, a Superintendência do Desenvolvimento da Amazônia – SUDAM; estabelece sua composição, natureza

jurídica, objetivos, área de competência e instrumentos de ação; dispõe sobre o Fundo de Desenvolvimento da Amazônia – FDA; altera a Medida Provisória no 2.157-5, de 24 de agosto de 2001; revoga a Lei Complementar no 67, de 13 de junho de 1991; e dá outras providências. 2007. Available from: https://www2.camara.leg.br/legin/fed/leicom/2007/leicomplementar-124-3-janeiro-2007-548988-norma-pl.html.

BRASIL. ITAMARATY. **Pretendida contribuição nacionalmente determinada para consecução do objetivo da Convenção-Quadro das Nações Unidas sobre Mudança do Clima**. 2020. Available from: http://www.itamaraty.gov.br/images/ed_desenvsust/BRASIL-iNDC-portugues.pdf.

BRASIL. MINISTÉRIO DA AGRICULTURA, PECUÁRIA E ABASTECIMENTO - MAPA. **Plano setorial de mitigação e de adaptação às mudanças climáticas para a consolidação de uma economia de baixa emissão de carbono na agricultura:** plano ABC (Agricultura de Baixa Emissão de Carbono). Brasília - DF: MAPA/ACS, 2012.

BRASIL. MINISTÉRIO DA CIÊNCIA, TECNOLOGIA, INOVAÇÕES E COMUNICAÇÕES - MCTIC. **Estimativas anuais de emissões de gases de efeito estufa no Brasil**. 5.ed. Brasília - DF: MCTIC, 2019.

BRASIL. MINISTÉRIO DA INFRAESTRUTURA - MINFRA. **Estatísticas:** frota de veículos - DENATRAN. Available from: https://www.gov.br/infraestrutura/pt-br/assuntos/transito/conteudo-denatran/estatisticas-frota-de-veiculos-denatran. Access on: 28 Dec. 2020.

BRASIL. MINISTÉRIO DA SAÚDE. **Padronização da nomenclatura do censo hospitalar**. 2.ed. Brasília - DF: Ministério da Saúde, 2002.

BRASIL. MINISTÉRIO DO MEIO AMBIENTE - MMA. **Download de dados geográficos**. Available from: http://mapas.mma.gov.br/i3geo/datadownload.htm.

BRASIL. MINISTÉRIO DO MEIO AMBIENTE. **Procedimentos técnicos para elaboração, apresentação, execução e avaliação técnica de Planos de Manejo Florestal Sustentável-PMFSs nas florestas primitivas e suas formas de sucessão na Amazônia Legal**. Brasília: MMA, 2006.

BRASIL. PRESIDÊNCIA DA REPÚBLICA. **Lei n°8.629, de 25 de fevereiro de 1993:** dispõe sobre a regulamentação dos dispositivos constitucionais relativos à reforma agrária, previstos no Capítulo III, Título VII, da Constituição Federal. 1993. Available from: https://www.planalto.gov.br/ccivil_03/leis/l8629.htm.

BRASIL. PRESIDÊNCIA DA REPÚBLICA. **Lei 12.187 de 29 de dezembro de 2009**: institui a política nacional sobre mudança do clima - PNMC e dá outras providências. 2009. Available from: https://www.planalto.gov.br/ccivil_03/_ato2007-2010/2009/lei/l12187.htm.

BRASIL. PRESIDÊNCIA DA REPÚBLICA. **Lei 12.651 de 25 de maio de 2012**: dispõe sobre a proteção da vegetação nativa (Novo Código Florestal). 2012 b. Available from: http://www.planalto.gov.br/ccivil_03/_ato2011-2014/2012/lei/l12651.htm.

BRASIL. PRESIDÊNCIA DA REPÚGLICA. **Lei n°9.605, de 12 de fevereiro de 1998**: dispõe sobre as sanções penais e administrativas derivadas de condutas e atividades lesivas ao meio ambiente, e dá outras providências. 1998. Available from: http://www.planalto.gov.br/ccivil_03/leis/l9605.htm.

BRASIL.PRESIDÊNDICA DA REPÚBLICA. **Lei n°9.985 de 18 de julho de 2000**: institui o Sistema Naciona de Unidades de Conservação da Natureza e dá outras providências. 2000. Available from: https://www.planalto.gov.br/ccivil_03/leis/l9985.htm.

BROWN, I. F. et al. **Brazil:** drought and fire response in the Amazon: world resources report case study. Washington, D. C.: World Resources Report, 2011. Available from: https://wriorg.s3.amazonaws.com/s3fs-public/uploads/wrr_case_study_amazon_fires.pdf.

BROWN, I. F. et al. Monitoring fires in southwestern Amazonia Rain Forests. **Eos, Transactions American Geophysical Union**, v. 87, n. 26, p. 253, 2006.

BUSETTO, L.; RANGHETTI, L. MODIStsp: An R package for automatic preprocessing of MODIS Land Products time series. **Computers & Geosciences**, v. 97, p. 40–48, 2016.

BUSH, M. B. et al. Holocene fire and occupation in Amazonia: records from two lake districts. **Philosophical Transactions of the Royal Society B: Biological Sciences**, v. 362, n. 1478, p. 209–218, 2007.

BUSH, M. et al. Amazonian paleoecological histories: one hill, three watersheds. **Palaeogeography, Palaeoclimatology, Palaeoecology**, v. 214, n. 4, p. 359–393, 2004.

CAAMANO-ISORNA, F. et al. Respiratory and mental health effects of wildfires: an ecological study in Galician municipalities (north-west Spain). **Environmental Health: A Global Access Science Source**, v. 10, n. 1, p. 1–9, 2011.

CAL FIRE. **2018 fire season**. Available from: https://www.fire.ca.gov/incidents/ 2018/. Access on: 12 jan. 2021.

CAMERON, A. C.; TRIVEDI, P. K. **Microeconometrics using Stata**. College Station, Tex: Stata Press, 2009.

CAMPANHARO, W. et al. Translating fire impacts in southwestern Amazonia into economic costs. **Remote Sensing**, v. 11, n. 7, p. 764, 2019.

CARLÉN, B. et al. EU ETS emissions under the cancellation mechanism: effects of national measures. **Energy Policy**, v. 129, p. 816–825, 2019.

CARMENTA, R. et al. Shifting cultivation and fire policy: insights from the Brazilian Amazon. **Human Ecology**, v. 41, n. 4, p. 603–614, 2013.

CARMO, C. N. et al. Associação entre material particulado de queimadas e doenças respiratórias na região sul da Amazônia brasileira. **Revista Panamericana de Salud Publica**, v. 27, n. 1, p. 10–16, 2010.

CASSOL, H. L. G. et al. Determination of region of influence obtained by aircraft vertical profiles using the density of trajectories from the HYSPLIT model. **Atmosphere**, v. 11, n. 10, p. 1073, 2020.

CASSOU, E. **Agricultural pollution: field burning**. Washington, D. C.: World Bank, 2018. Available from: https://openknowledge.worldbank.org/handle/10986/29504. Access on: 31 May 2021.

CAVIGLIA-HARRIS, J. et al. Busting the boom–bust pattern of development in the Brazilian Amazon. **World Development**, v. 79, p. 82–96, 2016.

CAVIGLIA-HARRIS, J. L. Agricultural innovation and climate change policy in the Brazilian Amazon: intensification practices and the derived demand for pasture. **Journal of Environmental Economics and Management**, v. 90, p. 232–248, 2018.

CENTRO DE ESTUDOS AVANÇADOS EM ECONOMIA APLICADA - CEPEA. **Consulta ao banco de dados de série de preços**. Available from: https://www.cepea.esalq.usp.br/br/consultas-ao-banco-de-dados-do-site.aspx. Access on: 9 Jan. 2018.

CENTRO DE ESTUDOS AVANÇADOS EM ECONOMIA APLICADA - CEPEA. **Indicador do boi gordo CEPEA/B3**. Available from: https://www.cepea.esalq.usp.br/br/indicador/boi-gordo.aspx. Access on: 19 Apr. 2021.

CHAGAS, A. L. S.; AZZONI, C. R.; ALMEIDA, A. N. A spatial difference-in-differences analysis of the impact of sugarcane production on respiratory diseases. **Regional Science and Urban Economics**, v. 59, p. 24–36, 2016.

CHUDNOVSKY, A. et al. A critical assessment of high-resolution aerosol optical depth retrievals for fine particulate matter predictions. **Atmospheric Chemistry and Physics**, v. 13, n. 21, p. 10907–10917, 2013.

CHUVIECO, E. et al. Historical background and current developments for mapping burned area from satellite Earth observation. **Remote Sensing of Environment**, v. 225, p. 45–64, 2019.

COMISSÃO ESTADUAL DE GESTÃO DE RISCOS AMBIENTAIS - CEGDRA. **Plano integrado de prevenção, controle e combate às queimadas e aos incêndios florestais do estado do Acre**. Rio Branco, AC: SEMA, 2011.

COMPANHIA NACIONAL DE ABASTECIMENTO - CONAB. **Planilhas de custos de produção:** séries históricas. Available from: https://www.conab.gov.br/info-agro/custos-de-producao/planilhas-de-custo-de-producao/itemlist/category/414-planilhas-de-custos-de-producao-series-historicas. Access on: 19 Apr. 2021b.

COMPANHIA NACIONAL DE ABASTECIMENTO - CONAB. **Preços agropecuários**. Available from: https://portaldeinformacoes.conab.gov.br/precos-agropecuarios.html. Access on: 19 abr. 2021c.

COMPANHIA NACIONAL DE ABASTECIMENTO - CONAB. **Safra**: série histórica dos grãos. Available from: https://portaldeinformacoes.conab.gov.br/safra-serie-historica-graos.html. Access on: 19 Apr. 2021a.

COPERNICUS CLIMATE CHANGE SERVICE. **ERA5 monthly averaged data on single levels from 1979 to present.** ECMWF, 2019. Available from: https://cds.climate.copernicus.eu/doi/10.24381/cds.f17050d7. Access on: 29 Dec. 2020.

COSTA, M. R. G. F. et al. Uso do fogo em pastagens naturais. **Pubvet**, v. 5, n. 9, 2011.

COSTA, N. L. Uso do fogo no manejo de pastagens. **AgroLink**, p. 12, 2008.

COUTINHO, A. C. et al. **Uso e cobertura da terra nas áreas desflorestadas da Amazônia Legal:** TerraClass 2008. São José dos Campos - SP: Embrapa, 2013.

COVINGTON, W. W.; MOORE, M. M. Post settlement changes in natural fire regimes and forest structure: ecological restoration of Old-Growth Ponderosa Pine Forests. **Journal of Sustainable Forestry**, v. 2, n. 1–2, p. 153–181, 1994.

DA MOTTA, R. S. et al. **O custo econômico do fogo na Amazônia**. Rio de Janeiro: IPEA, 2002.

DA ROCHA, V. R.; YAMASOE, M. A. Estudo da variabilidade espacial e temporal da profundidade óptida do aerossol obtida com Modis sobre a região Amazônica. **Revista Brasileira de Meteorologia**, v. 28, n. 2, p. 210–220, 2013.

DE CASTRO, A. L. C. **Manual de planejamento em defesa civil**. Brasília: Imprensa Nacional, 2007. v. I

DE CASTRO, C. F. et al. **Combate a incêndios florestais**. 2.ed. [S.l.]: Escola Nacional de Bombeiros, 2003.

DE MENDONÇA, M. J. C. et al. The economic cost of the use of fire in the Amazon. **Ecological Economics**, v. 49, n. 1, p. 89–105, 2004.

DE SOUZA BRAZ, A. M.; FERNANDES, A. R.; ALLEONI, L. R. F. Soil attributes after the conversion from forest to pasture in Amazon. **Land Degradation & Development**, v. 24, n. 1, p. 33–38, 2013.

DEPARTAMENTO DE INFORMÁTICA DO SUS - DATASUS. **Informações de saúde (TABNET)**. Available from: http://www2.datasus.gov.br/DATASUS/index.php?area=02. Access on: 28 Dec. 2020.

DEPARTAMENTO NACIONAL DE INFRAESTRUTURA DE TRANSPORTES - DNIT. **SICRO2**. Available from: www.dnit.gov.br/custos-e-pagamentos/sicro-2/norte/norte.

DERYUGINA, T. et al. The mortality and medical costs of air pollution: evidence from changes in wind direction. **American Economic Review**, v. 109, n. 12, p. 4178–4219, 2019.

DIAZ, J. M. **Economic impacts of wildfire**. Joint Fire Science Program; Southern Fire Exchange, 2012. Available from: https://fireadaptednetwork.org/wp-content/uploads/2014/03/economic_costs_of_wildfires.pdf. Access on: 19 July 2021.

DO CARMO, C. N.; ALVES, M. B.; HACON, S. DE S. Impact of biomass burning and weather conditions on children's health in a city of Western Amazon region. **Air Quality, Atmosphere & Health**, v. 6, n. 2, p. 517–525, 2013.

DOLMAN, D. I. et al. Re-thinking socio-economic impact assessments of disasters: the 2015 flood in Rio Branco, Brazilian Amazon. **International Journal of Disaster Risk Reduction**, v. 31, p. 212–219, 2018.

DUARTE, A. F. Aspectos da climatologia do Acre, Brasil, com base no intervalo 1971-2000. **Revista Brasileira de Meteorologia**, v. 21, p. 308–317, 2006.

DUARTE, M. et al. Pressões Ambientais em Unidades de Conservação: estudo de caso no sul do Estado do Amazonas. **GOT - Journal of Geography and Spatial Planning**, n. 18, p. 78–107, 2019.

EARL, N.; SIMMONDS, I. Spatial and temporal variability and trends in 2001–2016 global fire activity. **Journal of Geophysical Research: Atmospheres**, v. 123, n. 5, p. 2524–2536, 2018.

EMPRESA BRASILEIRA DE PESQUISA AGROPECUÁRIA - EMBRAPA. Principais focos e fontes de queimadas no Brasil, e suas causas. Campinas: EMBRAPA, 2000. p. 8–17.

EUROPEAN COMMISION. **EU Emissions Trading System - EU ETS**. Available from: https://ec.europa.eu/clima/policies/ets_en. Access on: 16 May 2021.

EUROPEAN STATISTICS - EUROSTAT. **Harmonised Index of Consumer Prices (HICP):** overview. Available from: https://ec.europa.eu/eurostat/web/hicp. Access on: 19 Apr. 2021.

FALLEIRO, R. M.; SANTANA, M. T.; BERNI, C. R. As contribuições do manejo integrado do fogo para o controle dos incêndios florestais nas Terras Indígenas do Brasil. **Bio Brasil,** v. 2, p. 18, 2016.

FELLOWS, M. et al. **Amazônia em chamas**: desmatamento e fogo nas terras indígenas: Amazônia em chamas. Brasilia - DF: Instituto de Pesquisa Ambiental da Amazônia, 2021. Available from: https://ipam.org.br/bibliotecas/amazonia-em- -chamas-6-desmatamento-e-fogo-nas-terras-indigenas-da-amazonia/.

FERNANDES, F. D. et al. **Produtividade da biomassa da parte aérea de genótipos de mandioca no Distrito Federal.** Embrapa cerrado, 2009. Available from: https://www.embrapa.br/busca-de-publicacoes/-/publicacao/748238/produtividade-da-biomassa-da-parte-aerea-de-genotipos-de-mandioca-no-distrito-federal-2009. Access on: 9 July 2018

FERNÁNDEZ-LÓPEZ, J.; SCHLIEP, K. rWind: download, edit and include wind data in ecological and evolutionary analysis. **Ecography**, v. 42, n. 4, p. 804–810, 2019.

FISCH, G.; MARENGO, J. A.; NOBRE, C. A. Clima da Amazônia. **Climanálise: Boletim de Monitoramento e Análise Climática**, esp., 1996.

FONTES, F.; PALMER, C. “Land sparing” in a von Thünen framework: theory and evidence from Brazil. **Land Economics**, v. 94, n. 4, p. 556-576, 2018.

FREITAS, F. L. M. et al. Nota técnica: malha fundiária do Brasil. In: MELO, D. S.; BRAZ, A. M.; NARDOQUE, S. (Ed.). **Atlas:** a geografia da agropecuária brasileira. [s.l: s.n.], 2018.

FREITAS, R. E.; MACIENTE, A. N. Mesorregiões brasileiras com expansão de área agrícola. **Radar: Tecnologia, Produção e Comércio Exterior**, v. 41, p. 7–18, 2015.

FUNDAÇÃO GETÚLIO VARGAS - FGV IBRE. **Arrendamento de terras:** exploração animal. Available from: http://www14.fgv.br/fgvdados20/consulta.aspx. Access on: 19 Apr. 2021.

FUNDAÇÃO NACIONAL DO ÍNDIO - FUNAI. **Terras indígenas do Brasil**. Available from: <http://www.funai.gov.br/index.php/shape>. Access on: 9 Jan. 2018.

FUNK, C. et al. The climate hazards infrared precipitation with stations: a new environmental record for monitoring extremes. **Scientific Data**, v. 2, n. 1, e150066, 2015.

GATTI, L. V. et al. Amazonia as a carbon source linked to deforestation and climate change. **Nature**, v. 595, n. 7867, p. 388–393, 15 jul. 2021.

GATTI, L. V. et al. Drought sensitivity of Amazonian carbon balance revealed by atmospheric measurements. **Nature**, v. 506, n. 7486, p. 76–80, 2014.

GIGLIO, L. et al. **MCD64A1 MODIS/Terra+Aqua burned area monthly L3 global 500m SIN grid V006**. NASA EOSDIS Land Processes DAAC, 2015. Available from: https://lpdaac.usgs.gov/products/mcd64a1v006/. Access on: 29 Dec. 2020

GIGLIO, L.; JUSTICE, C. **MYD14A1 MODIS/Aqua thermal anomalies/fire daily L3 global 1km SIN Grid V006.** NASA EOSDIS Land Processes DAAC, 2015. Available from: https://lpdaac.usgs.gov/products/myd14a1v006/. Access on: 28 Dec. 2020

GIGLIO, L. et al. An active-fire based burned area mapping algorithm for the MODIS sensor. **Remote Sensing of Environment**, v. 113, n. 2, p. 408–420, 2009.

GIGLIO, L. et al. **MODIS collection 6 active fire product user's guide (revision c)**, 2020.Available from: https://modis-fire.umd.edu/files/MODIS_C6_Fire_User_Guide_C.pdf. Access on: 23 Feb. 2021

GIORGINO, T. Computing and visualizing dynamic time warping alignments in *R* : the dtw package. **Journal of Statistical Software**, v. 31, n. 7, 2009.

GLOBAL WILDFIRE INFORMATION SYSTEM - GWIS. **Brazil:** country profile. Available from: https://gwis.jrc.ec.europa.eu/apps/country.profile/charts/BRA/BRA/2019/2002/2019. Access on: 26 Mar. 2021.

GODAR, J. et al. Actor-specific contributions to the deforestation slowdown in the Brazilian Amazon. **Proceedings of the National Academy of Sciences**, v. 111, n. 43, p. 15591–15596, 2014.

GOLGHER, A. B. **Introdução à econometria espacial**. Jundiaí-SP: Paco Editorial, 2015.

GONÇALVES, K. S. et al. Development of non-linear models predicting daily fine particle concentrations using aerosol optical depth retrievals and ground-based measurements at a municipality in the Brazilian Amazon region. **Atmospheric Environment**, v. 184, p. 156–165, 2018.

GONÇALVES, W. A.; MACHADO, L. A. T.; KIRSTETTER, P. E. Influence of biomass aerosol on precipitation over the Central Amazon: an observational study. **Atmospheric Chemistry and Physics**, v. 15, n. 12, p. 6789–6800, 2015.

GOULDER, L. H.; SCHEIN, A. R. Carbon taxes versus cap and trade: a critical review. **Climate Change Economics**, v. 4, n. 3, e1350010, 2013.

GRAF, R. **Agroecologia dos indígenas do Acre:** ética do bem viver. In: AGOECOL, 2016. **Anais...** Dourados -MS,2016. Available from: https://www.cpao.embrapa.br/cds/agroecol2016/PDF's/Mesa%20Redonda/MesaRedonda%20-%20Roberta%20Graf-

AGROECOLOGIA%20DOS%20IND%C3%8DGENAS%20DO%20ACRE%20%C3%89TICA%20DO%20BEM%20VIVER.pdf .

GUEDES, G. R. et al. Poverty and inequality in the rural brazilian Amazon: a multidimensional approach. **Human Ecology**, v. 40, n. 1, p. 41–57, 2012.

GUO, J. et al. Impact of diurnal variability and meteorological factors on the PM2.5 - AOD relationship: implications for PM2.5 remote sensing. **Environmental Pollution**, v. 221, p. 94–104, 2017.

HALL, S. C.; CAVIGLIA-HARRIS, J. Agricultural development and the industry life cycle on the Brazilian frontier. **Environment and Development Economics**, v. 18, n. 3, p. 326–353, 2013.

HARRIS, M. C.; KOHN, J. L. Reference health and the demand for medical care. **The Economic Journal**, v. 128, n. 615, p. 2812–2842, 2018.

HE, G.; LIU, T.; ZHOU, M. Straw burning, PM2.5, and death: evidence from China. **Journal of Development Economics**, v. 145, e102468, 2020.

HEINSELMAN, M. L. **Fire intensity and frequency as factors in the distribution and structure of northern ecosystems**: fire regimes and ecosystem properties. [S.l.]: USDA Forest Service, 1978.

HINTERMAYER, M. A carbon price floor in the reformed EU ETS: design matters! **Energy Policy**, v. 147, e111905, 2020.

HIPEL, K. W.; MCLEOD, A. I. **Time series modelling of water resources and environmental systems.** Burlington: Elsevier Science, 1994.

HUGHES, L. et al. **Summer of crisis**. [S.l.]: Climate Coincil of Australia, 2020.

IEG - FNP. **Agrianual 2012**: anuário da agricultura brasileira. São Paulo - SP: FNP Consultoria, 2012.

IGNOTTI, E. et al. Impact on human health of particulate matter emitted from burnings in the Brazilian Amazon region. **Revista de Saúde Pública**, v. 44, n. 1, p. 121–130, 2010.

INSTITUTO BRASILEIRO DE GEOGRAFIA E ESTATÍSTICA - IBGE. **Amazônia Legal**. Rio de Janeiro: IBGE, 2020.

INSTITUTO BRASILEIRO DE GEOGRAFIA E ESTATÍSTICA - IBGE. **Bases e referências**: malhas digitais. Available from: https://mapas.ibge.gov.br/bases-e-referenciais/bases-cartograficas/malhas-digitais. Access on: 10 Mar. 2018a.

INSTITUTO BRASILEIRO DE GEOGRAFIA E ESTATÍSTICA - IBGE. **Censo demográfico 2010:** sinopse. Available from: https://sidra.ibge.gov.br/pesquisa/censo-demografico/demografico-2010/sinopse. Access on: 9 Feb. 2021a.

INSTITUTO BRASILEIRO DE GEOGRAFIA E ESTATÍSTICA - IBGE. **Malha municipal**. Available from: https://www.ibge.gov.br/geociencias/organizacao-do-territorio/malhas-territoriais/15774-malhas.html?=&t=sobre. Access on: 1 July 2021c.

INSTITUTO BRASILEIRO DE GEOGRAFIA E ESTATÍSTICA - IBGE. **PAM - Produção Agrícola Municipal**. Available from: https://sidra.ibge.gov.br/pesquisa/pam/tabelas. Access on: 9 July 2018.

INSTITUTO BRASILEIRO DE GEOGRAFIA E ESTATÍSTICA - IBGE. **Pesquisa da pecuária municipal**. Available from: https://sidra.ibge.gov.br/tabela/3939. Access on: 30 Sept. 2018b.

INSTITUTO BRASILEIRO DE GEOGRAFIA E ESTATÍSTICA - IBGE. **Produto Interno Bruto dos municípios**. Available from: https://www.ibge.gov.br/estatisticas/economicas/contas-nacionais/9088-produto-interno-bruto-dos-municipios.html. Access on: 23 Mar. 2021b.

INSTITUTO BRASILEIRO DE GEOGRAFIA E ESTATÍSTICA - IBGE. **Séries históricas:** PIB a preços de mercado. Available from: https://www.ibge.gov.br/estatisticas/economicas/contas-nacionais/9300-contas-nacionais-trimestrais.html?=&t=series-historicas&utm_source=landing&utm_medium=explica&utm_campaign=pib#evolucao-taxa. Access on: 23 Mar. 2021e.

INSTITUTO BRASILEIRO DE GEOGRAFIA E ESTATÍSTICA - IBGE. **Sistema nacional de índices de preços ao consumidor - SNIPC**. Available from:

https://sidra.ibge.gov.br/pesquisa/snipc/ipca/quadros/brasil/janeiro-2021. Access on: 10 Mar. 2021g.

INSTITUTO BRASILEIRO DE GEOGRAFIA E ESTATÍSTICA - IBGE. **Tabela 5457:** área plantada ou destinada à colheita, área colhida, quantidade produzida, rendimento médio e valor da produção das lavouras temporárias e permanentes. Available from: https://sidra.ibge.gov.br/tabela/5457#notas-tabela. Access on: 17 Mar. 2021d.

INSTITUTO DE PESQUISA ECONÔMICA APLICADA - IPEA. **Ipeadata**. Available from: http://www.ipeadata.gov.br/Default.aspx. Access on: 30 Sept. 2018.

INSTITUTO DE PESQUISA ECONÔMICA APLICADA - IPEA. **Taxa de câmbio para R$/US$ referente a taxa comercial para compra em fim de período**. Available from: http://www.ipeadata.gov.br/Default.aspx. Access on: 22 mar. 2021.

INSTITUTO NACIONAL DE COLONIZAÇÃO E REFORMA AGRÁRIA - INCRA. **Tabela com módulo fiscal dos municípios Brasileiros**. Available from: http://www.incra.gov.br/tabela-modulo-fiscal. Access on: 9 July 2018.

INSTITUTO NACIONAL DE PESQUISAS ESPACIAS - INPE. **Banco de dados de queimadas**. Available from: https://queimadas.dgi.inpe.br/queimadas/bdqueimadas. Access on: 10 May 2021a.

INSTITUTO NACIONAL DE PESQUISAS ESPACIAS - INPE. **Monitoramento dos focos ativos por Estado/Região/Bioma**. Available from: http://www.inpe.br/queimadas/portal/estatistica_estados. Access on: 26 Nov. 2020.

INSTITUTO NACIONAL DE PESQUISAS ESPACIAS - INPE. **PRODES:** desmatamento UF. Available from: http://terrabrasilis.dpi.inpe.br/app/dashboard/deforestation/biomes/legal_amazon/rates. Access on: 22 June 2021b.

INSTITUTO NACIONAL DE PESQUISAS ESPACIAS - INPE. **TerraClass**. Available from: http://www.inpe.br/cra/projetos_pesquisas/dados_terraclass.php. Access on: 9 July 2018.

INTERGOVERNMENTAL PANEL ON CLIMATE CHANGE - IPCC. **Sixth assessment report:** regional fact sheet – Central and South America, 2021b. Available from: https://www.ipcc.ch/report/ar6/wg1/downloads/factsheets/IPCC_AR6_WGI_Regional_Fact_Sheet_Central_and_South_America.pdf. Access on: 9 Sept. 2021

INTERGOVERNMENTAL PANEL ON CLIMATE CHANGE - IPCC. Summary for Policymakers. In: MASSON-DELMONTTE, V. et al. (Ed.). **Climate change 2021:** the physical science basis: contribution of Working Group I to the sixth assessment report of the Intergovernmental Panel on Climate Change. [S.l.]: Cambridge University Press, 2021a.

JACOBSON, L. S. V. et al. Acute effects of particulate matter and black carbon from seasonal fires on peak expiratory flow of schoolchildren in the brazilian Amazon. **PLoS ONE**, v. 9, n. 8, e104177, 2014.

KUMAR, N. What can affect AOD–PM2.5 association? **Environmental Health Perspectives**, v. 118, n. 3, 2010.

KUMAR, P. et al. The economics of ecosystem services: from local analysis to national policies. **Current Opinion in Environmental Sustainability**, v. 5, n. 1, p. 78–86, 2013.

KUMAR, P.; KUMAR, S.; JOSHI, L. Valuation of the health effects. In: KUMAR, P.; KUMAR, S.; JOSHI, L. (Ed.). **Socioeconomic and environmental implications of agricultural residue surning**. New Delhi: Springer, 2015. p. 35–67.

LAGOUVARDOS, K. et al. Meteorological conditions conducive to the rapid spread of the deadly wildfire in eastern Attica, Greece. **Bulletin of the American Meteorological Society**, v. 100, n. 11, p. 2137–2145, 2019.

LAUGHARNE, J.; VAN DE WATT, G.; JANCA, A. After the fire: the mental health consequences of fire disasters. **Current Opinion in Psychiatry**, v. 24, n. 1, p. 72–77, 2011.

LENOBLE, J.; REMER, L. A.; TANRÉ, D. Introduction. In: LENOBLE, J.; REMER, L.; TANRE, D. (Ed.). **Aerosol remote sensing**. Berlin, Heidelberg: Springer, 2013. p. 1–11.

LEONEL, M. O uso do fogo: o manejo indígena e a piromania da monocultura. **Estudos Avançados**, v. 14, n. 40, p. 231–250, 2000.

LEWIS, S. L. et al. The 2010 Amazon drought. **Science**, v. 331, n. 6017, p. 554–554, 2011.

LI, W.; FU, R.; DICKINSON, R. E. Rainfall and its seasonality over the Amazon in the 21st century as assessed by the coupled models for the IPCC AR4. **Journal of Geophysical Research**, v. 111, n. D02111, p. 14, 2006.

LIBONATI, R. et al. Twenty-first century droughts have not increasingly exacerbated fire season severity in the Brazilian Amazon. **Scientific Reports**, v. 11, n. 1, p. 4400, 2021.

LIESENFELD, M. V. A.; VIEIRA, G.; MIRANDA, I. P. DE A. Ecologia do fogo e o impacto na vegetação da Amazônia. **Pesquisa Florestal Brasileira**, v. 36, n. 88, p. 505, 2016.

LIMA, A. et al. Land use and land cover changes determine the spatial relationship between fire and deforestation in the Brazilian Amazon. **Applied Geography**, v. 34, p. 239–246, 2012.

LIU, Y.; AO, C. Effect of air pollution on health care expenditure: evidence from respiratory diseases. **Health Economics**, v. 30, n. 4, p. 858–875, 2021.

LYAPUSTIN, A.; WANG, Y. **MCD19A2 MODIS/Terra+Aqua land aerosol optical depth daily L2G global 1km SIN grid V006.** NASA EOSDIS Land Processes DAAC, 2018. Available from: https://lpdaac.usgs.gov/products/mcd19a2v006/. Access on: 29 Dec. 2020

MACHADO-SILVA, F. et al. Drought and fires influence the respiratory diseases hospitalizations in the Amazon. **Ecological Indicators**, v. 109, p. 105817, 2020.

MAGOMANI, M. I.; VAN TOL, J. J. The impact of fire frequency on selected soil physical properties in a semi-arid savannah Thornveld. **Acta Agriculturae Scandinavica, Section B — Soil & Plant Science**, v. 69, n. 1, p. 43–51, 2019.

MALTA, D. C. et al. Mortalidade por doenças crônicas não transmissíveis no Brasil e suas regiões, 2000 a 2011. **Epidemiologia e Serviços de Saúde**, v. 23, n. 4, p. 599–608, 2014.

MAPBIOMAS. **Coleção 5 da série anual de mapas de cobertura e uso de solo do Brasil**. Available from: http://mapbiomas.org. Access on: 24 Mar. 2021.

MAPBIOMAS. **Mapeamento de cicatrizes de fogo no Brasil (versão beta)**.Available from: https://plataforma.brasil.mapbiomas.org/. Access on: 22 June 2021.

MARENGO, J. A. et al. The drought of 2010 in the context of historical droughts in the Amazon region: drought Amazon 2010. **Geophysical Research Letters**, v. 38, n. 12, 2011.

MARENGO, J. A.; ESPINOZA, J. C. Extreme seasonal droughts and floods in Amazonia: causes, trends and impacts. **International Journal of Climatology**, v. 36, n. 3, p. 1033–1050, 2016.

MARKETS INSIDERS. **Historical prices CO2 emission**. Available from: https://markets.businessinsider.com/commodities/historical-prices/co2-emissionsrechte/euro/15.11.2007_31.12.2009. Access on: 30 Sept. 2018.

MARTINS, J. S. **O poder do atraso: ensaios de sociologia da história lenta**. São Paulo: Hucitec, 1994.

MARTINS, V. S. et al. Validation of high-resolution MAIAC aerosol product over South America. **Journal of Geophysical Research: Atmospheres**, v. 122, n. 14, p. 7537–7559, 2017.

MATO GROSSO. GOVERNO DO ESTADO. **Decreto nº 173, de 12 de julho de 2019**: dispõe sobre o período proibitivo de queimadas no Estado de Mato Grosso. 2019. Available from: https://www.legisweb.com.br/legislacao/?id=379587.

MATO GROSSO. GOVERNO DO ESTADO. **Decreto nº 535, de 26 de junho de 2020**: dispõe sobre o período proibitivo de queimadas no Estado de Mato Grosso. 2020. Available from: https://www.legisweb.com.br/legislacao/?id=397642.

MATO GROSSO. GOVERNO DO ESTADO. **Decreto nº 938, de 18 de maio de 2021**: declara estado de emergência ambiental nos meses de maio a novembro de 2021 e dispõe sobre o período proibitivo de queimadas no Estado de Mato Grosso. 2021. Available from: https://www.legisweb.com.br/legislacao/?id=414518.

MEADOWS, D.; VIS, P.; ZAPFEL, P. The EU emissions trading system. In: DELBEKE, J.; VIS, P. (Ed.). **Towards a climate-neutral Europe: curbing the trend**. New York: Routledge, 2020. p. 29.

MEDEIROS, M. B.; MIRANDA, H. S. Mortalidade pós-fogo em espécies lenhosas de campo sujo submetido a três queimadas prescritas anuais. **Acta Botanica Brasilica**, v. 19, n. 3, p. 493–500, 2005.

MENDELSOHN, R.; OLMSTEAD, S. The economic valuation of environmental amenities and disamenities: methods and applications. **Annual Review of Environment and Resources**, v. 34, n. 1, p. 325–347, 2009.

MENDONÇA, M. J. C.; SACHSIDA, A.; LOUREIRO, P. R. A. Estimation of damage to human health due to forest burning in the Amazon. **Journal of Population Economics**, v. 19, n. 3, p. 593–610, 2006.

MISTRY, J.; BILBAO, B. A.; BERARDI, A. Community owned solutions for fire management in tropical ecosystems: case studies from Indigenous communities of South America. **Philosophical Transactions of the Royal Society B: Biological Sciences**, v. 371, n. 1696, p. 20150174, 2016.

MORAES, V. H.F.; MORAES, L. A. C.; MOREIRA, A. **Cultivo de seringueira com copas enxertadas resistentes ao mal-das folhas**: documentos. Manaus-AM: Embrapa Amazônia Ocidental, 2008. Available from: https://ainfo.cnptia.embrapa.br/digital/bitstream/item/47135/1/Doc-63-A5.pdf.

MORELLO, T. F. et al. Fires in Brazilian Amazon: why does policy have a limited impact? **Ambiente & Sociedade**, v. 20, n. 4, p. 19–38, 2017b.

MORELLO, T. F. et al. Policy instruments to control Amazon fires: a simulation approach. **Ecological Economics**, v. 138, p. 199–222, 2017a.

MORELLO, T. F. et al. Predicting fires for policy making: Improving accuracy of fire brigade allocation in the Brazilian Amazon. **Ecological Economics**, v. 169, e106501, mar. 2020.

MORTON, D. C. et al. Understorey fire frequency and the fate of burned forests in southern Amazonia. **Philosophical Transactions of the Royal Society B: Biological Sciences**, v. 368, n. 1619, e 20120163, 2013.

MÜLLER, C. H. et al. **A cultura da castanha-do-Brasil**. Brasília - DF: EMBRAPA-SPI, 1995.

NASI, R. et al. Forest fire and biological diversity. **Unasylva**, **Forest Biological Diversity**, v. 53, n.209, 2002.

NEARY, D. G.; RYAN, K. C.; DEBANO, L. F. **Wildland fire in ecosystems**: effects of fire on soil and water. Ogden, UT: USDA, Forest Service, 2005. v. 4.

NELSON, K. J. et al. LANDFIRE 2010-updated data to support wildfire and ecological management. **Earthzine**, p. 1–11, 2013.

NEPSTAD, D. C. A.; MOREIRA, A.; ALENCAR, A. A. **Floresta em chamas**: origens, impactos e prevenção do fogo na Amazônia. Brasília: [s.n.]. 1999. 202p.

NEPSTAD, D. et al. Slowing Amazon deforestation through public policy and interventions in beef and soy supply chains. **Science**, v. 344, n. 6188, p. 1118–1123, 2014.

NEPSTAD, D. et al. **Unlocking jurisdictional REDD+ as a policy framework for low-emission rural development: research results and recommendations for governments.** IPAM, 2012. Available from: https://earthinnovation.org/wp-content/uploads/2014/09/re-framing_redd_english.pdf.

NOLASCO, M. I. M. **Global forest resources assessment 2005:** report on fires in the South American Region. Rome: FAO, 2006.Available from: www.fao.org/forestry/site/fire-alerts/en.

NUNES, K. V. R.; IGNOTTI, E.; HACON, S.S. Circulatory disease mortality rates in the elderly and exposure to PM2.5 generated by biomass burning in the Brazilian Amazon in 2005. **Cadernos de Saúde Pública**, v. 29, n. 3, p. 589–598, 2013.

NUNES, S. et al. Unmasking secondary vegetation dynamics in the Brazilian Amazon. **Environmental Research Letters**, v. 15, n. 3, p. 034057,2020.

OPEN STREET MAP - OSM. **Data for this region:** Brazil. Available from: https://download.geofabrik.de/south-america/brazil.html. Access on: 28 Dec. 2020.

ORGANIZAÇÃO PARA A COOPERAÇÃO E DESENVOLVIMENTO ECONÔMICO - OECD. **Cost-benefit analysis and the environment:** recent developments. [S.l.]: OECD, 2006.

PAOLUCCI, L. N. et al. Fire-induced forest transition to derived savannas: cascading effects on ant communities. **Biological Conservation**, v. 214, p. 295–302, 2017.

PELLEGRINI, A. F. A. et al. Repeated fire shifts carbon and nitrogen cycling by changing plant inputs and soil decomposition across ecosystems. **Ecological Monographs**, v. 90, n. 4, 2020.

PEREIRA, J. P.; LEAL, A. C.; CASTRO, A. MARIA G. Análise sistêmica da cadeia produtiva da borracha natural. In: FRAZÃO, D. A. C.; CRUZ, E. S.; VIÉGAS, I. J. M. (Ed.). **Seringueira na Amazônia**: situação atual e perspectivas. Manaus-AM: Embrapa, Amazônia Central, 2003.

PEREIRA, M. A. et al. **Pastagens**: condicionantes econômicos e seus efeitos nas decisões de formação e manejo. Campo Grande-MS: Embrapa Gado de Corte, 2020. Available from: https://ainfo.cnptia.embrapa.br/digital/bitstream/item/215118/1/COT-150-FInal-em-Alta.pdf.

PERMENTIER, K. et al. Carbon dioxide poisoning: a literature review of an often forgotten cause of intoxication in the emergency department. **International Journal of Emergency Medicine**, v. 10, n. 1, p. 14, 2017.

PESSÔA, A. C. M. et al. Intercomparison of burned area products and its implication for carbon emission estimations in the Amazon. **Remote Sensing**, v. 12, n. 23, p. 3864, 2020.

PIVELLO, V. R. The use of fire in the Cerrado and Amazonian rainforests of Brazil: past and present. **Fire Ecology**, v. 7, n. 1, p. 24–39, 2011.

PLETSCH, M. A. J. S. et al. The 2020 Brazilian Pantanal fires. **Anais da Academia Brasileira de Ciências**, v. 93, n. 3, e20210077, 2021.

POHLERT, T. **Trend**: non-parametric trend tests and change-point detection. 2020. Available from: https://CRAN.R-project.org/package=trend. Access on: 4 June 2021

POPE, C. A. Epidemiology of fine particulate air pollution and human health: biologic mechanisms and who's at risk? **Environmental Health Perspectives**, v. 108, n. suppl 4, p. 713–723, 2000.

POSEY, D. A. Indigenous management of tropical forest ecosystems: the case of the Kayapó indians of the Brazilian Amazon. **Agroforestry Systems**, v. 3, n. 2, p. 139–158, 1985.

PYNE, S. J. From pleistocene to pyrocene: fire replaces ice. **Earth's Future**, v. 8, n. 11, 2020.

RANGEL, M. A.; VOGL, T. S. Agricultural fires and health at birth. **The Review of Economics and Statistics**, v. 101, n. 4, p. 616–630, 2019.

REDDINGTON, C. L. et al. Air quality and human health improvements from reductions in deforestation-related fire in Brazil. **Nature Geoscience**, v. 8, n. 10, p. 768–771, 2015.

REDIN, M. **Composição bioquímica e decomposição da parte aérea e raízes de culturas comerciais e plantas de cobertura do solo**. Dissertação (Mestrado em Ciência do Solo) - Universidade Federal de Santa Maria, Santa Maria, 2010.

REIS, V. et al. **Manual de operação da unidade de situação de monitoramento de eventos hidrometeorológicos do estado do Acre.** Secretaria de Estado de Meio Ambiente - SEMA, 2015. Available from: https://progestao.ana.gov.br/progestao-1/acompanhamento-programa/aplicacao-dos-recursos/acompanhamento-das-metas-de-cooperacao-federativa/manuais-de-salas-de-situacao/manual-de-operacao-da-unidade-de-situacao_sema_ac.pdf.

REISEN, F. et al. Wildfire smoke and public health risk. **International Journal of Wildland Fire**, v. 24, n. 8, p. 1029, 2015.

ROCHA, R.; SANT'ANNA, A. **Winds of fire and smoke:** air pollution and health in the brazilian Amazon. São Paulo: IEPS, Instituto de Estudos para Políticas de Saúde, 2020.

RODRIGUES, M. A. **Dinâmica espacial do desmatamento no estado do Acre entre 1999 e 2010: o papel do zoneamento ecológico-econômico**. Tese (Doutorado em Geografia) - Universidade Estadual de Campinas, Campinas, 2014.

RYAN, K. C. et al. **Wildland fire in ecosystems:** effects of fire on cultural resources and archaeology. [S.l.]: USDA Fores ed. Fort Collins, 2012.

SÁ, C. P.; ANDRADE, C. M. S.; VALENTIM, J. F. **Análise econômica para a pecuária de corte em pastagens melhoradas no Acre**: circular técnica. Rio Branco, AC: EMBRAPA, 2010.

SALIMON, C. I. et al. Estimating state-wide biomass carbon stocks for a REDD plan in Acre, Brazil. **Forest Ecology and Management**, v. 262, n. 3, p. 555–560, 2011.

SANTÍN, C.; DOERR, S. H. Fire effects on soils: the human dimension. **Philosophical Transactions of the Royal Society B: Biological Sciences**, v. 371, n. 1696, e20150171, 2016.

SANTORO, M.; CARTUS, O. **ESA Biomass Climate Change Initiative (Biomass_CCI)**: global datasets of forest above-ground biomass for the years 2010, 2017 and 2018. Centre for Environmental Data Analysis (CEDA), 2021. Available from: https://catalogue.ceda.ac.uk/uuid/84403d09cef3485883158f4df2989b0c. Access on: 14 May 2021

SCHAFFER, M. E.; STILLMAN, S. **XTOVERID:** stata module to calculate tests of overidentifying restrictions after xtreg, xtivreg, xtivreg2, xthtaylor. Boston College Department of Economics, 2006. Available from: https://ideas.repec.org/c/boc/bocode/s456779.html. Access on: 26 Oct. 2020

SERVIÇO FLORESTAL BRASILEIRO - SFB. **Sistema Nacional de Cadastro Ambiental Rural - SICAR**. Available from: http://www.car.gov.br/publico/imoveis/index. Acesso em: 9 Jan. 2018.

SETZER, A. **Resumo do evento da tarde escura em São Paulo, 20/Agosto/2019 e sua relação com as nuvens de queimadas**. 2019. Available from: https://www.oeco.org.br/wp-content/uploads/2019/08/EventoNuvemEscuridaoFumaca_SaoPaulo_SP-1.pdf. Access on: 12 Jan. 2021

SHAO, H. et al. The pitfall of instrumental variables in big data: What the rule of thumb can't give you. **Communications in Statistics - Simulation and Computation**, v. 48, n. 7, p. 2118–2124, 2019.

SHELDON, T. L.; SANKARAN, C. The impact of indonesian forest fires on singaporean pollution and health. **American Economic Review**, v. 107, n. 5, p. 526–529, 2017.

SHIMABUKURO, Y. E. et al. Fraction images derived from Terra Modis data for mapping burnt areas in Brazilian Amazonia. **International Journal of Remote Sensing**, v. 30, n. 6, p. 1537–1546, 2009.

SHIMABUKURO, Y. E.; SMITH, J. A. The least-squares mixing models to generate fraction images derived from remote sensing multispectral data. **IEEE Transactions on Geoscience and Remote Sensing**, v. 29, n. 1, p. 16–20, 1991.

SHRIVASTAVA, M. et al. Urban pollution greatly enhances formation of natural aerosols over the Amazon rainforest. **Nature Communications**, v. 10, n. 1, p. 1046, 2019.

SILLS, E. O. et al. **REDD + on the ground**: a case book of subnational initiatives across the globe. Bogor Barat: Centre for International Forest Research (CIFOR), 2014.

SILVA JUNIOR, C. et al. Deforestation-induced fragmentation increases forest fire occurrence in central brazilian Amazonia. **Forests**, v. 9, n. 6, p. 305, 2018.

SILVA JUNIOR, C. H. L. et al. Benchmark maps of 33 years of secondary forest age for Brazil. **Scientific Data**, v. 7, n. 1, p. 269, 2020.

SILVA, C. V. J. et al. Drought-induced Amazonian wildfires instigate a decadal-scale disruption of forest carbon dynamics. **Philosophical Transactions of the Royal Society B: Biological Sciences**, v. 373, n. 1760, p. 20180043, 2018a.

SILVA, C. V. J. et al. Estimating the multi-decadal carbon deficit of burned Amazonian forests. **Environmental Research Letters**, v. 15, n. 11, p. 114023, 2020.

SILVA, R. G.; LIMA, J. E. Avaliação econômica da poluição do ar na Amazônia Ocidental: um estudo de caso do Estado do Acre. **Revista de Economia e Sociologia Rural**, v. 44, n. 2, p. 157–178, 2006.

SILVA, R. G.; SILVEIRA, B. C.; SILVEIRA, A. O. A. Relacionamento entre as queimadas e as morbidades respiratórias no Acre no período de 1998 a 2005: uma abordagem espacial. In: CONGRESSO DA SOCIEDADE BRASILEIRA DE ECONOMIA, ADMINISTRAÇÃO E SOCIOLOGIA RURAL, 46., 2008. **Anais...** Rio Branco, AC: SOBER, 2008.

SILVA, S. S. et al. Dynamics of forest fires in the southwestern Amazon. **Forest Ecology and Management**, v. 424, p. 312–322, 2018b.

SISTEMA DE ESTIMATIVAS DE EMISSÕES E REMOÇÕES DE GASES DE EFEITO ESTUFA - SEEG. **Emissões totais de CO2**. [S.l.]: SEEG, 2019.

SMITH, L. T. et al. Drought impacts on children's respiratory health in the Brazilian Amazon. **Scientific Reports**, v. 4, n. 1, e3726, 2015.

SOARES-FILHO, B. et al. Cracking Brazil's Forest Code. **Science**, v. 344, n. 6182, p. 363–364, 2014.

SOUZA, A. A.; OVIEDO, A.; SANTOS, T. M. DOS. **Impactos na qualidade do ar e saúde humana relacionados ao desmatamento e queimadas na Amazônia Legal brasileira**. São Paulo - SP: Instituto Socioambiental, 2020. Available from: https://acervo.socioambiental.org/sites/default/files/documents/prov85.pdf. Access on: 20 fev. 2021.

SOUZA, C. M. et al. Reconstructing three decades of land use and land cover changes in brazilian biomes with Landsat archive and Earth Engine. **Remote Sensing**, v. 12, n. 17, p. 2735, 2020.

STAIGER, D.; STOCK, J. H. Instrumental variables regression with weak instruments. **Econometrica**, v. 65, n. 3, p. 557, 1997.

STRAND, J. et al. Spatially explicit valuation of the brazilian Amazon Forest's ecosystem services. **Nature Sustainability**, v. 1, n. 11, p. 657–664, 2018.

SUPERINTENDÊNCIA DO DESENVOLVIMENTO DA AMAZÔNIA - SUDAM. **Boletim amazônia**: indicadores socioeconômico-ambientais e análise conjuntural da Amazônia Legal. Belém - PA: SUDAM, 2016.

TASKER, K. A.; ARIMA, E. Y. Fire regimes in Amazonia: the relative roles of policy and precipitation. **Anthropocene**, v. 14, p. 46–57, 2016.

THE WORLD BANK. **Carbon pricing dashboard**. Available from: https://carbonpricingdashboard.worldbank.org/map_data. Access on: 24 Mar. 2021.

TOCANTINS. GOVERNO DO ESTADO. **Portaria nº 180, de 28 de junho de 2019**: Suspensão de emissão e vigência de autorização ambiental de queima controlada. 2019.

TOCANTINS. GOVERNO DO ESTADO. **Portaria nº 223, de 29 de junho de 2018**: suspensão da emissão e vigência das autorizações de queima controlada até 30 de outubro. 2018.

TOCANTINS. GOVERNO DO ESTADO. **Portaria nº84, de 07 de julho de 2020**: suspende a emissão e vigência de autorização ambiental de queima controlada. 2020.

TORRES, F. T. P. et al. Perfil dos incêndios florestais em Unidades de Conservação brasileiras no período de 2008 a 2012. **Floresta**, v. 46, n. 4, p. 531, 2017.

TORRES, M.; CUNHA, C. N.; GUERRERO, N. R. Ilegalidade em moto contínuo: o aporte legal para destinação de terras públicas e a grilagem na Amazônia. In: OLIVEIRA, A. U. (Ed.). **A grilagem de terras na formação territorial brasileira**. São Paulo - SP: Universidade de São Paulo, 2020.

TOWNSEND, C. R.; COSTA, N. L. Aspectos econômicos da recuperação de pastagens na Amazônia brasileira. **Amazônia: Ciência & Desenvolvimento**, v. 5, n. 10, p. 27–50, 2010.

TOWNSEND, C. R.; COSTA, N. L.; PEREIRA, R. G. A. **Recuperação e práticas sustentáveis de manejo de pastagens na Amazônia**: série documentos. Porto Velho - RO: EMBRAPA, 2012.

TRITSCH, I.; ARVOR, D. Transition in environmental governance in the Brazilian Amazon: emergence of a new pattern of socio-economic development and deforestation. **Land Use Policy**, v. 59, p. 446–455, 2016.

TURCO, M. et al. Climate drivers of the 2017 devastating fires in Portugal. **Scientific Reports**, v. 9, n. 1, p. 13886, 2019.

U S FIRE ADMINISTRATION - FEMA. **Fire in the United States 2004-2013**. U.S. Fire Administration; National Fire Data Center, 2016. Available from: https://www.usfa.fema.gov/downloads/pdf/publications/fius17th.pdf.

UNITED NATIONS FRAMEWORK CONVENTION ON CLIMATE CHANGE - UNFCCC. **NDC registry - Brazil**. Available from: https://www4.unfccc.int/sites/NDCStaging/Pages/Party.aspx?party=BRA. Access on: 22 June 2021.

UNITED NATIONS FRAMEWORK CONVENTION ON CLIMATE CHANGE - UNFCCC. **Paris agreement**. 2015. Available from: https://unfccc.int/sites/default/files/english_paris_agreement.pdf.

UNITED NATIONS OFFICE FOR DISASTER RISK REDUCTION - UNDRR. **Sendai framework for disaster risk reduction 2015-2030.** United Nations, 2015. Available from: https://www.undrr.org/publication/sendai-framework-disaster-risk-reduction-2015-2030.

URBANSKI, S. P.; HAO, W. M.; BAKER, S. Chemical composition of wildland fire emissions. In: BYTNEROWICZ, A. et al. (Ed.). **Developments in environmental science**. [S.l.]: Elsevier, 2008. v. 8. p. 79–107.

VAN DER WERF, G. R. et al. **Global fire emissions estimates during 1997–2015**. Biosphere – Biogeosciences, 12 jan. 2017. Available from: https://essd.copernicus.org/preprints/essd-2016-62/essd-2016-62.pdf. Access on: 16 May 2021.

VARIAN, H. R. **Intermediate microeconomics: a modern approach**. 8.ed. New York: W.W. Norton & Co, 2010.

VAUGHAN, A. Dawn of the pyrocene. **New Scientist**, v. 243, n. 3245, p. 20–21, 2019.

VENABLES, W. N.; RIPLEY, B. D.; VENABLES, W. N. **Modern applied statistics with S**. 4.ed. New York: Springer, 2002.

VERÍSSIMO, A. et al. (Ed.). **Áreas protegidas na Amazônia Brasileira**: avanços e desafios. Belém: IMAZON, 2011.

VIAN, A. L. et al. **Estimativa de biomassa da parte aérea de milho através de imagens digitais e sensor de vegetação**. In: CONGRESSO NACIONAL DE MILHO E SORGO, 31., 2016, Bento Gonçalves - RS. **Anais...** 2016. Available from: https://www.researchgate.net/publication/308779186_Estimativa_de_biomassa_da_parte_aerea_de_milho_atraves_de_imagens_digitais_e_sensor_de_vegetacao/citations.

VUOLO, J. H. **Fundamentos da teoria de erros**. 2.ed. São Paulo - SP: Edgar Blücher, 1996.

WALLEMACQ, P.; HOUSE, R. **Economic losses, poverty & disasters: 1998-2017**. UNISDR, 2018. Available from: https://www.undrr.org/publication/economic-losses-poverty-disasters-1998-2017.

WAN, Z.; HOOK, S.; HULLEY, G. **MOD11A2 MODIS/Terra land surface temperature/emissivity 8-day L3 global 1km SIN grid V006.** NASA EOSDIS Land Processes DAAC, 2015. Available from: https://lpdaac.usgs.gov/products/mod11a2v006/. Access on: 29 Dec. 2020

WANG, K. et al. Spatial assessment of health economic losses from exposure to ambient pollutants in China. **Remote Sensing**, v. 12, n. 5, p. 1–20, 2020.

WATTS, J. D. et al. Incentivizing compliance: Evaluating the effectiveness of targeted village incentives for reducing burning in Indonesia. **Forest Policy and Economics**, v. 108, e101956, 2019.

WEINHOLD, D.; REIS, E. J.; VALE, P. M. Boom-bust patterns in the Brazilian Amazon. **Global Environmental Change**, v. 35, p. 391–399, 2015.

WILLIAMSON, G. J. et al. A transdisciplinary approach to understanding the health effects of wildfire and prescribed fire smoke regimes. **Environmental Research Letters**, v. 11, n. 12, p. 1–11, 2016.

WOOLDRIDGE, J. M. **Introductory econometrics: a modern approach**. 7.ed. Boston, MA: Cengage Learning, 2018.

## APPENDIX A - SUPPLEMENTARY MATERIAL FROM CHAPTER 4

Table A-1. Mean effect of the variation in the Aerosol Optical Depth (AOD) on the Total respiratory disease hospitalization counts due to the burned area.

| | IVc01 | | | IVc02 | | | IVc03 | | | IVc04 | | |
|---|---|---|---|---|---|---|---|---|---|---|---|---|
| | | | | | | OLS | | | | | | |
| AOD (OLS) | 0.0443*** | 0.0925*** | 0.0455*** | 0.0443*** | 0.0925*** | 0.0455*** | 0.0443*** | 0.0925*** | 0.0455*** | 0.0443*** | 0.0925*** | 0.0455*** |
| | (0.0072) | (0.0072) | (0.0067) | (0.0072) | (0.0072) | (0.0067) | (0.0072) | (0.0072) | (0.0067) | (0.0072) | (0.0072) | (0.0067) |
| # obs. | 118,335 | 118,335 | 118,335 | 118,335 | 118,335 | 118,335 | 118,335 | 118,335 | 118,335 | 118,335 | 118,335 | 118,335 |
| | | | | | | IV | | | | | | |
| AOD (2SLS) | 0.1383*** | 0.0771* | 0.1359*** | 0.1336*** | -0.9626*** | 0.1361*** | 0.1401** | 0.0942** | 0.1389*** | 0.0461 | -12.9107*** | 2.2891 |
| | (0.0294) | (0.0321) | (0.0243) | (0.0315) | (0.105) | (0.0262) | (0.0466) | (0.0322) | (0.0383) | (0.1037) | (2.5574) | (3.1566) |
| # obs. | 118,335 | 118,335 | 118,335 | 118,335 | 118,335 | 118,335 | 118,335 | 118,335 | 118,335 | 118,335 | 118,335 | 118,335 |
| Fixed effect | Y | N | Y | Y | N | Y | Y | N | Y | Y | N | Y |
| Controls | Y | Y | N | Y | Y | N | Y | Y | N | Y | Y | N |
| Exogeneity and IV validity tests | | | | | | | | | | | | |
| Exog | 13.82*** | 0.24$^{ns}$ | 21.50*** | 11.59*** | 120.06*** | 20.07*** | 4.33* | 0.0027$^{ns}$ | 5.58* | 0.0006$^{ns}$ | 742.87*** | 7.18** |
| Overid | 1.204$^{ns}$ | 779.886*** | 4.41$^{ns}$ | 0.774$^{ns}$ | 549.951*** | 4.409* | 1.176$^{ns}$ | 741.718*** | 4.396* | - | - | - |
| Weak Instrument tests | | | | | | | | | | | | |
| Joint | 1103.36 | 945.817 | 2617.91 | 1396.41 | 250.833 | 1396.41 | 576.324 | 576 | 991.908 | 252.589 | 20.5295 | 252.589 |
| Yogo: stat | 1445.95 | 2087.78 | 2764.63 | 1703.26 | 330.615 | 1703.26 | 1045.85 | 1045.85 | 1729.91 | 282.652 | 26.7979 | 282.652 |
| Yogo: crit | 22.3 | 22.3 | 22.3 | 19.93 | 19.93 | 19.93 | 19.93 | 19.93 | 19.93 | 16.38 | 16.38 | 16.38 |

Notes: Set of instruments: IVc01 is the Log_Ba plus the BaWSpeed and the BaWDirec; IVc02 is the Log_Ba plus the BaWSpeed; IVc03 is the Log_Ba plus the BaWDirec, and; IVc04 is only Log_Ba. "*Exog.*", computes a test of exogeneity for a fixed-effect regression estimated via instrumental variables; "*Overid*" is the Sargan-Hansen statistic for instrument overidentification test. "*Joint*", for the joint significance test of the instruments in the first stage regression; "*Yogo: stat*", is the value of the Stock and Yogo test for instrument weakness; "*Yogo: crit*", is the table value for the Stock and Yogo test. Significance level: "***" p<0.001, "**" p<0.01, "*" p<0.05, "."p<0.1, "*ns*" not significant.

Source: From Author.

Table A-2. Mean effect of the variation in the Aerosol Optical Depth (AOD) on the hospitalization of Small Children due to the burned area.

| | IVc01 | | | IVc02 | | | IVc03 | | | IVc04 | | |
|---|---|---|---|---|---|---|---|---|---|---|---|---|
| | | | | | | | OLS | | | | | |
| AOD (OLS) | 0.0177** | 0.0700*** | 0.0222** | 0.0177** | 0.0700*** | 0.0222** | 0.0177** | 0.0700*** | 0.0222** | 0.0177** | 0.0700*** | 0.0222** |
| | (0.0068) | (0.0056) | (0.0073) | (0.0068) | (0.0056) | (0.0073) | (0.0068) | (0.0056) | (0.0073) | (0.0068) | (0.0056) | (0.0073) |
| # obs. | 118,335 | 118,335 | 118,335 | 118,335 | 118,335 | 118,335 | 118,335 | 118,335 | 118,335 | 118,335 | 118,335 | 118,335 |
| | | | | | | | IV | | | | | |
| AOD (2SLS) | 0.0760** | -0.0403$^{ns}$ | 0.1129*** | 0.0761** | -0.4136*** | 0.1187*** | -0.0210$^{ns}$ | -0.0422$^{ns}$ | 0.0865* | -0.3381*** | -11.5719*** | 5.6374$^{ns}$ |
| | (0.0271) | (0.0258) | (0.0241) | (0.0292) | (0.0797) | (0.0258) | (0.0476) | (0.0259) | (0.0422) | (0.1047) | (2.2816) | (7.5374) |
| # obs. | 118,335 | 118,335 | 118,335 | 118,335 | 118,335 | 118,335 | 118,335 | 118,335 | 118,335 | 118,335 | 118,335 | 118,335 |
| Fixed effect | Y | N | Y | Y | N | Y | Y | N | Y | Y | N | Y |
| Controls | Y | Y | N | Y | Y | N | Y | Y | N | Y | Y | N |
| Exogeneity and IV validity tests | | | | | | | | | | | | |
| Exog | 7.23** | 19.35*** | 29.26*** | 6.73** | 39.26*** | 30.77*** | 0.91$^{ns}$ | 19.84*** | 3.59. | 20.9530*** | 929.26*** | 60.23*** |
| Overid | 21.757*** | 906.273*** | 32.163*** | 21.753*** | 833.464*** | 31.481*** | 15.014*** | 912.353*** | 31.604*** | - | - | - |
| Weak Instrument tests | | | | | | | | | | | | |
| Joint | 1103.36 | 945.817 | 2617.91 | 1396.41 | 250.833 | 1396.41 | 576.324 | 576.324 | 991.908 | 252.589 | 20.5295 | 252.589 |
| Yogo: stat | 1445.95 | 2087.78 | 2764.63 | 1703.26 | 330.615 | 1703.26 | 1045.85 | 1045.85 | 1729.91 | 282.652 | 26.7979 | 282.652 |
| Yogo: crit | 22.3 | 22.3 | 22.3 | 19.93 | 19.93 | 19.93 | 19.93 | 19.93 | 19.93 | 16.38 | 16.38 | 16.38 |

Notes: Set of instruments: IVc01 is the Log_Ba plus the BaWSpeed and the BaWDirec; IVc02 is the Log_Ba plus the BaWSpeed; IVc03 is the Log_Ba plus the BaWDirec, and; IVc04 is only Log_Ba. "*Exog.*", computes a test of exogeneity for a fixed-effect regression estimated via instrumental variables; "*Overid*" is the Sargan-Hansen statistic for instrument overidentification test. "*Joint*", for the joint significance test of the instruments in the first stage regression; "*Yogo: stat*", is the value of the Stock and Yogo test for instrument weakness; "*Yogo: crit*", is the table value for the Stock and Yogo test. Significance level: "***" p<0.001, "**" p<0.01, "*" p<0.05, "."p<0.1, "*ns*" not significant.

Source: From Author.

Table A-3. Mean effect of the variation in the Aerosol Optical Depth (AOD) on the hospitalization of children due to the burned area.

| | IVc01 | | | IVc02 | | | IVc03 | | | IVc04 | | |
|---|---|---|---|---|---|---|---|---|---|---|---|---|
| | | | | | | OLS | | | | | | |
| AOD (OLS) | -0.0061$^{ns}$ | 0.0500*** | -0.0047 | -0.0061$^{ns}$ | 0.0500*** | -0.0047 | -0.0061$^{ns}$ | 0.0500*** | -0.0047 | -0.0061$^{ns}$ | 0.0500*** | -0.0047$^{ns}$ |
| | (0.0051) | (0.0039) | (0.0053) | (0.0051) | (0.0039) | (0.0053) | (0.0051) | (0.0039) | (0.0053) | (0.0051) | (0.0039) | (0.0053) |
| # obs. | 118,335 | 118,335 | 118,335 | 118,335 | 118,335 | 118,335 | 118,335 | 118,335 | 118,335 | 118,335 | 118,335 | 118,335 |
| | | | | | | IV | | | | | | |
| AOD (2SLS) | 0.0094$^{ns}$ | -0.0464* | 0.0223 | 0.0177$^{ns}$ | -0.5826*** | 0.0312. | -0.0765* | -0.0347. | -0.0291$^{ns}$ | -0.1815* | -4.3372*** | 2.7389$^{ns}$ |
| | (0.0201) | (0.0182) | (0.0164) | (0.0212) | (0.0598) | (0.0173) | (0.0364) | (0.0182) | (0.0306) | (0.0761) | (0.8896) | (3.7735) |
| # obs. | 118,335 | 118,335 | 118,335 | 118,335 | 118,335 | 118,335 | 118,335 | 118,335 | 118,335 | 118,335 | 118,335 | 118,335 |
| Fixed effect | Y | N | Y | Y | N | Y | Y | N | Y | Y | N | Y |
| Controls | Y | Y | N | Y | Y | N | Y | Y | N | Y | Y | N |
| Exogeneity and IV validity tests | | | | | | | | | | | | |
| Exog | 0.84$^{ns}$ | 29.78*** | 3.98* | 1.79$^{ns}$ | 135.56*** | 6.48* | 4.58* | 22.86*** | 0.74$^{ns}$ | 7.6436** | 264.49*** | 21.68*** |
| Overid | 10.966** | 308.79*** | 20.107*** | 8.499** | 167.23*** | 15.235*** | 2.895. | 254.004*** | 15.81*** | - | - | - |
| Weak Instrument tests | | | | | | | | | | | | |
| Joint | 1103.36 | 945.817 | 2617.91 | 1396.41 | 250.833 | 1396.41 | 576.324 | 576.324 | 991.908 | 252.589 | 20.5295 | 252.589 |
| Yogo: stat | 1445.95 | 2087.78 | 2764.63 | 1703.26 | 330.615 | 1703.26 | 0.0174 | 1045.85 | 1729.91 | 282.652 | 26.7979 | 282.652 |
| Yogo: crit | 22.3 | 22.3 | 22.3 | 19.93 | 19.93 | 19.93 | 19.93 | 19.93 | 19.93 | 16.38 | 16.38 | 16.38 |

Notes: Set of instruments: IVc01 is the Log_Ba plus the BaWSpeed and the BaWDirec; IVc02 is the Log_Ba plus the BaWSpeed; IVc03 is the Log_Ba plus the BaWDirec, and; IVc04 is only Log_Ba. "*Exog.*", computes a test of exogeneity for a fixed-effect regression estimated via instrumental variables; "*Overid*" is the Sargan-Hansen statistic for instrument overidentification test. "*Joint*", for the joint significance test of the instruments in the first stage regression; "*Yogo: stat*", is the value of the Stock and Yogo test for instrument weakness; "*Yogo: crit*", is the table value for the Stock and Yogo test. Significance level: "***" p<0.001, "**" p<0.01, "*" p<0.05, "."p<0.1, "*ns*" not significant.

Source: From Author.

Table A-4. Mean effect of the variation in the Aerosol Optical Depth (AOD) on the hospitalization of the elderly due to the burned area.

| | IVc01 | | | IVc02 | | | IVc03 | | | IVc04 | | |
|---|---|---|---|---|---|---|---|---|---|---|---|---|
| | | | | | | **OLS** | | | | | | |
| AOD(OLS) | 0.0215*** | 0.0218*** | 0.0290*** | 0.0215*** | 0.0218*** | 0.0290*** | 0.0215*** | 0.0218*** | 0.0290*** | 0.0215*** | 0.0218*** | 0.0290*** |
| | (0.0051) | (0.0045) | (0.0052) | (0.0051) | (0.0045) | (0.0052) | (0.0051) | (0.0045) | (0.0052) | (0.0051) | (0.0045) | (0.0052) |
| # obs. | 118,335 | 118,335 | 118,335 | 118,335 | 118,335 | 118,335 | 118,335 | 118,335 | 118,335 | 118,335 | 118,335 | 118,335 |
| | | | | | | **IV** | | | | | | |
| AOD(2SLS) | 0.0428* | 0.0344. | 0.0590*** | 0.0581** | 0.3074*** | 0.0722*** | -0.0596. | 0.0187 | -0.0211 | -0.0720 | -6.2621*** | 1.9639 |
| | (0.0206) | (0.0204) | (0.0167) | (0.0218) | (0.0624) | (0.0179) | (0.0352) | (0.0205) | (0.0294) | (0.0719) | (1.2516) | (2.7017) |
| # obs. | 118,335 | 118,335 | 118,335 | 118,335 | 118,335 | 118,335 | 118,335 | 118,335 | 118,335 | 118,335 | 118,335 | 118,335 |
| Fixed effect | Y | N | Y | Y | N | Y | Y | N | Y | Y | N | Y |
| Controls | Y | Y | N | Y | Y | N | Y | Y | N | Y | Y | N |
| Exogeneity and IV validity tests: | | | | | | | | | | | | |
| Exog | 1.47$^{ns}$ | 0.40*** | 4.77* | 3.94* | 21.74*** | 9.11** | 6.02* | 0.02 | 3.15. | 2.1189$^{ns}$ | 428.08*** | 10.58** |
| Overid | 12.241** | 508.117*** | 17.086*** | 3.733. | 470.484*** | 7276** | 0.041$^{ns}$ | 428.019*** | 7.856** | - | - | - |
| Week Instrument tests: | | | | | | | | | | | | |
| Joint | 1103.36 | 945.817 | 2617 | 1396.41 | 250.833 | 1396.41 | 576.324 | 576.324 | 991.908 | 252.589 | 20.5295 | 252.589 |
| Yogo: stat | 1445.95 | 2087 | 2764 | 1703.26 | 330.615 | 1703.26 | 1045.85 | 1045.85 | 1729.91 | 282.652 | 26.7979 | 282.652 |
| Yogo: crit | 22.3 | 22.3 | 22.3 | 19.93 | 19.93 | 19.93 | 19.93 | 19.93 | 19.93 | 16.38 | 16.38 | 16.38 |

Notes: Set of instruments: IVc01 is the Log_Ba plus the BaWSpeed and the BaWDirec; IVc02 is the Log_Ba plus the BaWSpeed; IVc03 is the Log_Ba plus the BaWDirec, and; IVc04 is only Log_Ba. "*Exog.*", computes a test of exogeneity for a fixed-effect regression estimated via instrumental variables; "*Overid*" is the Sargan-Hansen statistic for instrument overidentification test. "*Joint*", for the joint significance test of the instruments in the first stage regression; "*Yogo: stat*", is the value of the Stock and Yogo test for instrument weakness; "*Yogo: crit*", is the table value for the Stock and Yogo test. Significance level: "***" p<0.001, "**" p<0.01, "*" p<0.05, "."p<0.1, "*ns*" not significant.

Source: From Author.

Table A-5. Mean effect of the variation in the Aerosol Optical Depth (AOD) on the Asthma hospitalizations due to the burned area.

| | IVc01 | | | IVc02 | | | IVc03 | | | IVc04 | | |
|---|---|---|---|---|---|---|---|---|---|---|---|---|
| | | | | | | OLS | | | | | | |
| AOD(OLS) | 0.0265*** | 0.0532*** | 0.0295*** | 0.0265*** | 0.0532*** | 0.0295*** | 0.0265*** | 0.0532*** | 0.0295*** | 0.0265*** | 0.0532*** | 0.0295*** |
| | (0.006) | (0.0047) | (0.0059) | (0.006) | (0.0047) | (0.0059) | (0.006) | (0.0047) | (0.0059) | (0.006) | (0.0047) | (0.0059) |
| # obs. | 118,335 | 118,335 | 118,335 | 118,335 | 118,335 | 118,335 | 118,335 | 118,335 | 118,335 | 118,335 | 118,335 | 118,335 |
| | | | | | | IV | | | | | | |
| AOD(2SLS) | 0.0792*** | -0.0356 | 0.0844*** | 0.0865*** | -0.9181*** | 0.0921*** | 0.0147 | -0.0111 | 0.0394 | -0.0423 | -2.4134*** | 2.3085 |
| | (0.0244) | (0.0217) | (0.0204) | (0.0254) | (0.0754) | (0.0214) | (0.0433) | (0.0218) | (0.0352) | (0.0843) | (0.5755) | (3.2576) |
| # obs. | 118,335 | 118,335 | 118,335 | 118,335 | 118,335 | 118,335 | 118,335 | 118,335 | 118,335 | 118,335 | 118,335 | 118,335 |
| Fixed effect | Y | N | Y | Y | N | Y | Y | N | Y | Y | N | Y |
| Controls | Y | Y | N | Y | Y | N | Y | Y | N | Y | Y | N |
| Exogeneity and IV validity tests | | | | | | | | | | | | |
| Exog | 6.63** | 17.72*** | 11.53*** | 7.96** | 224.02*** | 13.95*** | $0.09^{ns}$ | 9.21** | $0.09^{ns}$ | $0.8569^{ns}$ | 58.47*** | 10.87*** |
| Overid | $3.5598^{ns}$ | 228.13*** | 8.627* | $2.52^{ns}$ | 16.728*** | 7.011** | $0.727^{ns}$ | 55.595*** | 7.406** | - | - | - |
| Week Instrument tests: | | | | | | | | | | | | |
| Joint | 1103.36 | 945.817 | 2617 | 1396.41 | 250.833 | 1396.41 | 576.324 | 576.324 | 991.908 | 252.589 | 20.5295 | 252.589 |
| Yogo: stat | 1445.95 | 2087.78 | 2764 | 1703.26 | 330.615 | 1703.26 | 1045.85 | 1045.85 | 1729.91 | 282.652 | 26.7979 | 282.652 |
| Yogo: crit | 22.3 | 22.3 | 22.3 | 19.93 | 19.93 | 19.93 | 19.93 | 19.93 | 19.93 | 16.38 | 16.38 | 16.38 |

Notes: Set of instruments: IVc01 is the Log_Ba plus the BaWSpeed and the BaWDirec; IVc02 is the Log_Ba plus the BaWSpeed; IVc03 is the Log_Ba plus the BaWDirec, and; IVc04 is only Log_Ba. "*Exog.*", computes a test of exogeneity for a fixed-effect regression estimated via instrumental variables; "*Overid*" is the Sargan-Hansen statistic for instrument overidentification test. "*Joint*", for the joint significance test of the instruments in the first stage regression; "*Yogo: stat*", is the value of the Stock and Yogo test for instrument weakness; "*Yogo: crit*", is the table value for the Stock and Yogo test. Significance level: "***" p<0.001, "**" p<0.01, "*" p<0.05, "."p<0.1, "*ns*" not significant.

Source: From Author.

Table A-6. Mean effect of the variation in the Aerosol Optical Depth (AOD) on the Pneumonia hospitalizations due to the burned area.

| | IVc01 | | | IVc02 | | | IVc03 | | | IVc04 | | |
|---|---|---|---|---|---|---|---|---|---|---|---|---|
| | | | | | | **OLS** | | | | | | |
| AOD (OLS) | 0.0594*** | 0.0244*** | 0.0663*** | 0.0594*** | 0.0244*** | 0.0663*** | 0.0594*** | 0.0244*** | 0.0663*** | 0.0594*** | 0.0244*** | 0.0663*** |
| | (0.0069) | (0.0064) | (0.0069) | (0.0069) | (0.0064) | (0.0069) | (0.0069) | (0.0064) | (0.0069) | (0.0069) | (0.0064) | (0.0069) |
| # obs. | 118,335 | 118,335 | 118,335 | 118,335 | 118,335 | 118,335 | 118,335 | 118,335 | 118,335 | 118,335 | 118,335 | 118,335 |
| | | | | | | **IV** | | | | | | |
| AOD (2SLS) | 0.1207*** | -0.1005*** | 0.1544*** | 0.1285*** | -0.4372*** | 0.1655*** | 0.0122$^{ns}$ | -0.1046*** | 0.0928* | -0.1790$^{ns}$ | -12.6441*** | 5.2789$^{ns}$ |
| | (0.0281) | (0.0287) | (0.0242) | (0.0303) | (0.088) | (0.0262) | (0.0477) | (0.0288) | (0.0396) | (0.1098) | (2.4844) | (6.9921) |
| # obs. | 118,335 | 118,335 | 118,335 | 118,335 | 118,335 | 118,335 | 118,335 | 118,335 | 118,335 | 118,335 | 118,335 | 118,335 |
| Fixed effect | Y | N | Y | Y | N | Y | Y | N | Y | Y | N | Y |
| Controls | Y | Y | N | Y | Y | N | Y | Y | N | Y | Y | N |
| Exogeneity and IV validity tests | | | | | | | | | | | | |
| Exog | 6.36* | 20.07*** | 22.24*** | 7.51** | 28.92*** | 26.26*** | 1.13$^{ns}$ | 21.25*** | 0.49$^{ns}$ | 7.6513** | 889.09*** | 42.23*** |
| Overid | 11.308** | 868*** | 27.217*** | 9.99** | 818.263*** | 23.546*** | 4.768* | 865.478*** | 23.765*** | - | - | - |
| Week Instrument tests: | | | | | | | | | | | | |
| Joint | 110336 | 945.817 | 2617 | 1396 | 250.833 | 1396.41 | 576.324 | 576.324 | 991.908 | 252.589 | 20.5295 | 252.589 |
| Yogo: stat | 1445.95 | 2087 | 2764 | 1703 | 330.615 | 1703.26 | 1045 | 1045.85 | 1729.91 | 282.652 | 26.7979 | 282.652 |
| Yogo: crit | 22.3 | 22.3 | 22.3 | 19.93 | 19.93 | 19.93 | 19.93 | 19.93 | 19.93 | 16.38 | 16.38 | 16.38 |

Notes: Set of instruments: IVc01 is the Log_Ba plus the BaWSpeed and the BaWDirec; IVc02 is the Log_Ba plus the BaWSpeed; IVc03 is the Log_Ba plus the BaWDirec, and; IVc04 is only Log_Ba. "*Exog.*", computes a test of exogeneity for a fixed-effect regression estimated via instrumental variables; "*Overid*" is the Sargan-Hansen statistic for instrument overidentification test. "*Joint*", for the joint significance test of the instruments in the first stage regression; "*Yogo: stat*", is the value of the Stock and Yogo test for instrument weakness; "*Yogo: crit*", is the table value for the Stock and Yogo test. Significance level: "***" p<0.001, "**" p<0.01, "*" p<0.05, "."p<0.1, "*ns*" not significant.

Source: From Author.

Table A-7. Mean effect of the variation in the Aerosol Optical Depth (AOD) on the Bronchitis hospitalizations due to the burned area.

| | IVc01 | | | IVc02 | | | IVc03 | | | IVc04 | | |
|---|---|---|---|---|---|---|---|---|---|---|---|---|
| | | | | | | OLS | | | | | | |
| AOD (OLS) | 0.0103** | 0.0075*** | 0.0121*** | 0.0103** | 0.0075*** | 0.0121*** | 0.0103** | 0.0075*** | 0.0121*** | 0.0103** | 0.0075*** | 0.0121*** |
| | (0.0032) | (0.002) | (0.0037) | (0.0032) | (0.002) | (0.0037) | (0.0032) | (0.002) | (0.0037) | (0.0032) | (0.002) | (0.0037) |
| # obs. | 118,335 | 118,335 | 118,335 | 118,335 | 118,335 | 118,335 | 118,335 | 118,335 | 118,335 | 118,335 | 118,335 | 118,335 |
| | | | | | | IV | | | | | | |
| AOD (2SLS) | 0.0011$^{ns}$ | 0.0111$^{ns}$ | 0.0072$^{ns}$ | -0.0023$^{ns}$ | -0.0958*** | 0.0046 | 0.0169$^{ns}$ | 0.0149$^{ns}$ | 0.0240$^{ns}$ | -0.0020$^{ns}$ | 0.4608** | 0.1545$^{ns}$ |
| | (0.0139) | (0.0099) | (0.0127) | (0.0151) | (0.0299) | (0.0138) | (0.0215) | (0.0099) | (0.0191) | (0.0412) | (0.1709) | (0.4591) |
| # obs. | 118,335 | 118,335 | 118,335 | 118,335 | 118,335 | 118,335 | 118,335 | 118,335 | 118,335 | 118,335 | 118,335 | 118,335 |
| Fixed effect | Y | N | Y | Y | N | Y | Y | N | Y | Y | N | Y |
| Controls | Y | Y | N | Y | Y | N | Y | Y | N | Y | Y | N |
| Exogeneity and IV validity tests | | | | | | | | | | | | |
| Exog | 0.60$^{ns}$ | 0.14$^{ns}$ | 0.28$^{ns}$ | 1.06$^{ns}$ | 12.24*** | 0.62$^{ns}$ | 0.11$^{ns}$ | 0.59$^{ns}$ | 0.46$^{ns}$ | 0.0867$^{ns}$ | 9.54** | 0.14$^{ns}$ |
| Overid | 0.854$^{ns}$ | 29.635*** | 1.042$^{ns}$ | 0$^{ns}$ | 14.716*** | 0.127$^{ns}$ | 0.276$^{ns}$ | 9.267** | 0.095$^{ns}$ | - | - | - |
| Week Instrument tests: | | | | | | | | | | | | |
| Joint | 1103.36 | 945.817 | 2617.91 | 1396.41 | 250.833 | 1396.41 | 576.324 | 576 | 991.908 | 252.589 | 20.5295 | 252.589 |
| Yogo: stat | 1445.95 | 2087.78 | 2764.63 | 1703.26 | 330615 | 1703.26 | 1045 | 1045 | 1729.91 | 282.652 | 26.7979 | 282.652 |
| Yogo: crit | 22.3 | 22.3 | 22.3 | 19.93 | 19.93 | 19.93 | 19.93 | 19.93 | 19.93 | 16.38 | 16.38 | 16.38 |

Notes: Set of instruments: IVc01 is the Log_Ba plus the BaWSpeed and the BaWDirec; IVc02 is the Log_Ba plus the BaWSpeed; IVc03 is the Log_Ba plus the BaWDirec, and; IVc04 is only Log_Ba. "*Exog.*", computes a test of exogeneity for a fixed-effect regression estimated via instrumental variables; "*Overid*" is the Sargan-Hansen statistic for instrument overidentification test. "*Joint*", for the joint significance test of the instruments in the first stage regression; "*Yogo: stat*", is the value of the Stock and Yogo test for instrument weakness; "*Yogo: crit*", is the table value for the Stock and Yogo test. Significance level: "***" p<0.001, "**" p<0.01, "*" p<0.05, "."p<0.1, "*ns*" not significant.

Source: From Author.

## APPENDIX B - SUPPLEMENTARY MATERIAL FOR CHAPTER 5

Figure B-1. Evolution of LULC for the BLA region and its biomes.

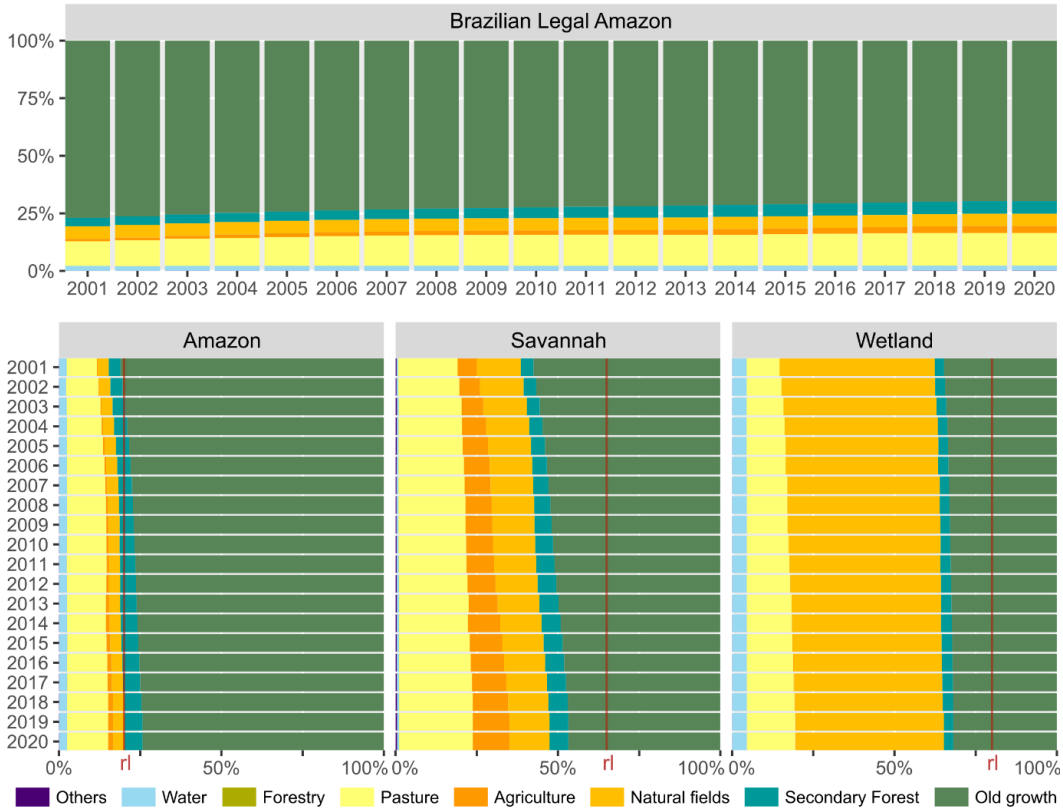


Notes: rl represents the mininum percentage of forest cover for each phytophysiognomy within the BLA region, following the instruction of legal reserve established in the New Forest Code (BRASIL, 2012).
Source: From Author.

Figure B-2. Trends in burned area for each public land tenure.

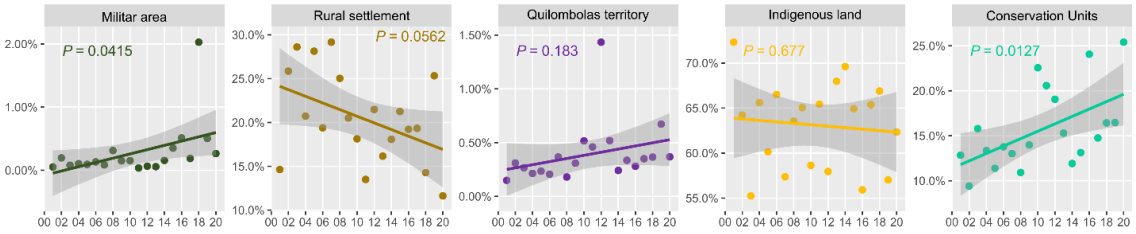


Source: From Author.

Table B-1. Percentage of each land tenure type and category over the BLA territory.

| Category | Type | Area (%) | |
|---|---|---|---|
| | | by Type | by Category |
| Not Designated | Without information | 8.85% | 19.69% |
| | Undesignated land from Terra Legal Program | 3.89% | |
| | Undesignated public forests | 6.02% | |
| | Public properties at INCRA system | 0.94% | |
| Private | CAR premium | 3.48% | 30.69% |
| | CAR poor | 7.79% | |
| | Private properties at INCRA system | 17.47% | |
| | Private properties from Terra Legal Program | 1.95% | |
| Public | Rural settlements | 6.61% | 47.03% |
| | Communitarian lands | 0.35% | |
| | Military areas | 0.56% | |
| | Quilombola lands | 0.47% | |
| | Homologated indigenous land | 21.44% | |
| | Non-homologated indigenous land | 0.41% | |
| | Full protection conservation unit | 7.18% | |
| | Sustainable use conservation unit | 10.01% | |
| Urban, Water | Water bodies | 2.17% | 2.58% |
| | Transportation network | 0.33% | |
| | Urban areas | 0.08% | |

Source: From Author.

Figure B-3. Total of municipalities affected by fire per year in the BLA region.

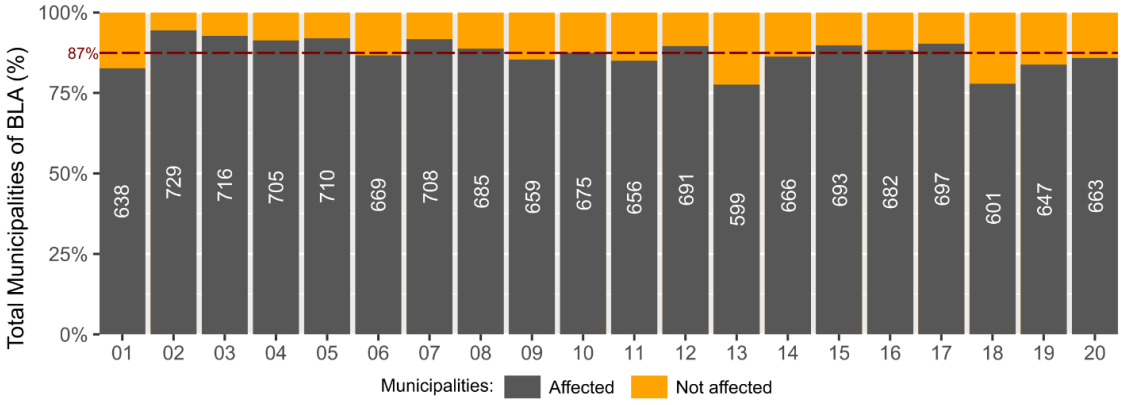


Note: Red line represents the average of municipalities affected by fire along the 20 years.
Source: From Author.

Table B-2. Trends in each state, considering the total burned area by different methods

| | Linear | | | Mann-kendal | | | Seasonal Mann-kendall | | |
|---|---|---|---|---|---|---|---|---|---|
| UF | COEF | pval | | Tau | pval | | Tau | pval | |
| RO | -0.243 | 0.207 | ns | 0.113 | 0.009 | *** | 0.119 | 0.011 | ** |
| AC | -1.616 | 0.085 | * | 0.025 | 0.593 | ns | -0.043 | 0.436 | ns |
| AM | 0.593 | 0.088 | * | 0.023 | 0.599 | ns | 0.042 | 0.381 | ns |
| RR | 0.469 | 0.169 | ns | 0.038 | 0.390 | ns | 0.053 | 0.264 | ns |
| PA | -0.029 | 0.532 | ns | 0.057 | 0.187 | ns | 0.104 | 0.028 | ** |
| AP | -0.562 | 0.537 | ns | -0.002 | 0.964 | ns | -0.048 | 0.336 | ns |
| TO | 0.008 | 0.762 | ns | 0.110 | 0.011 | ** | 0.210 | 0.000 | *** |
| MA | 0.032 | 0.610 | ns | 0.052 | 0.236 | ns | 0.049 | 0.300 | ns |
| MT | -0.007 | 0.710 | ns | 0.068 | 0.118 | ns | 0.020 | 0.667 | ns |

Note: significance levels: "***" p<0.01, "**" p<0.05, "*" p<0.1 e "ns" not significant.
Source: From Author.

Figure B-4. Total of CO2 emission through the years analyzed, considering the National estimate (SIRENE) and the BLA's immediate fire emission.

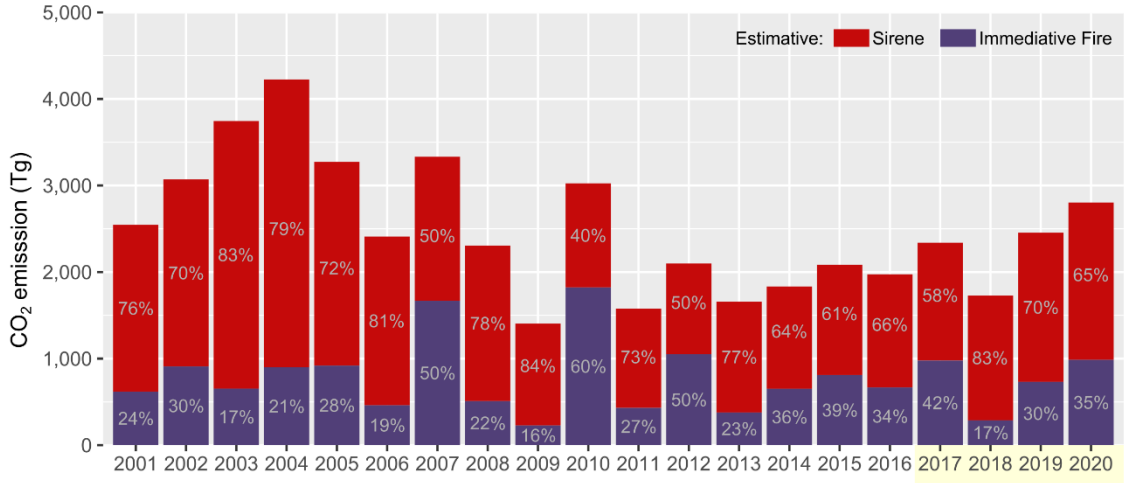


Note: Following the estimate of the 5th national emission report until 2016 (MCTIC, 2019). For the remaining years (2017-2020), we use the trend in each category to extrapolate, with exception of the lad use change category that we use the correlation of it with deforestation rates by Terrabrasilis (INPE, 2021b).
Source: From Author.

## B.1. Fire and its evolution with deforestation

Considering the interannual subdivision of the series into four groups (G1, G2, G3 and G4) some relations with deforestation were made (Figure B-5). The first group, from 2001 to 2005 is characterized by its majority of years before the PPCDAm measures. In this period, the highest deforestation rates were observed (average of 22,399 km²) while the total burned area remained constant and high (average of 129,584 km²), in which about

26% of the total burned area in the time series occurred. During this period the use of fire is closely related to deforestation (ARAGÃO et al., 2008).

The second group (G2: from 2006 to 2010) covers the end of phases 1 and part of phase 2 of the plan, which is characterized by the greatest drop in deforestation levels for the region (reduction of approximately 7.286 km²), while the temporal pattern of the burned area remained with higher average (142,501 km²) in relation to previous years, mainly taken by the years 2007 and 2010, years of El Niño, when the change in weather patterns causes a significant increase in the occurrence of fires in the region. During this period, the highest amounts of burned area for the region were recorded, representing 29% of the total burned during the last 20 years.

The third group (G3: from 2011 to 2015) in turn, covers the end of phase 2 and phase 3 in full. In this period, deforestation levels are the lowest in the entire series (average of 5,620 km²), however, an increase in rates begins, mainly in recent years. During the same period, there is an increase in the levels of burned area for the region, but there is no significant correlation between these variables. This phase is the one with the lowest total value of burned area, representing approximately 21% of the total burned within the analyzed time series.

Figure B-5. Deforestation and Fire relation through the age groups.

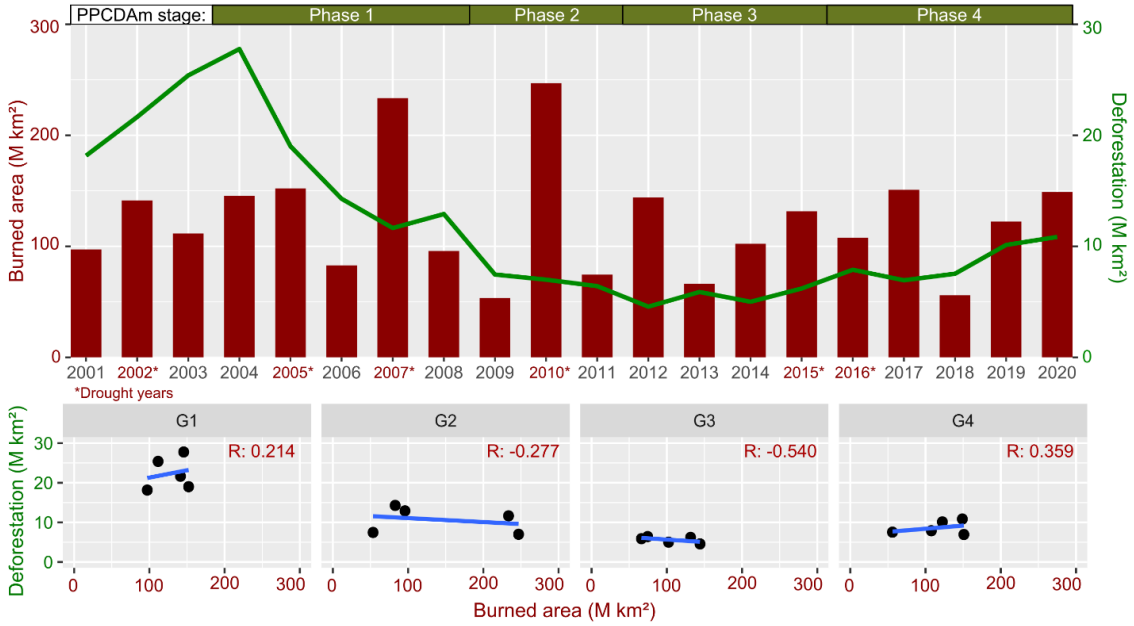


Source: From Author.

Finally, the fourth group (G4: from 2016 to 2020) covers the years of phase 4 of the PPCDAm program, in addition to including a year of extreme drought and significant changes in policy with the weakening, among others, of the environmental agenda. In this period, the average of the burned area is in the order of 117.196 km², similar to those at the beginning of the data series (G1). The burned area data is beginning to resemble the deforestation data, presenting the last two years with high rates.